ISSN: 2153-1196 Volume 11, Number 4, April 2020

Scientific Research Publishing

Journal of Modern Physics

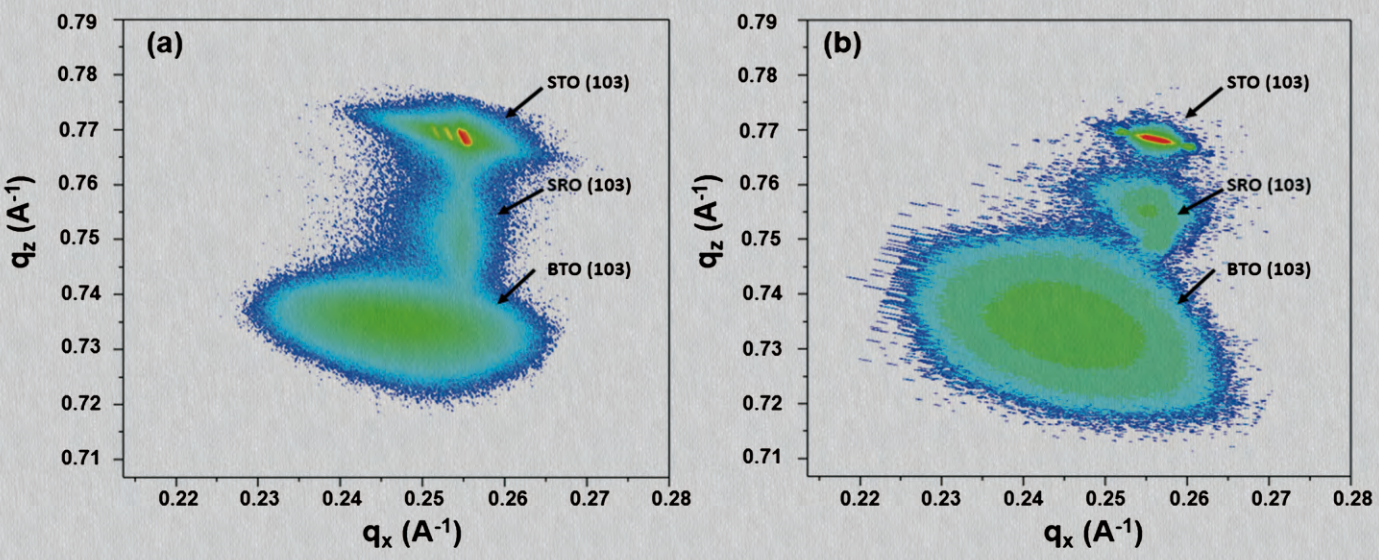

ISSN: 2153-1196
9 772153 119007 04

https://www.scirp.org/journal/jmp

Journal Editorial Board

ISSN: 2153-1196 (Print) ISSN: 2153-120X (Online)
https://www.scirp.org/journal/jmp

Editor-in-Chief

Editorial Board

Scientific Research Publishing

Journal of Modern Physics, 2020, 11, 487-592
https://www.scirp.org/journal/jmp
ISSN Online: 2153-120X
ISSN Print: 2153-1196

Table of Contents

Volume 11 Number 4 April 2020

Most Intense X-Ray Lines of the Helium Isoelectronic Sequence for Plasmas Diagnostic

I. Sakho.....487

Noise-Induced Origin of the Fundamental Scalar Field

B. I. Lev, A. G. Zagorodny.....502

Comparison of Epitaxial and Textured Ferroelectric $BaTiO_3$ Thin Films

B. Wague, N. Baboux, P. R. Romeo, Y. Robach, B. Vilquin.....509

The Mathematical Foundations of Quantum Thermodynamics

A. Suzuki, H. Taira.....517

The Relativistic Rydberg's Formula in Greater Depth and for Any Atom

E. G. Haug.....528

Classification of Relativity

V. B. Ho.....535

Recent QFT of Einstein's Gravity Simplified via Ultrahyperfunctions

A. Plastino, M. C. Rocca.....565

Complete Solution for Quasicrystals

A. J. Bourdillon.....581

The figure on the front cover is from the article published in Journal of Modern Physics, 2020, Vol. 11, No. 4, pp. 509-516 by Baba Wague, Nicolas Baboux, Pedro Rojo Romeo, Yves Robach, Bertrand Vilquin.

Journal of Modern Physics (JMP)
Journal Information

SUBSCRIPTIONS

The *Journal of Modern Physics* (Online at Scientific Research Publishing, https://www.scirp.org/) is published monthly by Scientific Research Publishing, Inc., USA.

Subscription rates:
Print: $89 per issue.
To subscribe, please contact Journals Subscriptions Department, E-mail: sub@scirp.org

SERVICES

Advertisements
Advertisement Sales Department, E-mail: service@scirp.org

Reprints (minimum quantity 100 copies)
Reprints Co-ordinator, Scientific Research Publishing, Inc., USA.
E-mail: sub@scirp.org

COPYRIGHT

PRODUCTION INFORMATION

For manuscripts that have been accepted for publication, please contact:
E-mail: jmp@scirp.org

Journal of Modern Physics, 2020, 11, 487-501
https://www.scirp.org/journal/jmp
ISSN Online: 2153-120X
ISSN Print: 2153-1196

Most Intense X-Ray Lines of the Helium Isoelectronic Sequence for Plasmas Diagnostic

Ibrahima Sakho*

Department of Experimental Sciences, UFR Sciences and Technologies, University of Thies, Thies, Senegal
Email: *aminafatima_sakho@yahoo.fr

How to cite this paper: Sakho, I. (2020) Most Intense X-Ray Lines of the Helium Isoelectronic Sequence for Plasmas Diagnostic. *Journal of Modern Physics*, **11**, 487-501.
https://doi.org/10.4236/jmp.2020.114031

Received: January 23, 2020
Accepted: March 23, 2020
Published: March 26, 2020

Abstract

We report accurate wavelengths for the three most intense lines (resonance line: $1s^2\ ^1S0$ - $1s2p\ ^1P1$, intercombination line: $1s^2\ ^1S0$ - $1s2p\ ^3P1$ and forbidden line: $1s^2\ ^1S0$ - $1s2s\ ^3S1$) along with wavelengths for the $1s^2\ ^1S0$ - $1snp\ ^1P1$ and $^1S0$ - $1snp\ ^3P2$ ($2 \le n \le 25$) transitions in He-like systems ($Z = 2 - 13$). The first spectral lines that belong to the above transitions are established in the framework of the Screening Constant per Unit Nuclear Charge method. The results obtained agree excellently with various experimental and theoretical literature data. The uncertainties in wavelengths between the present calculations and the available literature data are less than 0.004 Å. A host of new data listed in this paper may be of interest in astrophysical and laboratory plasmas diagnostic.

Keywords

He-Like Systems, Semi-Empirical, Screening Constant Per Unit Nuclear Charge, Excited States, X-Ray Spectra

1. Introduction

The helium-like isoelectronic series emit strong X-ray wavelengths. The most intense lines of these systems are the resonance line designated by ω (also labelled r: $1s^2\ ^1S_0$ - $1s2p^1P_1$), the intercombination lines ($x + y$) (or i: $1s^2\ ^1S_0$ - $1s2p^3P_{2,1}$) and the forbidden line z (or f: $1s^2\ ^1S_0$ - $1s2s\ ^3S_1$). These three lines correspond to the transitions between the $n = 2$ excited shell and the $n = 1$ ground state shell. The determination of these lines is of great interest because the line ratios f/i and $(f + i)/r$ provided respectively electrons density ($n_e \sim 10^8$ - 10^{13} cm^{-3}) and electrons temperature ($T_e \sim 1$ - 10 MK) as first shown by Gabriel and Jordan [1] and are widely used for collisional solar plasma diagnostics [1] [2] [3]. On the other hand, these line ratios enable also to determine the prevailed ioni-

zation processes (photo-ionization and/or collisional ionization) in the plasma [4] [5] [6]. Traditionally, He-like ions f/i line ratios have been used to derive electron densities of X-ray line-emitting regions since the populations of the 2^3P level are controlled by collisional excitation from the 2^3S level [1]. At low density, the $n = 2$ states are populated by electron excitation and then decay radiatively. Then, the relative intensities of the three lines are independent of the density [7]. Above the critical density (n_{crtit}): (n_{crit} *C* ~ *A*, *C being the rate coefficient for collisional excitation* $2^3S \rightarrow 2^3P$ *and A denotes the radiative transition probability of* $2^3S \rightarrow 1^1S$), the 2^3S upper level of the forbidden line becomes to be depleted by collision to the 2^3P upper levels of the intercombination line. As a result, when the electron density increases, the intensity of the forbidden line decreases strongly whereas that of the intercombination line increases. However, in the case of a strong UV radiation, the photo-excitation $2^3S \rightarrow 2^3P$ becomes no negligible. Subsequently, the ratio (f/i) of the forbidden line on the intercombination line is no longer an electron density diagnostic. As concern the ratio ($f + i$)/r, it is sensitive to electron temperature as the dependence of the collisional excitation rates with the temperature for the resonance line is not the same for the forbidden and intercombination lines. In short, for plasma dominated by photo-ionization and recombination, the forbidden line (or the intercombination line at high density) becomes much stronger than the resonance line. In the case of plasma dominated by collisional ionization and excitation, the resonance line is stronger or comparable to the forbidden line and the intercombination line [4]. The following considerations indicate that the determination of the most intensive lines of Helium-like ions in the X-ray range is of great interest in laboratory and astrophysical plasma diagnostics.

On the experimental side, high-precision measurements of the energy difference between S and P levels in the helium isoelectronic series were made three decades ago. Robinson [7] presents measurements of the $1s^2\ ^1S_0$ - $1snp\ ^1P_1$ series of the Helium isoelectronic sequence for Be III, B IV and C V. Since that time, many experiments have been improved. Twelve lines in the region 20 - 100 Å belonging to the resonance series of Be III, B IV, C V and O VII are remeasured by Svensson [8] using spectrograms. Beiersdorfer *et al.* [9] use the tokamak plasmas from the Princeton Large Torus (PLT) high-resolution Johann spectrometer to report the $n = 2 \rightarrow 1$ X-ray transitions of Helium-like potassium, scandium, titanium, vanadium, chromium, and iron ($Z = 19$ - 26) along with wavelengths belonging to the $1s^2\ ^1S_0$ - $1snp\ ^1P_1$ ($n = 3$ - 5) transitions. Furthermore, Engtröm and Litzén [10] generate spectra of C, N and O simultaneously by focusing 1 GW laser pulses on targets made of either ammonium hydrogen carbonate or ammonium oxalate and then determine the wavelengths of the $1s^2\ ^1S$ - $1snp\ ^1P$ ($n = 2$ - 4) resonance lines in N VI and O VII (17 - 30 ÅÅ) with uncertainties ranging from 0.2 to 0.7 mÅÅ. Bartnik *et al.* [11] measure the wavelengths of the $1snp\ ^1P$ - $1s^2\ ^1S$ ($n = 4$ - 10) transitions in He-like O VII in laser-produced gas puff plasmas with an accuracy measurement ranging between (1.5 - 3.0 mÅ).

On the theoretical side, many techniques are presented. Acaad *et al.* [12] con-

struct wave function expanded in a triple series of Laguerre polynomials of the *perimertric* coordinates to study the S and P states of the helium isoelectronic sequence and report nonrelativistic wavelengths and total wavelengths including mass polarization relativistic and, the Lamb shift corrections for $Z = 2$ - 9 belonging to the $1snp\ ^1P$ - $1s^{21}S$ ($n = 2$ - 5) transitions. In addition, Safronova *et al.* [13] apply the MZ code through a perturbation theory based on hydrogen-like functions to compute wavelengths of highly charged He-like ions ($Z = 6$ - 54) for both satellite lines ($1s2l'nl$ - $1s^2n'l'$, n, $n' = 2$, 3) and ($1snp\ ^{1,3}P$ - $1s^2$, $n = 2$, 3 and $1s2s\ ^{1,3}S$ - $1s^2$) transitions. Additionally, the plasma simulation code CLOUDY is used by Porter [14] to present wavelengths of the UV, intercombination, forbidden, and resonance transitions oh He-like ions for $Z = 6$ - 14 and for $Z = 16$, 18, 20, and 26. But, as far as we know, the wavelengths cannot be directly determined within a single analytical formula for a whole members of He-like ions using one of the preceding method or one of the other existing computational techniques. Then, analytical spectral lines in two-electron systems such as the Balmer or the Lyman spectral lines of the hydrogen-like systems are not yet established. In this paper, we intend to present analytical spectral lines belonging to the resonance line: $1s^2\ ^1S_0$ - $1s2p\ ^1P_1$ and intercombination line: $1s^2\ ^1S_0$ - $1s2p\ ^3P_{2,1}$ along the $1s^2\ ^1S_0$ - $1snp\ ^1P_1$ ($n \le 10$) transitions in the helium isoelectronic sequence. In our study, we use the Screening Constant per Unit Nuclear Charge (SCUNC) method suitable in the analysis of atomic spectra [15] [16]. All the results obtained in the present work compared very well to the available experimental and theoretical literature data. A host of data listed in this paper may be of interest in astrophysical and laboratory plasmas diagnostic.

In section 2, we present the theoretical procedure adopted in this work. In section 3, the presentation and the discussion of the results are made. A comparison of our results with available experimental and theoretical results is also made.

2. Theory

2.1. Brief Description of the SCUNC Formalism

In the framework of Screening Constant per Unit Nuclear Charge formalism, total energy of $\left(N\ell, n\ell'\right)^{2S+1}L^{\pi}$ excited states are expressed in the form (in rydberg units)

$$E\left(N\ell n\ell';\ ^{2S+1}L^{\pi}\right) = -Z^2\left(\frac{1}{N^2} + \frac{1}{n^2}\left[1-\beta\left(N\ell n\ell';\ ^{2S+1}L^{\pi};Z\right)\right]^2\right). \quad (1)$$

In this equation, the principal quantum numbers N and n, are respectively for the inner and the outer electron of He-isoelectronic series. In this equation, the β-parameters are screening constant by unit nuclear charge expanded in inverse powers of Z and given by

$$\beta\left(N\ell n\ell';\ ^{2S+1}L^{\pi};Z\right) = \sum_{k=1}^{q} f_k \times \left(\frac{1}{Z}\right)^k. \quad (2)$$

where $f_k = f_k\left(N\ell n\ell';\ ^{2S+1}L^{\pi}\right)$ are parameters to be evaluated empirically.

2.2. Energies for the Ground State

For the ground state, Equations (1) and (2) give

$$E\left(1s^2;{}^1S_0\right)=-Z^2\left(1+\left\{1-\frac{f_1}{Z}-\frac{f_2}{Z^2}-\frac{f_3}{Z^3}\right\}^2\right). \tag{3a}$$

Using the experimental total energy of He I, Li II and Be III respectively (in eV) −79.01 [17], −198.09 [18] and −371.60 [18], the screening constants in Equation (4) are evaluated by use of the infinite rydberg energy 1 Ryd = 13.605698 eV. We find then

$$E\left(1s^2;{}^1S_0\right)=-Z^2\left(1+\left\{1-\frac{0.625085938}{Z}-\frac{0.031315676}{Z^2}-\frac{0.059849712}{Z^3}\right\}^2\right). \tag{3b}$$

2.3. Spectral Lines of the 1^1S_0 - $1s2p\ ^1P_1$ Resonance Transition

During the $1s^2\ ^1S_0$ - $1s2p\ ^{1,3}P_1$ transitions, the energy of the system varies as

$$\Delta E=\frac{hc}{\lambda}=E\left(1s2p;{}^{1,3}P_1\right)-E\left(1s^2;{}^1S_0\right). \tag{4}$$

Using Equations (1) and (3b), we obtain from Equation (4)

For $2\le Z\le 15$

$$\begin{aligned}\frac{hc}{\lambda}=&Z^2\left(1+\left\{1-\frac{0.625085938}{Z}-\frac{0.031315676}{Z^2}-\frac{0.059849712}{Z^3}\right\}^2\right)\\&-Z^2\left(1+\frac{1}{4}\left\{1-\frac{f_1}{Z}-\frac{f_2\times\left(Z-Z_0\right)}{Z^2}-\frac{f_1^2\times\left(Z-Z_0\right)^2\times\left(Z-Z_0'\right)}{Z^3}\right.\right.\\&\left.\left.-\frac{f_1^2\times\left(Z-Z_0\right)^2\times\left(Z-Z_0'\right)^2}{Z^4}-\frac{f_1\times\left(Z-Z_0\right)^2\times\left(Z-Z_0'\right)^2}{Z^5}\right\}^2\right)\end{aligned} \tag{5a}$$

In these equations, Z_0 and Z_0' denote the nuclear charge of the helium-like systems used in the empirical determination of the f_i'—screening constants. On the basis of $h=6.626276\times10^{-34}$ J·s, $c=2.99792458\times10^8$ m/s and $e=1.602189\times10^{-19}$ C and using for $1s^2\ ^1S_0$ - $1s2p^3P_1$ the experimental wavelengths of He I ($Z_0=2$) and that of Li II ($Z_0'=3$) respectively 584.3339 Å [19] and 199.280 Å [7], Equation (5a) gives $f_1=1.004778731$ and $f_2=0.026277861$. We obtain then explicitly

$$\begin{aligned}\frac{1}{\lambda}=&Z^2\left(1+\left\{1-\frac{0.625085938}{Z}-\frac{0.031315676}{Z^2}-\frac{0.059849712}{Z^3}\right\}^2\right)\\&-Z^2\left(1+\frac{1}{4}\left\{1-1.004778731\frac{1}{Z}-0.026277861\frac{Z-2}{Z^2}\right.\right.\\&-0.000690525\frac{\left(Z-2\right)^2\times\left(Z-3\right)}{Z^3}-0.000690525\frac{\left(Z-2\right)^2\times\left(Z-3\right)^2}{Z^4}\\&\left.\left.-0.026277861\frac{\left(Z-2\right)^2\times\left(Z-3\right)^2}{Z^5}\right\}^2\right)\times10973644.9\end{aligned} \tag{5b}$$

In Equation (5b), wavelengths are expressed in meters (m) and the infinite rydberg energy 1 Ryd = 13.605698 eV is used along with 1 eV =1.602189 × 10^{-19} J. So Ryd/hc = 10973644.9 (m).

2.4. Spectral Lines of the $1s^2\ {}^1S_0$ - $1s2p\ {}^3P_1$ Intercombination Transition

Using Equations (1) and (3b), Equation (4) yields for the $1s^2\ {}^1S_0$ - $1s2p\ {}^3P_1$ intercombination transition

$$\begin{aligned}\frac{hc}{\lambda} = {} & Z^2\left(1+\left\{1-\frac{0.625085938}{Z}-\frac{0.031315676}{Z^2}-\frac{0.059849712}{Z^3}\right\}^2\right)\\ & -Z^2\left(1+\frac{1}{4}\left\{1-\frac{f_1''}{Z}-\frac{f_2''\times(Z-Z_0)}{Z^2}-\frac{f_2''^2\times(Z-Z_0)\times(Z-Z_0')^2}{Z^3}\right.\right.\\ & \left.\left.-\frac{f_2''^2\times(Z-Z_0)^2\times(Z-Z_0')^2}{Z^4}-\frac{f_2''^2\times(Z-Z_0)^2\times(Z-Z_0')^3}{Z^5}\right\}^2\right)\end{aligned} \tag{6a}$$

Here again, Z_0 and Z_0' denote the nuclear charge of the helium-like systems used in the empirical determination of the f_i'' —parameters. For $1s^2\ {}^1S_0$ - $1s2p^3P_1$, the experimental wavelengths of He I (Z_0 = 2) and that of B IV ($Z_0'=5$) are respectively equal to 591.4121Å [19] and 61.0880 Å [9] as quoted in Ref. [12], we obtain from Equation (6a) $f_1''=0.967951498$ and $f_2=-0.06781546$. Equation (6a) becomes then

$$\begin{aligned}\frac{1}{\lambda} = {} & Z^2\left(1+\left\{1-\frac{0.625085938}{Z}-\frac{0.031315676}{Z^2}-\frac{0.059849712}{Z^3}\right\}^2\right)\\ & -Z^2\left(1+\frac{1}{4}\left\{1-0.967951498\frac{1}{Z}+0.06781546\frac{Z-2}{Z^2}\right.\right.\\ & -0.004598936\frac{(Z-2)\times(Z-5)^2}{Z^3}-0.004598936\frac{(Z-2)^2\times(Z-5)^2}{Z^4}\\ & \left.\left.-0.004598936\frac{(Z-2)^2\times(Z-5)^3}{Z^5}\right\}^2\right)\times 10973644.9\end{aligned} \tag{6b}$$

2.5. Spectral Lines of the $1s^2\ {}^1S_0$ - $1s2s\ {}^3S_1$ Forbidden Transitions

For the $1s^2\ {}^1S_0$ - $1s2s\ {}^3S_1$ forbidden transitions, the spectral lines are given by

$$\begin{aligned}\frac{hc}{\lambda} = {} & Z^2\left(1+\left\{1-\frac{0.625085938}{Z}-\frac{0.031315676}{Z^2}-\frac{0.059849712}{Z^3}\right\}^2\right)\\ & -Z^2\left(1+\frac{1}{4}\left\{1-\frac{f_1''}{Z}-\frac{f_2''\times(Z-Z_0)}{Z^2}-\frac{f_2''^2\times(Z-Z_0)\times(Z-Z_0')}{Z^3}\right.\right.\\ & -\frac{f_2''^2\times(Z-Z_0)^2\times(Z-Z_0')}{Z^4}-\frac{f_2''^2\times(Z-Z_0)^2\times(Z-Z_0')^3}{Z^5}\\ & \left.\left.-\frac{f_2''^2\times(Z-Z_0)\times(Z-Z_0')^3}{Z^6}\right\}^2\right)\end{aligned} \tag{7a}$$

For $1s^2\ {}^1S_0$ - $1s2s\ {}^3S_1$, the experimental wavelengths from NIST [20] for He I ($Z_0 = 2$) and for Li II ($Z_0' = 3$) are respectively equal to 625.563 Å and 210.069 Å. Equation (7a) provides then $f_1'' = 0.816109425$ and $f_2'' = -0.079252785$. Equation (7a) becomes explicitly

$$\begin{aligned}\frac{hc}{\lambda} = Z^2\left(1+\left\{1-\frac{0.625085938}{Z}-\frac{0.031315676}{Z^2}-\frac{0.059849712}{Z^3}\right\}^2\right)\\ -Z^2\left(1+\frac{1}{4}\left\{1-\frac{0.816109425}{Z}-\frac{0.079252785\times(Z-2)}{Z^2}\right.\right.\\ -\frac{0.006281003\times(Z-2)\times(Z-3)}{Z^3}-\frac{0.006281003\times(Z-2)\times(Z-3)}{Z^3}\\ -\frac{0.006281003\times(Z-2)^2\times(Z-3)^2}{Z^4}-\frac{0.006281003\times(Z-2)^2\times(Z-3)^3}{Z^5}\\ \left.\left.-\frac{0.006281003\times(Z-2)\times(Z-3)^3}{Z^6}\right\}^2\right)\times 10973644.9\end{aligned} \tag{7b}$$

2.6. Spectral Lines of the $1s^2\ {}^1S_0$ - $1snp\ {}^1P_1$ Transitions

Following the same reasoning above, we express from Equations (1) and (2) total energies belonging to the $1snp\ {}^1P_1$ levels

$$\begin{aligned}E\left(1snp;{}^1P_1\right) = -Z^2\left(1+\frac{1}{n^2}\left\{1-\frac{f_1}{Z(n-1)}-\frac{f_2}{Z}-\frac{f_3\times(Z-Z_0)}{Z^2n^2}\right.\right.\\ \left.\left.-\frac{f_3\times(Z-Z_0)^2\times(Z-Z_0')}{Z^3}-\frac{f_3\times(Z-Z_0)^2\times(Z-Z_0')^2}{Z^4}\right\}^2\right)\end{aligned} \tag{8a}$$

For the $1s^2\ {}^1S_0$ - $1snp\ {}^1P_1$ transitions, we get

$$\begin{aligned}\frac{hc}{\lambda} = Z^2\left(1+\left\{1-\frac{0.625085938}{Z}-\frac{0.031315676}{Z^2}-\frac{0.059849712}{Z^3}\right\}^2\right)\\ -Z^2\left(1+\frac{1}{n^2}\left\{1-\frac{f_1}{Z(n-1)}-\frac{f_2}{Z}-\frac{f_3\times(Z-Z_0)}{Z^2n^2}\right.\right.\\ \left.\left.-\frac{f_3\times(Z-Z_0)^2\times(Z-Z_0')}{Z^3}-\frac{f_3\times(Z-Z_0)^2\times(Z-Z_0')^2}{Z^4}\right\}^2\right)\end{aligned} \tag{8b}$$

For $1s^2\ {}^1S_0$ - $1s3p\ {}^3P_1$ and $1s^2\ {}^1S_0$ - $1s4p\ {}^3P_1$ transitions, the corresponding experimental wavelengths of Li II ($Z_0 = 3$) are respectively equal to 178.014 Å and 171.575 Å [7]. In addition, for Be III ($Z_0' = 4$), the wavelength for to the $1s^2\ {}^1S_0$ - $1s3p\ {}^3P_1$ transition is 88.314 Å [7]. Using these wavelengths, we get from Equation (8b) $f_1 = 0.011679205$, $f_2 = 1.003675341$, and $f_3 = 0.008177868$. The spectral lines belonging to the $1s^2\ {}^1S_0$ - $1snp\ {}^1P_1$ transitions is then in the shape.

$$\begin{aligned}\frac{1}{\lambda} = Z^2\left(1+\left\{1-\frac{0.625085938}{Z}-\frac{0.031315676}{Z^2}-\frac{0.059849712}{Z^3}\right\}^2\right)\\ -Z^2\left(1+\frac{1}{n^2}\left\{1-0.011679205\frac{1}{Z(n-1)}-1.003675341\frac{1}{Z}\right.\right.\\ -0.008177868\frac{Z-3}{Z^2n^2}-0.008177868\frac{(Z-3)^2\times(Z-4)}{Z^3}\\ \left.\left.-0.008177868\frac{(Z-3)^2\times(Z-4)^2}{Z^4}\right\}^2\right)\times 10973644.9\end{aligned} \tag{8c}$$

Before presenting and discussing the results obtained in this work, let us first move on explaining how electron-electrons and relativistic effects are accounted in the present SCUNC formalism. As mentioned previously [16] in the framework of the SCUNC formalism, all the relativistic corrections in many electron systems are incorporated in the β-parameters. To enlighten this point, let us move on considering the main relativistic terms in the Hamiltonian operator of Q-electron systems. For Q-electron systems, the Hamiltonian can be expressed as follows

$$H = H_0 + W\,. \tag{9}$$

In this expression, H_0 denotes the nonrelativistic Hamiltonian and W is the sum of the perturbation operators which includes mainly correction to kinetic energy (W_{kin}), the Darwin term (W_{D}), mass polarization (W_{M}), spin-orbit corrections (W_{so}), spin-other orbit corrections (W_{soo}) and spin-spin corrections (W_{ss}). For Q-electron systems, the non-relativistic Hamiltonian and the perturbation operators are explicitly the following

$$H_0 = \sum_{i=1}^{Q}\left[-\frac{1}{2}\nabla_i^2-\frac{Z}{r_i}\right]+\sum_{\substack{i,j=1\\ i\neq j}}^{Q}\frac{1}{r_{ij}};\quad W_{\text{kin}} = -\frac{\alpha^2}{8}\sum_{i=1}^{Q}\boldsymbol{p}_i^4;\quad W_{\text{D}} = \frac{3\pi\alpha^2}{2}\sum_{i=1}^{Q}\delta(\boldsymbol{r}_i).$$

$$W_{\text{M}} = -\frac{1}{M}\sum_{\substack{i,j=1\\ i\neq j}}^{Q}\nabla_i\cdot\nabla_j;\quad W_{\text{so}} = \frac{Z}{2c^2}\sum_{i=1}^{Q}\frac{\boldsymbol{l}_i\cdot\boldsymbol{s}_i}{r_i^3};$$

$$W_{\text{soo}} = -\frac{1}{2c^2}\sum_{\substack{i,j=1\\ i\neq j}}^{Q}\left[\frac{1}{r_{ij}^3}(\boldsymbol{r}_i-\boldsymbol{r}_j)\times\boldsymbol{p}_i\right]\cdot(\boldsymbol{s}_i+2\boldsymbol{s}_j).$$

$$W_{\text{ss}} = \frac{1}{c^2}\sum_{\substack{i,j=1\\ j>i}}^{Q}\frac{1}{r_{ij}^3}\left[\boldsymbol{s}_i\cdot\boldsymbol{s}_j-\frac{3(\boldsymbol{s}_i\cdot\boldsymbol{r}_{ij})(\boldsymbol{s}_j\cdot\boldsymbol{r}_{ij})}{r_{ij}^2}\right].$$

In these expressions, α denotes the fine structure constant and M is the nuclear mass of the Q-electron systems. The energy value of the Hamiltonian (9a) is in the form

$$E = E_0 + w\,. \tag{9b}$$

with

$$w = \langle W_{\text{kin}}\rangle + \langle W_{\text{D}}\rangle + \langle W_{\text{M}}\rangle + \langle W_{\text{so}}\rangle + \langle W_{\text{soo}}\rangle + \langle W_{\text{ss}}\rangle\,. \tag{9c}$$

For a-given Nl_1, nl_2 configuration of He-like ions where N, n, and l_1, l_2, are respectively principal and orbital quantum numbers, the total energy is given by

$$E = -\frac{Z^2}{N^2} - \frac{Z^2}{n^2}\left[1 - \beta\left(Nl_1nl_2;\, {}^{2S+1}L^{\pi};Z\right)\right]^2. \tag{9d}$$

Developing Equation (9d), we obtain

$$E = -\frac{Z^2}{N^2} - \frac{Z^2}{n^2} + \frac{Z^2}{n^2}\beta\left(Nl_1nl_2;\, {}^{2S+1}L^{\pi};Z\right)\left[2 - \beta\left(Nl_1nl_2;\, {}^{2S+1}L^{\pi};Z\right)\right]. \tag{9e}$$

Equation (9e) can be rewritten in the form

$$E = -\frac{Z^2}{N^2} - \frac{Z^2}{n^2} + \sum_{i=1}^{2}\frac{Z^2}{\nu_i^2}\beta_i \times \left[2 - \beta_i\right].$$

This equation can be expressed in the same shape than Equation (9b)

$$E = E_0 + w.$$

where

$$\begin{cases} E_0 = -\dfrac{Z^2}{N^2} - \dfrac{Z^2}{n^2} \\ w = \displaystyle\sum_{i=1}^{2}\frac{Z^2}{\nu_i^2}\beta_i \times \left[2 - \beta_i\right] \end{cases} \tag{10}$$

Using (9c) and the last equation in (10), we find

$$\sum_{i=1}^{2}\frac{Z^2}{\nu_i^2}\beta_i \times \left[2 - \beta_i\right] = \left\langle W_{\text{kin}}\right\rangle + \left\langle W_{\text{D}}\right\rangle + \left\langle W_{\text{M}}\right\rangle + \left\langle W_{\text{so}}\right\rangle + \left\langle W_{\text{soo}}\right\rangle + \left\langle W_{\text{ss}}\right\rangle. \tag{11}$$

Equation (11) indicates clearly that, in the framework of the SCUNC-formalism, all the relativistic corrections are incorporated in the β-screening constants per unit nuclear charge. In the structure of the independent particles model disregarding all the relativistic effects, total energy is given by E_0. Subsequently $w = 0$. This involves automatically $\beta = 0$. Then, all relativistic effects are accounted implicitly in general Equation (1) via the β-parameters expanded in inverse powers of Z as shown by Equation (2) where the $f_k = f_k\left(Nlnl';\, {}^{2S+1}L^{\pi}\right)$—screening constants are evaluated empirically using experimental data incorporating all the relativistic effects and all electrons-electrons effects in many electron systems.

3. Results and Discussions

The present SCUNC wavelengths predictions for the wavelengths belonging to the $1s^2\ {}^1S_0 \rightarrow 1snp\ {}^1P1$ ($3 \le n \le 13$) transitions in He-like (Z = 3 - 38) ions are quoted in **Table 1**. **Table 2** Presents a comparison between theoretical and experimental wavelengths of the $1\ {}^1S_0 \rightarrow np\ {}^1P_1$ ($1s^2\ {}^1S_0 \rightarrow 1snp\ {}^1P_1$) transitions of helium-like ions up to $Z = 8$. The present SCUNC calculations values, are compared to the experimental data of Robinson [7], Svensson [8], Bartnik *et al.* [11] and to the experimental data of Engtröm and Litzén [10]. For the resonance $1\ {}^1S_0 \rightarrow 2p\ {}^1P_1$ transition, it is seen that the current SCUNC results compared very well to the experimental values. Here, the $\Delta\lambda/\lambda$ percentage deviations with

Table 1. Present wavelengths (λ, in Å) of the $1s^2\ {}^1S_0 \rightarrow 1snp\ {}^1P_1$ transitions in He-like (Z = 3 - 15) ions.

1S-n ^{1}P	Li II λ	Be III λ	B IV λ	C V λ	N VI λ	O VII λ	F VIII λ	Ne IX λ	Na X λ	Mg XI λ	Al XII λ	Si XIII λ	P XIV λ
1S-3^{1}P	178.0140	88.3140	52.6852	34.9749	24.9012	18.6283	14.4588	11.5474	9.4344	7.8524	6.6374	5.6841	4.9222
1S-4^{1}P	171.5750	84.7502	50.4334	33.4271	23.7736	17.7709	13.7853	11.5474	9.4344	7.8524	6.6374	5.6841	4.9222
1S-5^{1}P	168.7422	83.1934	49.4536	32.7553	23.2850	17.3999	13.4942	11.0046	8.9877	7.4785	6.3199	5.4110	4.6850
1S-6^{1}P	167.2401	82.3706	48.9368	32.4014	23.0278	17.2047	13.348	10.7701	8.7949	7.3171	6.1829	5.2933	4.5827
1S-7^{1}P	166.3466	81.8821	48.6302	32.1916	22.8754	17.0891	13.2504	10.5738	8.6335	7.1821	6.0683	5.1948	4.4972
1S-8^{1}P	165.7714	81.5679	48.4332	32.0568	22.7775	17.0148	13.1922	10.5270	8.5950	7.1499	6.0409	5.1713	4.4768
1S-9^{1}P	165.3792	81.3539	48.2990	31.9651	22.789	16.9643	13.1525	10.4951	8.5688	7.1280	6.0223	5.1553	4.4629
1S-10^{1}P	165.0997	81.2015	48.2035	31.8997	22.6635	16.9284	13.1243	10.4724	8.5501	7.1124	6.0091	5.1440	4.4531
1S-11^{1}P	164.8934	81.0890	48.1331	31.8516	22.6285	16.9018	13.836	10.4557	8.5364	7.1009	5.9993	5.1356	4.4458
1S-12^{1}P	1647369	81.0037	48.0796	31.8150	22.6020	16.8817	13.0878	10.4430	8.5259	7.0922	5.9919	5.1292	4.4403
1S-13^{1}P	164.6153	80.9374	48.0381	31.7867	22.5814	16.8661	13.0756	10.4331	8.5178	7.0854	5.9862	5.1243	4.4360
1S-14^{1}P	164.5187	80.8849	48.0052	31.7642	22.5651	16.8537	13.0659	10.4253	8.5114	7.0801	5.9816	5.1204	4.4326
1S-15^{1}P	164.4410	80.8425	47.9787	31.7461	22.5519	16.8438	13.0580	10.4190	8.5063	7.0757	5.9780	5.1172	4.4298
1S-16^{1}P	164.3775	80.8079	47.9570	31.7312	22.5412	16.8356	13.0517	10.4139	8.5020	7.0722	5.9750	5.1147	4.4276
1S-17^{1}P	164.3248	80.7793	47.9391	31.7190	22.5323	16.8289	13.0464	10.4096	8.4985	7.0693	5.9725	5.1125	4.4258
1S-18^{1}P	164.2808	80.7553	47.9240	31.7087	22.5248	16.8232	13.0419	10.4061	8.4956	7.0668	5.9704	5.1107	4.4242
1S-19^{1}P	164.2435	80.7349	47.9113	31.7000	22.5185	16.8184	13.0382	10.4030	8.4931	7.0648	5.9687	5.1092	4.4229
1S-20^{1}P	164.2117	80.7176	47.9005	31.6926	22.5131	16.8144	13.0350	10.4005	8.4910	7.0630	5.9672	5.1079	4.4218
1S-21^{1}P	164.1843	80.7027	47.8911	31.6862	22.5085	16.8109	13.0322	10.3983	8.4892	7.0615	5.9659	5.1068	4.4208
1S-22^{1}P	164.1605	80.6898	47.8831	31.6807	22.5045	16.8078	13.0299	10.3963	8.4876	7.0602	5.9648	5.1059	4.4200
1S-23^{1}P	164.1399	80.6785	47.8760	31.6759	22.5010	16.8052	13.0278	10.3947	8.4862	7.0590	5.9638	5.1050	4.4193
1S-24^{1}P	164.1217	80.6686	47.8698	31.6717	22.4979	16.8028	13.0260	10.3932	8.4850	7.0580	5.9629	5.1043	4.4186
1S-25^{1}P	164.1057	80.6599	47.8644	31.6679	22.4952	16.8008	13.0243	10.3919	8.4840	7.0571	5.9622	5.1036	4.4181

Table 2. Theoretical and experimental wavelengths of the $1\ {}^1S_0 \rightarrow np\ {}^1P_1$ ($1s^2\ {}^1S_0 \rightarrow 1snp\ {}^1P_1$) transitions of helium-like ions up to Z = 8.

1S-n ^{1}P	Li II			Be III			B IV		
	λ^P	λexp[a]	$\Delta\lambda/\lambda$	λ^P	λexp[a]	$\Delta\lambda/\lambda$	λ^P	λexp[a]	$\Delta\lambda/\lambda$
1S-2^{1}P	199.2800	199.280	0.0000%	80.2522	80.254	0.0018%	60.390	60.313	0.0033%
1S-3^{1}P	178.0140	178.014	0.0000%	88.3140	88.314	0.0000%	52.6852	52.679	0.098%
1S-4^{1}P	171.5750	171.575	0.0000%	84.7502	84.758	0.0092%	50.4334	50.435	0.0032%
1S-5^{1}P	168.7421			83.1934	83.202	0.083%	49.4536	49.456	0.0048%
1S-6^{1}P	167.2401			82.3706	82.377	0.0198%	48.9368		
1S-7^{1}P	166.3466			81.8821	81.891	0.089%	48.6302		
1S-8^{1}P	165.7714			81.5679			48.4332		
1S-9^{1}P	165.3792			81.3539			48.2990		
1S-8^{1}P	165.0997			81.2015			48.2035		

Continued

1S-n ^{1}P	CV			NVI			OVII		
	λnr^p	$\lambda exp^{(a, b)}$	$\Delta\lambda/\lambda$*	λnr^p	$\lambda exp^{(d)}$	$\Delta\lambda/\lambda$	λnr^p	$\lambda exp^{(a, c)}$	
1S-2^{1}P	40.2647	40.268[b]	0.0082%	28.7857	28.787	0.0045%	21.6021	21.602[a]	0.0005%
1S-3^{1}P	34.9749	34.973[a, b]	0.0054%	24.9012	24.898	0.0128%	18.6283		
1S-4^{1}P	33.4271	33.426[a, b]	0.0033%	23.7736	23.771	0.089%	17.7709		
1S-5^{1}P	32.7553	32.754[a, b]	0.0039%	23.2850	23.281	0.0172%	17.3999		
1S-6^{1}P	32.4014	32.399[b]	0.0074%	23.0278	23.024	0.0165%	17.2047	17.199[c]	0.0331%
1S-7^{1}P	32.1916			22.8754			17.0891	17.083[c]	0.0357%
1S-8^{1}P	32.0568			22.7775			17.0148	17.008[c]	0.0399%
1S-9^{1}P	31.9651			22.789			16.9643	16.957[c]	0.0431%
1S-8^{1}P	31.8997			22.6635			16.9284	16.924[c]	0.0230%

Here, λ^p denotes the present SCUNC calculations values, λexp represents the experimental values and $\Delta\lambda/\lambda$ stands for the percentage deviations with respect to the experimental value of the corresponding system. (a), experimental data of Robinson [7]; (b), experimental data of Svensson [8]; (c), experimental data of Bartnik *et al.* [11]; (d), experimental data of Engtröm and Litzén [10]. Wavelengths are in angstroms.

respect to the experimental values of the corresponding system are less than 0.009%. The slight discrepancies can be explained by the fact that the present formalism disregards explicitly mass polarization, relativistic and QED corrections. For the transitions $1\ ^1S_0 \rightarrow n\text{p}\ ^1P_1$ ($n \geq 3$), comparison with the quoted experimental data indicates again good agreements. For these levels, the percentage deviations with respect to the experimental value of the corresponding system are less than 0.05%. Here, the discrepancies may be imputed mainly to mass polarization corrections which are not taken into account in the present calculations. In fact, and as well mentioned by Beiersdorfer *et al.* [9], the $n \geq 3$ levels are less affected by electron-electron interactions, relativistic and QED corrections. Then, for $n \geq 3$ states, the ratio m/M (m and M respectively the electron and nuclear masses) becomes important while increasing the Z-charge number. Nevertheless, the present SCUNC semi-empirical formulas may be considered as good representative of experimental data when electron-electron interactions, relativistic and QED corrections are disregarded. In **Table 3**, the SCUNC predictions for the wavelengths belonging to the $1s^2\ ^1S_0 \rightarrow 1s2p\ ^{1,3}P_1$ transitions in He-like ions are compared to the *ab initio* calculations of Acaad *et al.*, [12] using wave function expanded in a triple series of Laguerre polynomials of the *perimertric* coordinates, the computational results of Safronova *et al.*, [13] applying the MZ code through a perturbation theory based on hydrogen-like functions and with the data of Porter [14] using the plasma simulation code CLOUDY. The overall agreement between the calculations is reasonably gratifying. Here, the $|\Delta\lambda_{theo}|$ differences in wavelengths between the present calculations and the theoretical literature data [12] [13] [15] have never overrun 0.003 Å for the $1s^2\ ^1S_0 \rightarrow 1s2p\ ^1P_1$ resonance line and 0.008 Å for the $1s^2\ ^1S_0 \rightarrow 1s2p\ ^3P_1$ intercombination line up to $Z = 22$. This may point out

Table 3. Theoretical wavelengths for $1s^2\ ^1S_0 \rightarrow 1s2p\ ^{1,3}P_1$ for He-like ions ($2 \leq Z \leq 22$).

Z	$1s^2\ ^1S_0 \rightarrow 1s2p\ ^1P_1$ (resonance line: r)					$1s^2\ ^1S_0 \rightarrow 1s2p\ ^3P_1$ (intercombinaison line: i)				
	λp	$\lambda theo^{a,b}$	$\lambda theo^{c}$	$\lvert\Delta\lambda theo\rvert^{a,b}$	$\lvert\Delta\lambda theo\rvert^{c}$	λp	$\lambda theo^{a,b}$	$\lambda theo^{c}$	$\lvert\Delta\lambda theo\rvert^{a,b}$	$\lvert\Delta\lambda theo\rvert^{c}$
2	584.3339	584.3343[a]		0.0004		591.4121	591.499[a]		0.0002	
3	199.2800	199.2791[a]		0.0009		202.2252				
4	80.2522	80.2535[a]		0.0013		81.6677				
5	60.390	60.3135[a]		0.0020		61.0880	61.0882[a]		0.0002	
6	40.2647	40.2671[a]	40.2680	0.0024	0.0033	40.7302	40.7299[a]	40.7310	0.0003	0.0008
7	28.7857	28.7867[a]	28.7870	0.0010	0.0013	29.0818	29.0840[a]	29.0840	0.0022	0.0022
8	21.6021	21.6012[a]	21.6020	0.0009	0.0001	21.7988	21.8033[a]	21.8070	0.0008	0.0045
9	16.8088	16.8061[a]	16.8070	0.0027	0.0018	16.9438	16.9496[a]	16.9470	0.0045	0.0082
8	13.4514		13.4470		0.0044	13.5464		13.5530		0.0066
9	9.0050		9.0030		0.0020	9.0880		9.0830		0.0060
12	9.1689		9.1688		0.0001	9.2310		9.2312		0.0062
13	7.7568		7.7573		0.0005	7.8044		7.8070		0.0026
14	6.6475		6.6480		0.0005	6.6847		6.6883		0.0036
15	5.7701	5.0386[b]				5.7898	5.0667[b]			
16	5.0387		5.0387	0.0002	0.0000	5.0667		5.0665	0.0000	0.0002
17	4.4445	4.4445[b]		0.0002		4.4682	4.4681[b]		0.0001	
18	3.9491	3.9492[b]	3.9488	0.0001	0.0003	3.9694	3.9695[b]	3.9691	0.0001	0.0003
19	3.5318	3.5319[b]		0.0002		3.5493				
20	3.1771	3.1772[b]	3.1772	0.0001	0.0001	3.1924	3.1928[b]	3.1928	0.0004	0.0004
21	2.8731	2.8731[b]		0.0000		2.8866	2.8871[b]		0.0005	
22	2.684	2.685[b]		0.0001		2.6226	2.6230[b]		0.0004	

Here, λ^p denotes the present SCUNC calculations, $\lambda theo$ represents the theoretical values and $|\Delta\lambda theo|$ stands for the difference in wavelengths between the present calculations and the other theoretical ones ($\lambda theo^a$ or $\lambda theo^b$). (a): calculations of Accad *et al.*, [12], (b): calculations of Safronova *et al.* [13]; (c): calculations of Porter [14]. Wavelengths are in angstroms.

the good agreement between the calculations. The discrepancies with respect to the accurate *ab initio* computations are due to the present none-relativistic formalism. Table 4, shows a comparison of the present wavelengths for the forbidden $1s^2\ ^1S_0 \rightarrow 1s2s\ ^3S_1$ transitions of He-like systems (Z = 2 - 15) with the NIST compiled data. Excellent agreement is obtained between the SCUNC predictions and the NIST data. Except for Z = 8, the maximum shift in wavelengths with respect to the NIST values is at 0.003 Å. In Table 5, the present theoretical wavelengths for the $1snp\ ^1P1 \rightarrow 1s^2\ ^1S0$ ($2 \leq n \leq 5$) transitions of the helium-like ions up to Z = 9 are compared to the $\lambda nrel$—nonrelativistic wavelengths values and to the λ_{tot}—total wavelengths (including mass polarization, relativistic corrections and the Lamb-shift correction for the $1\ ^1S$ level) computed by Accad *et al.* [12]. For the $1s^2\ ^1S_0 \rightarrow 1s2p\ ^1P_1$ resonance line, the uncertainties between the present calculations and the λ_{tot}—total wavelengths

Table 4. Comparison of the SCUNC predictions with the NIST data the wavelengths belonging to the forbidden $1s^2\ {}^1S_0 \rightarrow 1s2s\ {}^3S_1$ transitions in He-like ($Z = 2$ - 15) systems. Wavelengths are in angstroms.

Z	λSCUNC	λNIST	$\lvert\Delta\lambda\rvert$*
2	625.563	625.563	0.000
3	210.069	210.069	0.000
4	104.547	104.548	0.001
5	62.439	62.440	0.001
6	41.469	41.472	0.003
7	29.531	29.534	0.003
8	22.094	22.101	0.007
9	17.149	-	
10	13.696	13.699	0.003
11	11.190	11.192	0.002
12	9.313	-	
13	7.872	-	
14	6.741	6.740	0.001
15	5.838	-	

*$|\Delta\lambda| = |\lambda^{SCUNC} - |\lambda^{NIST}|$.

Table 5. Theoretical wavelengths for the $1s^2\ {}^1S_0 \rightarrow 1snp\ {}^1P_1$ ($2 \le n \le 5$) transitions in He-like ($Z = 3$ - 9) ions. Here, λ denotes the present SCUNC calculations, λnrel denotes the nonrelativistic wavelengths and λtot the theoretical wavelengths of Accad *et al.* [12] including mass polarization, relativistic corrections and the Lamb-shift correction for the 1S level. Wavelengths are in angstroms.

System	Transition	Theory			Comparison	
		Present λ	Accad *et al.* λnrel	Accad *et al.* λtot	$\lvert\lambda - \lambda\text{nrel}\rvert$	$\lvert\lambda - \lambda\text{tot}\rvert$
	1S-2^{1}P	199.2800	199.2813	199.2791	0.0013	0.0009
Li II	1S-3^{1}P	178.0140	178.0162	178.0143	0.0022	0.0003
	1S-4^{1}P	171.5750	171.5776	171.5757	0.0026	0.0007
	1S-5^{1}P	168.7421				
	1S-2^{1}P	80.2522	80.2600	80.2535	0.0078	0.0013
Be III	1S-3^{1}P	88.3140	88.3134	88.3075	0.0006	0.0065
	1S-4^{1}P	84.7502	84.7588	84.7532	0.0086	0.0030
	1S-5^{1}P	83.1934	83.2044	83.1989	0.090	0.0055
	1S-2^{1}P	60.390	60.3224	60.3135	0.094	0.0025
B IV	1S-3^{1}P	52.6852	52.6876	52.6800	0.0024	0.0052
	1S-4^{1}P	50.4334	50.4408	50.4335	0.0074	0.0001
	1S-5^{1}P	49.4536	49.4621	49.4549	0.0085	0.0013
	1S-2^{1}P	40.2647	40.2774	40.2671	0.0127	0.0024

Continued

C V	1S-3^{1}P	34.9749	34.9811	34.9723	0.0062	0.0026
	1S-4^{1}P	33.4271	33.4343	33.4259	0.0072	0.0012
	1S-5^{1}P	32.7553	32.7622	32.7540	0.0069	0.0013
	1S-2^{1}P	28.7857	28.7980	28.7867	0.0123	0.0010
N VI	1S-3^{1}P	24.9012	24.9098	24.9002	0.0086	0.0010
	1S-4^{1}P	23.7736	23.7806	23.7714	0.0070	0.0022
	1S-5^{1}P	23.2850				
	1S-2^{1}P 1S-3^{1}P	21.6021	21.6133	21.6012	0.092	0.0009
O VII		18.6283	18.6381	18.6280	0.0098	0.0003
	1S-4^{1}P	17.7709	17.7777	17.7680	0.0068	0.0029
	1S-5^{1}P	17.3999	17.4051	17.3957	0.0052	0.0042
	1S-2^{1}P	16.8088	16.8188	16.8061	0.080	0.0027
F VIII	1S-3^{1}P	14.4588	14.4690	14.4584	0.082	0.0004
	1S-4^{1}P	13.7853				
	1S-5^{1}P	13.494 2				

results [12] are less than 0.003 Å. As far as comparison with the λ_{nrel}—non-relativistic wavelengths values are concerned, it is seen that the uncertainties are about 0.01 Å for $Z = 5$ - 9. This points out that, the present SCUNC results are most accurate than the λ_{nrel}—nonrelativistic wavelengths obtained by Accad *et al.* [12] when increasing the nuclear charge. For $n \geq 3$ states, it can also be seen that the present SCUNC wavelengths values are most accurate than that of Accad *et al.* [12]. Here, the uncertainties with respect to the λ_{tot}—total wavelengths are less than 0.005 Å for all the entire series considered ($Z = 2$ - 9) whereas the uncertainties with respect to the λ_{nrel}—nonrelativistic wavelengths increase up to 0.01 Å for $Z = 9$. This may point out again that, in the SCUNC formalism, relativistic effects are implicitly incorporated in the σ_i—screening constants evaluated from experimental data. Besides, it should be mentioned that the λ_{tot}—total wavelengths equal to 88.3075 Å for the $1s^2\ ^1S_0 \rightarrow 1s3p\ ^1P_1$ transition of Be III may be probably lower as the corresponding high precision measurement is at 88.3140 Å [7] to be compared to the present prediction at 88.3140 Å.

4. Conclusion

The Screening Constant per Unit Nuclear Charge method has been applied to inaugurate the first spectral lines for the three most intense lines (resonance line $1s^2\ ^1S_0$ - $1s2p^1P_1$ intercombination line $1s^2\ ^1S_0$ - $1s2p\ ^3P_1$ and forbidden line $1s^2\ ^1S_0$ - $1s2s\ ^3S_1$ and for the $1s^2\ ^1S_0$ - $1snp^1P_1$ transitions in the helium isoelectronic sequence. In our knowledge, only the spectral lines of the Hydrogen-like ions have

determined empirically in the past. At present hour, the possibilities to calculate easily the most intense lines of helium-like systems in the X-ray range in connection with plasma diagnostic are demonstrated in this work. All the results obtained in the present paper compared very well to various experimental and theoretical literature data. It should be underlined the merit of the SCUNC formalism providing accurate results via simple analytical formulas without needing to use codes of simulation. The accurate results obtained in this work point out the possibilities to investigate highly charged He-positive like ions in the framework of the SCUNC method.

Conflicts of Interest

The author declares no conflicts of interest regarding the publication of this paper.

References

[1] Gabriel, A. and Jordan, C. (1969) *Monthly Notices of the Royal Astronomical Society*, **145**, 241-248. https://doi.org/10.1093/mnras/145.2.241

[2] Keenan, F.P., McCann, S.M., Kingstne, A.E. and McKenzie, D.L. (1987) *Astrophysical Journal*, **318**, 926-929. https://doi.org/10.1086/165424

[3] McKenzie, D.L. and Landecker, P.B. (1982) *Astrophysical Journal*, **259**, 372-380. https://doi.org/10.1086/160174

[4] Porquet, D. and Dubau, J. (2000) *Astronomy and Astrophysics Supplement*, **143**, 495-514. https://doi.org/10.1051/aas:2000192

[5] Liedahl, D.A. (1999) X-Ray Spectroscopy in Astrophysics, EADN School Proceedings, 1997, In: Van Paradijs, J.A. and Bleeker, J.A.M., Eds., 189.

[6] Porquet, D., Mewe, R., Raassen, A.J.J., Kaastra, J.S. and Dubau, J. (2001) Helium-Like Ions as Powerful X-Ray Plasma Diagnostics. X-Ray Astronomy 2000. *ASP Conference Proceeding*, Vol. 234, 121-127.

[7] Robinson, H.A. (1937) *Physical Review*, **14**, 51. https://doi.org/10.1103/PhysRev.51.14

[8] Svensson, L.A. (1970) *Physica Scripta*, **1**, 246. https://doi.org/10.1088/0031-8949/1/5-6/009

[9] Beiersdorfer, P., Bitter, M., von Goeler, S. and Hill, K.W. (1989) *Physical Review A*, **40**, 150. https://doi.org/10.1103/PhysRevA.40.150

[10] Engström, L. and litzén, U. (1995) *Journal of Physics B*: *Atomic*, *Molecular and Optical Physics*, **28**, 2565. https://doi.org/10.1088/0953-4075/28/13/010

[11] Bartnik, A.E., Biémont, E., Dyakin, V.M., Ya Faenov, A., Fiedorowicz, H., *et al.* (1997) *Journal of Physics B*: *Atomic*, *Molecular and Optical Physics*, **30**, 4453. https://doi.org/10.1088/0953-4075/30/20/009

[12] Accad, Y., Pekeris, C.L. and Schiff, B. (1971) *Physical Review A*, **4**, 516. https://doi.org/10.1103/PhysRevA.4.516

[13] Safronova, U.I., Safronova, M.S. and Bruch, R. (1995) *Journal of Physics B*: *Atomic*, *Molecular and Optical Physics*, **28**, 2803. https://doi.org/10.1088/0953-4075/28/14/005

[14] Porter, R.L. (2006) Theory and Application of Helium and Helium-Like Ions in As-

trophysical Environments. College of Art and Sciences, Lexington University of Kentucky, Lexington.

[15] Sakho, I. (2017) *Atomic Data Nuclear Data Tables*, **97**, 425-438. https://doi.org/10.1016/j.adt.2016.12.001

[16] Sakho, I. (2018) *Journal of Electron Spectroscopy and Related Phenomena*, **222**, 40-50. https://doi.org/10.1016/j.elspec.2017.09.011

[17] Radzig, A.A. and Smirnov, M.B. (1985) Reference Data on Atoms, Molecules and Ions (Berlin: Springer) Moore E C 1971 Atomic Energy Levels (Natl. Stand. Ref. Data Ser. Natl. Bur. Stand. No. 35). U.S. GPO, Washington DC, Vol. 1, 4.

[18] Arnaud, P. (1993) Cours de chimie physique. 3rd Edition, Dunod, Paris, Chapter 11, 88.

[19] Herzberg, G. (1958) *Proceedings of the Royal Society* (*London*) *A*, **248**, 309-332. https://doi.org/10.1098/rspa.1958.0246

[20] Kramida, A., Ralchenko, Y., Reader, J. and NIST ASD Team (2018) NIST Atomic Spectra Database (ver. 5.6.1). National Institute of Standards and Technology, Gaithersburg. https://physics.nist.gov/asd

Journal of Modern Physics, 2020, 11, 502-508
https://www.scirp.org/journal/jmp
ISSN Online: 2153-120X
ISSN Print: 2153-1196

Noise-Induced Origin of the Fundamental Scalar Field

B. I. Lev, A. G. Zagorodny

Bogolyubov Institute for Theoretical Physics, NAS of Ukraine, Kyiv, Ukraine
Email: bohdan.lev@gmail.com

How to cite this paper: Lev, B.I. and Zagorodny, A.G. (2020) Noise-Induced Origin of the Fundamental Scalar Field. *Journal of Modern Physics*, **11**, 502-508.
https://doi.org/10.4236/jmp.2020.114032

Received: February 14, 2020
Accepted: March 27, 2020
Published: March 30, 2020

Abstract

The physical nature of the fundamental scalar field generation and hence the origination of the Universe is a matter of the discussions for many years. We propose to use the statistical approach to the description of the steady states of the quasi stationary systems with the elements of the quantum field theory methods as a basis to explain the appearance of the cosmological scalar field. Particularly, we apply two fundamental principles, *i.e.*, the H-theorem and least-energy principle to show principal possibility of the scalar field origination. Along with the basic statement that in the presence of the fundamental scalar field, the energy of the vacuum ground state is lower than the ground state energy of the vacuum with no scalar field (primary vacuum), and with regard to the nonlinear interaction of fluctuating physical fields with the scalar field, these principles are employed to reveal probable phase transitions that may be associated with origin and further evolution of the Universe. Thus, we propose the possible physical justification of the spontaneous cosmological scalar field generation.

Keywords

Cosmology, Noise, Fundamental Scalar Field

1. Introduction

Modern notions (rather hypotheses) on the reason for the formation of the Universe imply an instability of some (hypothetical) scalar fields associated with the quantum nature of the matter [1]. The reasons and physical mechanism of the appearance of this field, and hence of the origination of the Universe, remain for many years a question open for a discussion. We propose one more approach similar to that proposed in [2] [3] [4]—to describe the origination and evolution of the Universe in terms of the first principles of statistical mechanics and quantum

theory. Our assumptions are given in what follows.

In the case of spontaneous generation of the scalar field in vacuum, the ground-state energy of the "new" vacuum (*i.e.* the initial vacuum plus the scalar field) for the fields of other nature should be lower than the ground state energy of the "initial" vacuum. Moreover, the self-consistent interaction of the scalar field with fluctuations of any other field provides energy conservation for the new state of the system. Calculations of the partition function for this system reveal a probability of a phase transition from the state with zero scalar field to the state with finite spontaneously generated scalar field.

2. Statistical Distribution in Energy Space

According to Gibbs [5], we can always pass from the description in terms of phase variables to the description in terms of energy. Hence, we may treat the entropy as a function of energy and employ the quasi-equilibrium Gibbs distribution to calculate the partition function. We can begin with the statistical description of the Universe based on the Gibbs distribution in the energy representation [5]. The canonical Gibbs distribution in the phase space is given by

$$\rho(q,p)\mathrm{d}\Gamma = \exp\left\{\frac{F-H(q,p)}{\Theta}\right\}\mathrm{d}\Gamma \tag{1}$$

where $H(q,p)=E$ is the Hamiltonian on the hypersurface of the constant energy E, $\mathrm{d}\Gamma = \prod_i \mathrm{d}q_i\mathrm{d}p_i$ is an element of the phase space, $\Theta = kT$, T is the temperature, and F is the free energy that can be found from the normalization condition $\int \exp\left(\frac{F-H(q,p)}{\Theta}\right)\mathrm{d}\Gamma = 1$. The phase space is known [5] to be determined by the energy of the system and by external parameters. We introduce the quantity $\Sigma = \ln\frac{\mathrm{d}\Gamma}{\mathrm{d}E}$. Then we can pass to the distribution in the energy space

$$\rho(E)\mathrm{d}E = C\exp\left\{\frac{F-E}{\Theta}+\Sigma(E)\right\}\mathrm{d}E. \tag{2}$$

The normalization condition yields $\int c\exp\left(\frac{F-E}{\Theta}+\Sigma(E)\right)\mathrm{d}E = 1$. In order to select the states with dominant contributions in the partition function, we employ the condition for the temperature given by $\frac{\mathrm{d}\Sigma}{\mathrm{d}E} = \frac{1}{\Theta}$.

We assume that the relation between the changes of the value of the phase space from the energy E is known. In terms of this definition and within the context of fundamental principles of statistical mechanics [6] that $\Sigma = \ln\frac{\mathrm{d}\Gamma}{\mathrm{d}E} = S$ reproduces the entropy of the system bearing in mind that the temperature describes dependence of entropy only on energy but not on the other thermodynamic functions. It also follows that integration over energy in the continual sense yields an expression for the partition function. It is obvious that the extreme contribution in the partition function is associated with the states for

which $F = E - \theta S$ and that for any deviations from the latter condition the contribution in the partition function is negligibly small similarly to the contribution of quantum corrections to the classical trajectories [7] [8].

The Universe is non-equilibrium from origination, so in order to describe its evolution we introduce an additional intrinsic parameter "time". We assume that both the statistical distribution and the evolution of the Universe can be described in terms of the distribution function that depends only on energy. An example of how this idea is applied to describe the properties of the statistical distribution is given in [7] [8]. It seems quite natural to suggest the evolution of the system in the energy space to be analogous to the Brownian motion in such a space. This raises the question which system can serve for the Universe as a thermostat. It is reasonable to suggest that such thermostat is the vacuum with fluctuations of all physical fields that interact with the fundamental scalar field and thus influence even the ground state of the vacuum. On the other hand, this suggestion opens the possibility to describe the Universe evolution in the energy space by the appropriate distribution function governed by the Fokker-Planck equations with nonlinear energy dependence of the diffusion and dissipation coefficients associated with relevant nonlinear Langevine equations [7] [8]. Just this assumption shows the way to describe the evolution of the Universe both before and after origin.

Now let us apply the above speculations to the description of the Universe. First, we suggest that the vacuum ground state possesses energy. We also assume that fluctuations of all fields existing in vacuum can occur and thus we can write the equation of state for the vacuum. The thermodynamic relations yield the pressure given by $P = -\Theta \dfrac{\mathrm{d}S}{\mathrm{d}V}$ where V is the volume. For pure vacuum, we have $P = -\Theta \dfrac{\mathrm{d}S}{\mathrm{d}E_v}\dfrac{\mathrm{d}E_v}{\mathrm{d}V} = -\dfrac{\mathrm{d}E_v}{\mathrm{d}V} = -\rho_v$ under the assumption that energy with density ρ_v is additive, *i.e.*, $E_v = \rho_v V$ and constant entropy. Obtained equation reproduces the known equation of state for the vacuum. In order to describe its evolution we introduce an additional intrinsic parameter, "time", and write $\dot{S} = \dfrac{\mathrm{d}S}{\mathrm{d}E}\dot{E} = \dfrac{1}{\Theta}\dot{E}$. The latter equation implies that time changes of the entropy are related to the time changes of energy. Inasmuch as $\dot{S} > 0$, relaxation to the equilibrium state occurs for $\dot{E} > 0$, *i.e.*, energy growth is accompanied by the increase of entropy. Thermodynamics regards heat as energy distributed between the degrees of freedom that are not macroscopic observable. Hence we suggest that under the change of the vacuum state the heat $\mathrm{d}Q = \Theta \mathrm{d}S$ varies as $\dfrac{\mathrm{d}Q}{\mathrm{d}t} = \dfrac{\mathrm{d}E}{\mathrm{d}t}$ which in turn implies that heating can occur only under the relaxation towards equilibrium state.

3. Origin of Classical Fundamental Scalar Field

The above consideration and relations are well known. Now we employ them to

propose one more possible explanation of the origin of fundamental scalar field. We begin with the assumption that the phase transition from the "initial" vacuum to the new vacuum state is accompanied by the appearance of new scalar field. This means that the presence of the scalar field makes the "new" vacuum different from the "primary" vacuum for any field that may exist. The scalar field decreases the energy of the "new" vacuum with respect to the energy of the "primary" vacuum. Hence, the ground-state energy of the "new" vacuum is given by

$$E = E_v - \frac{\mu_0^2}{2}\varphi^2 \tag{3}$$

Here the second term is the scalar field energy; the coefficient μ_0^2 describes the coupling of the new field and the "primary" vacuum, *i.e.*, the self-consistent interaction of the new field with the fluctuations of all other fields that can exist in the "primary" vacuum. Notice, that the coupling coefficient is now positive so there is no need to use the explanations accepted in the standard approach. The contribution of the above interaction to the partition function (2) is given by

$$Z \sim \int D\varphi \int D\xi \exp\frac{1}{\Theta}\left\{-E_v + \frac{1}{2}\mu^2\varphi^2 - \frac{1}{2}\xi\varphi^2 - \frac{\xi^2}{\sigma^2}\right\} \tag{4}$$

where the coupling coefficient is presented in terms of its average value plus the fluctuation caused by the nonlinear coupling of the scalar field with a fluctuation field of other nature. We also assume that the mean-square value of the fluctuation is equal to $\mu_0^2 = \mu^2 + \xi$. σ^2 is dispersion of the couples coefficient fluctuations. Integration over fluctuation fields yields

$$Z \sim \int D\varphi \exp\frac{1}{\Theta}\left\{-E_v + \frac{1}{2}\mu^2\varphi^2 - \frac{\sigma^2\varphi^4}{4}\right\} \tag{5}$$

This means that we have a system with the effective energy (averaged over the fluctuations of the other field coupled with the scalar field) given by

$$E = E_v - \frac{1}{2}\mu^2\varphi^2 + \frac{\sigma^2\varphi^4}{4} \tag{6}$$

where the last two-term is the well-known expression for the energy of the fundamental scalar field $V(\varphi) = -\frac{1}{2}\mu^2\varphi^2 + \frac{\sigma^2\varphi^4}{4}$. The total effective energy of the "new" vacuum with the fundamental scalar field is given by

$$E = E_v - \frac{\mu^4}{4\sigma^2} + \frac{\sigma^2}{4}\left(\varphi^2 - \frac{\mu^2}{\sigma^2}\right)^2 \tag{7}$$

In the case of no scalar field $\varphi = 0$, $E = E_v$ while for $\varphi^2 = \frac{\mu^2}{\sigma^2}$ the expression for the effective ground state energy of the "new" vacuum reduces to $E = E_v - \frac{\mu^4}{4\sigma^2}$. As follows from last relation, the energy of the "new" vacuum is lower than the energy of the primary vacuum and can vanish for $E_v = \frac{\mu^4}{4\sigma^2}$.

This relation can be applied to estimate the maximum dispersion of the field fluctuations. If σ^2 tends to infinity, then the energy of the new state tends to the initial energy of the ground state. Thus, we come to the standard form of the energy of the fundamental scalar field, but with different behavior of the energy of vacuum at the presence of the scalar field. The coefficient of non-linearity in the potential energy is determined by the coupling of the fundamental scalar field with the fluctuations of the field of different nature. This means that there could be a new scenario of the Universe formation. In this scenario, the energy of pure vacuum does not contribute to the energy-momentum tensor and thus we cannot introduce dynamic presentation (and geometry) for such state. Only, if the fundamental scalar field appears and the matter is originated we can tell about the geometry. In this sense, the potential of scalar field determines the vacuum state of the Universe.

4. Conclusions

Standard cosmological models involve a scenario of the Universe nucleation and expansion based on a scalar field which is of fundamental importance for the unified theories of weak, strong, and electromagnetic interactions with spontaneous symmetry breaking [1]. A theory of new-phase bubble nucleation and expansion was proposed in Ref. [1]. Various cosmological models describe tunneling through the potential barrier in terms of the potentials $V(\varphi)$ of arbitrary forms. Here we propose a modification of the standard cosmological model. As was mentioned above, we assume that the fundamental scalar field interacts with possible fluctuations of fields of the other nature. To proceed further and to calculate the size of the bubble, we have to violate the equivalence of the local minima. Attempts have been made [1] to obtain non-linearity of such type associated with the fluctuations of the medium and produced by the interaction with the fields of different nature [9] [10]. Similar ideas are used in the description of phase transitions in condensed media, e.g., liquid crystals, superconductors etc. [11]. In order to explain the fact that the transition in such systems is the first-order one, the physical mechanism has been reduced to the interaction of the scalar order parameter with the vector field that includes information on possible fluctuations in the system [11] [12]. This means that the contribution of all existing configurations of such fields results in the additional part in the potential energy which proportional φ^3 in turn violates the equivalence of the local minima and opens the possibility to determine the bubble size of new phase with nonzero fundamental scalar field [12]. Thus the "condensing" value of fluctuations of the field that is "external" with respect to the scalar field completely determines both the mean critical size of the new phase bubble and the probability of its formation. In this case characteristics of such formation have no free parameters other than fluctuation dispersion.

As mentioned above, only the fundamental scalar field and its symmetry breaking generate the matter, and equilibrium distribution of this matter deter-

mines the geometry [13]. Obviously, the size of the bubble of the new phase is a finite one that is in agreement with the observations. And here we notice that in the Einstein equation the energy of primary vacuum is not present and the dynamics of the Universe are determined only by the potential energy of the fundamental scalar field which produces the matter. The distribution of matter in its turn determines the geometry. For our Universe, the vacuum is different from the primary one and its state depends on the fundamental scalar field which determines all possible processes. So, the dispersion of the fluctuations fully determines the conditions of new phase bubble formation.

Thus, the assumption of the vacuum ground state energy decrease for all physical fields due to the presence of the fundamental scalar field makes it possible to reveal the probability of a phase transition caused by the spontaneous generation of the field, *i.e.* the phase transition from vacuum with zero scalar field to the "new" vacuum with the spontaneously generated field. Combining this assumption with the idea that the Universe interacts with the fluctuations of various physical fields in vacuum we can get a consistent picture of the Universe origination and evolution. The decrease of the initial ground state energy does not contradict the H-theorem, because the distribution functions describing the evolution governed by the Fokker-Planck equation are known to satisfy it [14] [15].

Acknowledgements

This work was supported by the Target Program of Fundamental Research of the Department of Physics and Astronomy of the National Academy of Sciences of Ukraine (N0120U100857).

Conflicts of Interest

The authors declare no conflicts of interest regarding the publication of this paper.

References

[1] Linde, A.D. (1990) Particle Physics and Inflationary Cosmology. CRC Press, London, New-York, Washington D.C. https://doi.org/10.1016/B978-0-12-450145-4.50004-9

[2] Fomin, P.I. and Fomina, A.P. (2015) Dark Energy and Dark Matter in the Universe. In: Shulga, V., Ed., Kyiv, Akademperiodik, Vol. 3, 15.

[3] Fomin, P.I. (1976) *Physics of Elementary Particles and Atomic Nuclei*, **7**, 682.

[4] Boyle, L., Finn, K. and Turok, N. (2018) *Physical Review Letters*, **121**, Article ID: 251301. https://doi.org/10.1103/PhysRevLett.121.251301

[5] Gibbs, J.W. (1902) Elementary Principles in Statistical Mechanics, Developed with Especial Reference to the Rational Foundation of Thermodynamics. Charles Scriener's Sons, New York; Edward Arnold, London. https://doi.org/10.5962/bhl.title.32624

[6] Landau, L.D. (1973) Statistical Mechanics. Nauka, Moskwa.

[7] Lev, B.I. (2013) *The European Physical Journal Special Topics*, **216**, 37-48. https://doi.org/10.1140/epjst/e2013-01727-1

[8] Lev, B.I. and Kiselev, A.D. (2010) *Physical Review E*, **82**, Article ID: 031101. https://doi.org/10.1103/PhysRevE.82.031101

[9] Horsthemke, W. and Lefever, R. (1984) Noise-Induced Transition. In: Theory, Applications in Physics, Chemistry and Biology, Springer-Verlag, New-York.

[10] Lev, B.I. (2018) *Journal of Modern Physics*, **9**, 2223-2232. https://doi.org/10.4236/jmp.2018.912140

[11] Chaikin, P.M. and Luensky, T.C. (1995) Principles of Comdensed Matter Physics. Cambridge University Press, Cambridge.

[12] Lev, B. and Yokoyama, H. (2003) *International Journal of Modern Physics B*, **17**, 4913-4933. https://doi.org/10.1142/S021797920302274X

[13] Rebesh, A.P. and Lev, B.I. (2017) *Physics Letter A*, **381**, 2538-2543. https://doi.org/10.1016/j.physleta.2017.05.051

[14] Balesku, R. (1978) Equilibrium and Non-Equilibrium Statistical Mechanics. J. Wiley and Sons, New York.

[15] Nelson, E. (2001) Dynamical Theories of Brownian Motion. 2nd Edition. Princeton University Press, Princeton, 114.

Journal of Modern Physics, 2020, 11, 509-516
https://www.scirp.org/journal/jmp
ISSN Online: 2153-120X
ISSN Print: 2153-1196

Comparison of Epitaxial and Textured Ferroelectric $BaTiO_3$ Thin Films

Baba Wague[1], Nicolas Baboux[2], Pedro Rojo Romeo[1], Yves Robach[1], Bertrand Vilquin[1]

[1]Université de Lyon, Ecole Centrale de Lyon, Institut des Nanotechnologies de Lyon, CNRS UMR, Ecully Cedex, France
[2]Université de Lyon, INSA de Lyon, Institut des Nanotechnologies de Lyon, CNRS UMR, Villeurbanne Cedex, France
Email: bertrand.vilquin@ec-lyon.fr

How to cite this paper: Wague, B., Baboux, N., Romeo, P.R., Robach, Y. and Vilquin, B. (2020) Comparison of Epitaxial and Textured Ferroelectric $BaTiO_3$ Thin Films. *Journal of Modern Physics*, **11**, 509-516.
https://doi.org/10.4236/jmp.2020.114033

Received: February 27, 2020
Accepted: April 5, 2020
Published: April 8, 2020

Abstract

The properties of $BaTiO_3$ (BTO) thin films deposited on different substrates by RF magnetron sputtering were investigated. Two representative substrates were selected and different heterostructures were studied. 1) $SrTiO_3$ (STO) single crystals as a bulk oxide reference material, and 2) silicon as a semiconductor. $SrRuO_3$ (SRO) and Pt bottom electrodes were deposited on the silicon substrate. The BTO structural characterizations show that all the films have (001) crystallographic orientation. We have compared the electrical properties of the different samples: the same dielectric constant and polarization values were obtained independently of the nature of the substrate.

Keywords

Ferroelectric, Barium Titanate, Thin Film, Silicon, Sputtering, Epitaxy

1. Introduction

Among the ferroelectric perovskites, $BaTiO_3$ (BTO) has intensively been studied for a wide range of applications [1], MEMS devices [2], non-volatile memories, electro-optical devices [3], and piezoelectric and electro-optical properties [4]. Especially the fact that its composition is lead-free makes BTO very interesting for applications and many papers have discussed electrical and structural properties of BTO thin films [5] [6]. Various deposition techniques were used to grow thin films such as molecular beam epitaxy (MBE) [7] [8] [9], sol-gel deposition [10], pulsed laser deposition [11], chemical vapor deposition (CVD) [12], and RF sputtering [13] [14] [15]. RF sputtering is known to be one of the best compromises between deposition area size, stoichiometry, smoothness and de-

position speed problematics. High quality BTO thin films have generally been grown on lattice matched substrate such as MgO and $SrTiO_3$ (STO). In most cases, STO single-crystal is used as substrate as it also has a perovskite structure and its lattice parameters are close to those of BTO [16]. It is then easy to obtain epitaxially growth of BTO on STO. To check the electrical properties, conductive electrodes are needed. One can use a metal such as Pt, or a conductive oxide layer such as $SrRuO_3$ (SRO). The substrate and the bottom contact layer have to ensure good quality growth, and sufficient mechanical and thermal stabilities. In the present work, we investigate the structural and dielectric properties of 300 nm thick BTO thin films deposited by RF sputtering on different stacks of electrode/substrate: 1) $SrRuO_3/SrTiO_3$, 2) $Pt/TiO_2/SiO_2/Si$ and 3) $SrRuO_3/SrTiO_3/Si$.

2. Experimental Procedure

In this work, the substrates were cleaned before performing the deposition process with acetone and ethanol in an ultrasonic bath. Firstly, bulk STO (001) and STO buffered Si (001) were used as a substrate to deposit the BTO/SRO. SRO (30 nm thick) was deposited with Ar/O_2 gas ratio = 10/1 at 4 mTorr and at 620˚C. The STO buffer layer growth was performed by Molecular Beam Epitaxy on Si (004) wafer thanks to McKee process [17] [18]. Strontium was deposited on the native silica layer of the wafer and used for the reduction of SiO_2 and passivation layer on silicon, before the $SrTiO_3$ direct deposition around 360˚C under oxygen atmosphere. Secondly, on Si (001) with native silica layer was deposited at room temperature by RF sputtering 120 nm-thick platinum bottom electrode. A thin TiO_2 layer (5 nm-thick) was used as buffer and adhesion layer between Pt and SiO_2. Then, the BTO thin films on all substrates were prepared by RF magnetron sputtering from a stoichiometric $BaTiO_3$ ceramic target. The deposition was carried out in gas ratio Ar/O_2 = 4/1 maintained at a pressure of 15 mTorr and a temperature of 650˚C. After deposition, a rapid thermal annealing (RTA) at 650˚C for 3 minutes under oxygen atmosphere was performed in order to reduce oxygen vacancies in BTO thin films and improve their structural and electrical properties. The crystalline nature of BTO thin films was checked by X-ray diffraction analysis with a Rigaku Smartlab diffractomter using CuKα radiation (λ = 1.5406 Å). For electrical measurements, platinum top electrodes (50 µm × 50 µm area and 250 nm-thick) were deposited by lift-off on all samples at room temperature. A sketch of the different samples can be found in Figure 1. To perform the capacitance-voltage (C-V) measurements, a HP 4284A precision

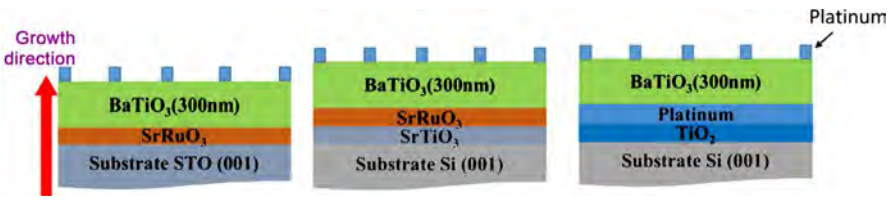

Figure 1. Schematic of the different samples. Pt top electrodes were deposited by lift-off at room temperature.

LCR meter was used. The ferroelectric hysteresis loops were evaluated with PUND (Positive Up Negative Down) method in order to extract the P-E hysteresis loop [19]. The PUND pulse train was programmed by LabView and a NF WF1966 2-channel generator. After application by a KEITHLEY 428 current amplifier, the current response was recorded by Nicolet INTEGRA-40 oscilloscope.

3. Results and Discussion

- **Structural characterization**

As a bulk material, BTO is normally crystallized in a tetragonal phase at room temperature. The difference between tetragonal phase and cubic phase in general is confirmed by the separation of diffraction peaks (002) and (200). **Figure 2(a)**, **Figure 2(c)** and **Figure 2(e)** show $2\theta/\omega$ patterns of 300 nm thick BTO grown on the different substrates. All diagrams indicate a preferential diffraction peak along the [001] direction, with no sign of secondary crystallographic orientation. Moreover, no other phase than the pure perovskite phase with a tetragonal structure is observed. The position corresponding to the 002 BTO reflection of bulk is obtained by angle determination (2θ = 44.86˚). The BTO thin films on all substrates are c-oriented and strained with elongated c-axis. These results are consistent with experimental data from previous sputtering depositions [20]. The diffractograms for all samples are qualitatively similar: on ω scan, the rocking curves display a full width at half maximum (FWHM) between 1.16 ˚ and 1.36˚, indicating the similar good crystallinity of BTO films, as shown in **Figure 2(b)**, **Figure 2(d)** and **Figure 2(f)**. These values are similar to those found in [21]. On the one hand, the phi-scan and reciprocal space mapping (RSM) patterns on the 103 reflections, shown in **Figure 3(a)** and **Figure 3(b)**, reveal the epitaxy of BTO films on bulk STO and STO buffered silicon substrates. The RSM measurements also show that the BTO films are relaxed on the substrates. On the other hand, the BTO deposited on $Pt/TiO_2/SiO_2/Si$ is textured with out-of-plane c-axis. The $2\theta/\omega$ patterns allow calculating the out-of-plane c-parameter of BTO for all samples. Based on fitting of 002 reflection peaks, these *c*-parameter values are 4.07 Å, 4.06 Å and 4.03 Å (±0.01 Å) respectively for BTO films deposited on BTO/SRO/STO and BTO/SRO/STO/Si and $Pt/TiO_2/SiO_2/Si$. This expansion of c parameter (bulk value of 4.038 Å) can be due to the epitaxial strain from the substrate for the epitaxial samples and/or the oxygen vacancies in BTO films. However, with a very low leakage current in the films (about 50 nA/cm^2 at 100 kV/cm applied field), it is expected that the films are vacancies-free. From RSM measurements, the in-plane *a*-parameter values were extracted and equal to 4.03 Å and 4.02 Å (±0.01 Å) respectively for BTO/SRO/STO and BTO/SRO/STO/Si. Then, it was possible to calculate their $\frac{c}{a}\text{ratio} = 1.01$—equal to the bulk value one—which confirms the tetragonal structure of the BTO films. Although the substrates are different for BTO/SRO/STO and BTO/SRO/

STO/Si heterostructures, their structural properties are quite similar with same out-of-plane orientation and close lattice parameters.

- **Dielectric and ferroelectric properties**

Electrical and ferroelectric measurements were performed on the 3 samples. The investigation on the variation of the dielectric constant versus the applied

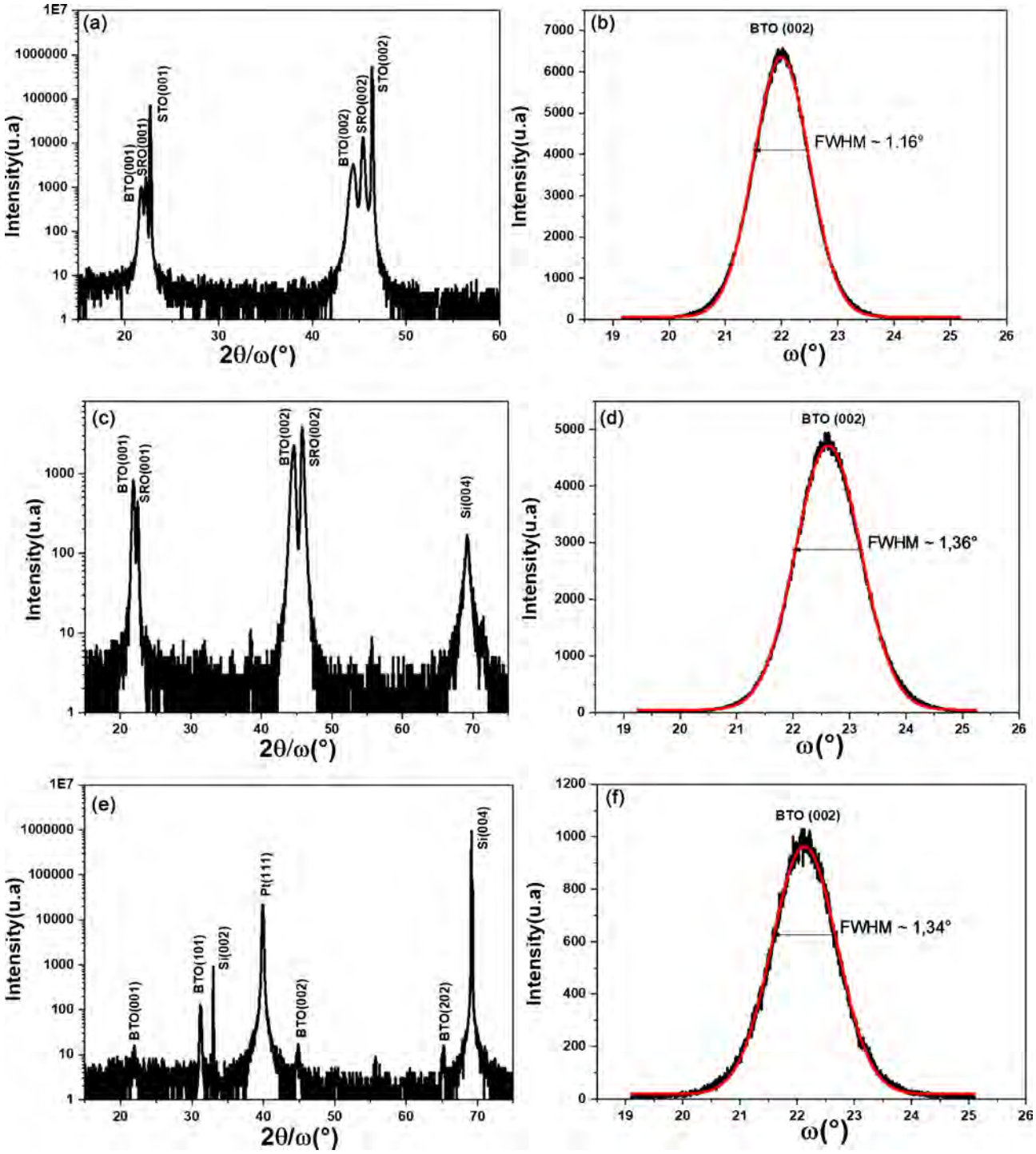

Figure 2. Out-of-plane XRD measurements of 300 nm thick BTO thin films on: (a) SRO/STO, (c) SRO/STO/Si and (e) Pt/TiO_2/SiO_2/Si. Rocking curve measurements around the BTO 002 respectively on (b) STO, (d) STO-Si and (f) Pt/TiO_2/SiO_2/Si.

electric field (C-V) is one of the methods for gaining insight into the behavior of the ferroelectric materials and has been used to characterize ferroelectric thin films [22] [23]. The C-V (**Figure 4**) characteristics measured on BTO films show the dielectric constant extracted from the small signal capacitance as a function of a DC bias voltage. The butterfly shape observed for all samples indicates the ferroelectric nature of the BTO tetragonal films. Very low leakage current (about 50 nA/cm^2 at 100 kV/cm applied field) was measured on the 3 samples. From **Figure 4**, the relative permittivity extracted using the parallel-plate capacitor equation was found $\varepsilon_r = 115$ for all substrates, corresponding to its dielectric contribution. On all samples, we can observe a shift of the dielectric constant along the X-axis for positive values of the electric field. This can be explained by the fact that top and bottom electrodes were made of different materials, which

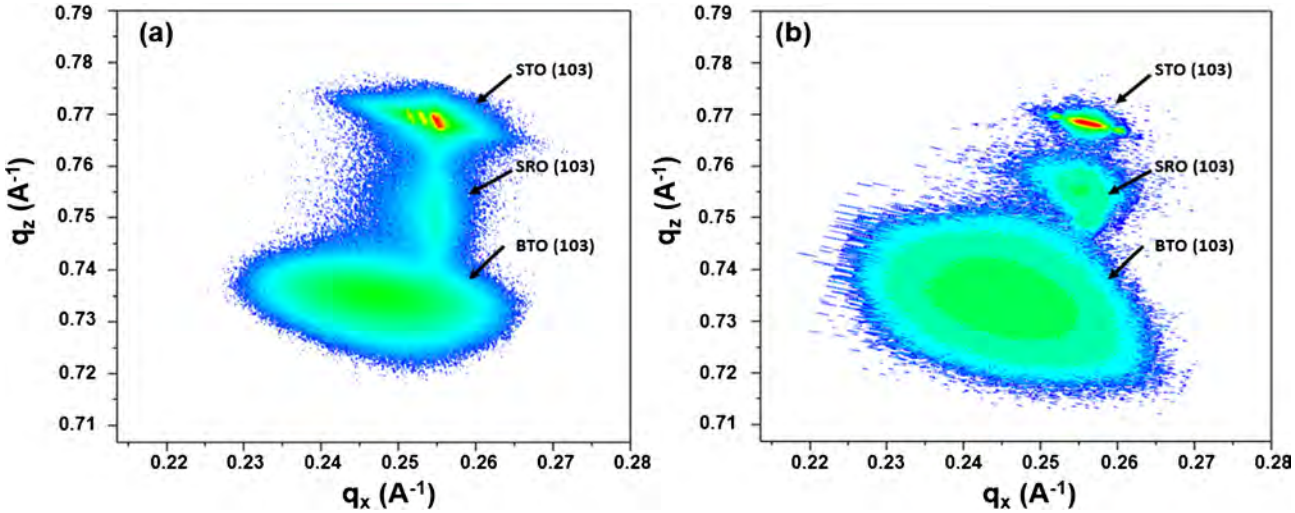

Figure 3. RSM measurements around the 103 STO, SRO and BTO reflections for BTO films deposited respectively on (a) STO substrate and (b) STO/Si template.

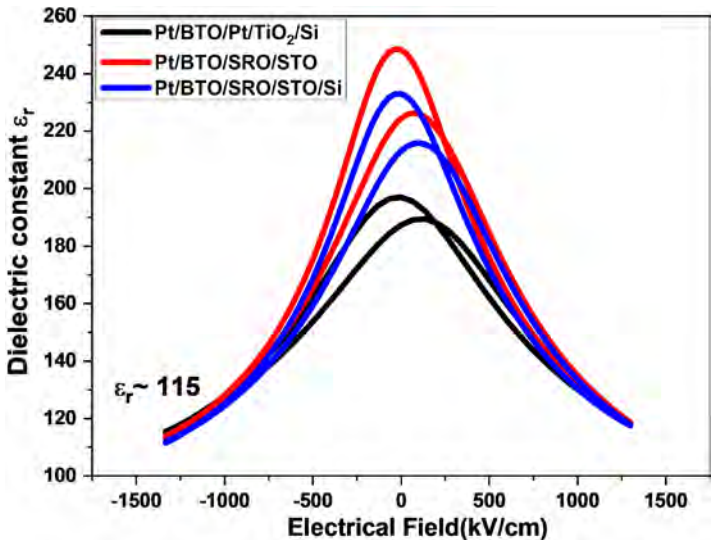

Figure 4. Dielectric constant curves of different samples: BTO/SRO/STO, BTO/SRO/STO/Si and BTO/Pt/TiO$_2$/SiO$_2$/Si.

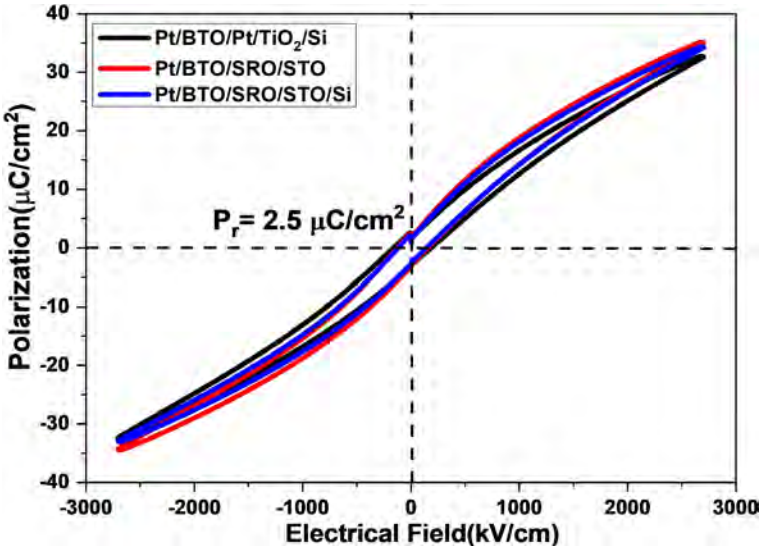

Figure 5. Ferroelectric hysteresis loops of different samples: BTO/SRO/STO, BTO/SRO/STO/Si and BTO/Pt/TiO_2/SiO_2/Si.

results in asymmetric properties of the upper and lower electrode-thin film interfaces, e.g. their work-function. The ferroelectric properties of BTO films on substrates were confirmed by hysteresis measurement as shown in **Figure 5**. It can be seen that all loops are normal P-E hysteresis ones. The corresponding remanent polarization value is $P_r = 2.5\mu c/\text{cm}^2$ and the coercive field about $E_c = 170\ \text{kV/cm}$ for all samples. These results agree with other results close to state of art obtained for BTO films deposited by MOCVD [23] [24] [25] or sputtering [20] [26]. The small value of the Pr in BTO films can be due to the presence of space-charges within the films [26]. As all the BTO films have out-of-plane c-axis orientation, it is obvious that the remanent polarization and the coercive field are similar. In this work, the same values are obtained on all substrates. We obtained BTO films with similar out-of-plane structure and electrical properties regardless of the nature of the substrate. It seems that the same crystallization process by sputtering with post-deposition annealing under oxygen atmosphere used to realize all the samples leads to similar film properties independently of the nature of the substrate.

4. Conclusion

Ferroelectric BTO thin films were successfully deposited on bulk STO, STO- and Pt-buffered silicon substrates. We achieved epitaxial growth of BTO on STO and STO-buffered Si and texturation on Pt-buffered Si. The BTO films show similar electrical properties on the substrates used in this work (STO or Si). These results offer promise for low cost integration of ferroelectric BTO film on silicon wafer.

Acknowledgements

This work was realized on the Nanolyon technology platform. The authors thank Agence Nationale de la Recherche (funding grant ANR-14-CE26-0010—INTENSE

project), Region Rhone-Alpes (ARC4 funding grant) and GDR OXYFUN for their financial support.

Conflicts of Interest

The authors declare no conflicts of interest regarding the publication of this paper.

References

[1] Roy, B.K. and Cho, J. (2012) *Journal of the American Ceramic Society*, **95**, 1189-1192. https://doi.org/10.1111/j.1551-2916.2012.05104.x

[2] Bakhoum, E.G., Member, S. and Cheng, M.H.M. (2010) *Journal of Microelectromechanical Systems*, **19**, 443-450. https://doi.org/10.1109/JMEMS.2010.2047632

[3] Dicken, M.J., Sweatlock, L.A., Pacifici, D., Lezec, H.J., Bhattacharya, K. and Atwater, H.A. (2008) *Nano Letters*, **8**, 4048-4052. https://doi.org/10.1021/nl802981q

[4] Wang, D.Y., Wang, J., Chan, H.L.W. and Choy, C.L. (2007) *Integrated Ferroelectrics*, **88**, 12-20. https://doi.org/10.1080/10584580601098522

[5] Beckers, L., Schubert, J., Zander, W., Ziesmann, J., Eckau, A., Leinenbach, P. and Buchal, C. (1998) *Journal of Applied Physics*, **83**, 3305-3310. https://doi.org/10.1063/1.367099

[6] Kim, Y.S., Kim, D.H., Kim, J.D., Chang, Y.J., Noh, T.W., Kong, J.H., Char, K., Park, Y.D., Bu, S.D., Yoon, J.G. and Chung, J.S. (2005) *Applied Physics Letters*, **86**, Article ID: 102907. https://doi.org/10.1063/1.1880443

[7] Niu, G., Yin, S., Saint-Girons, G., Gautier, B., Lecoeur, P., Pillard, V., Hollinger, G. and Vilquin, B. (2011) *Microelectronic Engineering*, **88**, 1232-1235. https://doi.org/10.1016/j.mee.2011.03.028

[8] Niu, G., Gautier, B., Yin, S., Saint-Girons, G., Lecoeur, P., Pillard, V., Hollinger, G. and Vilquin, B. (2012) *Thin Solid Films*, **520**, 4595-4599. https://doi.org/10.1016/j.tsf.2011.10.182

[9] Dubourdieu, C., Bruley, J., Arruda, T.M., Posadas, A., Jordan-Sweet, J., Frank, M.M., Cartier, E., Frank, D.J., Kalinin, S.V., Demkov, A.A. and Narayanan, V. (2013) *Nature Nanotechnology*, **8**, 748-754. https://doi.org/10.1038/nnano.2013.192

[10] Sharma, H.B. and Mansingh, A. (1994) Sol-Gel Processed Barium Titanate Thin Films and Ceramics. *IEEE International Symposium on Applications of Ferroelectrics*, Vol. 4, 1385-1390.

[11] García, T., Bartolo-Pérez, P., de Posada, E., Peña, J.L. and Villagrán-Muniz, M. (2006) *Surface and Coatings Technology*, **201**, 3621-3624. https://doi.org/10.1016/j.surfcoat.2006.08.117

[12] Kim, T.W., Yoon, Y.S., Yom, S.S. and Kim, C.O. (1995) *Applied Surface Science*, **90**, 75-80. https://doi.org/10.1016/0169-4332(95)00058-5

[13] Nagatomo, T., Kosaka, T., Omori, S. and Omoto, O. (1981) *Ferroelectrics*, **37**, 681-684. https://doi.org/10.1080/00150198108223520

[14] Zhang, W., Kang, L., Yuan, M., Yang, Q. and Ouyang, J. (2013) *Journal of Alloys and Compounds*, **580**, 363-368. https://doi.org/10.1016/j.jallcom.2013.06.093

[15] Zhu, J.S., Lu, X.M., Jiang, W., Tian, W., Zhu, M., Zhang, M.S., Chen, X.B., Liu, X. and Wang, Y.N. (1997) *Journal of Applied Physics*, **81**, 1392. https://doi.org/10.1063/1.363875

[16] Yang, Y., Priya, S., Wang, Y.U., Li, J. and Viehland, D. (2009) *Journal of Materials*

Chemistry, **28**, 4998-5002. https://doi.org/10.1039/b903762d

[17] Niu, G., Saint-Girons, G., Vilquin, B., Delhaye, G., Maurice, J.L., Botella, C., Robach, Y. and Hollinger, G. (2009) *Applied Physics Letters*, **95**, Article ID: 062902. https://doi.org/10.1063/1.3193548

[18] Niu, G., Peng, W.W., Saint-Girons, G., Penuelas, J., Roy, P., Brubach, J.B., Maurice, J.L., Hollinger, G. and Vilquin, B. (2011) *Thin Solid Films*, **519**, 5722-5725. https://doi.org/10.1016/j.tsf.2010.12.208

[19] Feng, S.M., Chai, Y.S., Zhu, J.L., Manivannan, N., Oh, Y.S., Wang, L.J., Yang, Y.S., Jin, C.Q. and Kim, K.H. (2010) *New Journal of Physics*, **12**, Article ID: 073006. https://doi.org/10.1088/1367-2630/12/7/073006

[20] Zhang, W., Hu, F., Zhang, H. and Ouyang, J. (2017) *Materials Research Bulletin*, **95**, 23-29. https://doi.org/10.1016/j.materresbull.2017.07.012

[21] El Marssi, M., Le Marrec, F., Lukyanchuk, I.A., Karkut, M.G., El Marssi, M., Le Marrec, F., Lukyanchuk, I.A. and Karkut, M.G. (2014) *Journal of Applied Physics*, **94**, 3307. https://doi.org/10.1063/1.1596720

[22] Sreenivas, K., Mansingh, A. and Sayer, M. (1987) *Journal of Applied Physics*, **62**, 4475-4481. https://doi.org/10.1063/1.339037

[23] Zeng, J., Wang, H., Wang, M., Shang, S., Wang, Z. and Lin, C. (1998) *Thin Solid Films*, **322**, 104-107. https://doi.org/10.1016/S0040-6090(97)00965-6

[24] Stawski, T.M., Vijselaar, W.J.C., Göbel, O.F., Veldhuis, S.A., Smith, B.F., Blank, D.H.A. and Ten Elshof, J.E. (2012) *Thin Solid Films*, **520**, 4394-4401. https://doi.org/10.1016/j.tsf.2012.02.029

[25] Yanase, N., Abe, K., Fukushima, N. and Kawakubo, T. (1999) *Journal of Applied Physics*, **38**, 5305-5308. https://doi.org/10.1143/JJAP.38.5305

[26] Zhang, W., Gao, Y., Kang, L., Yuan, M., Yang, Q., Cheng, H., Pan, W. and Ouyang, J. (2015) *Acta Materialia*, **85**, 207-215. https://doi.org/10.1016/j.actamat.2014.10.063

Journal of Modern Physics, 2020, 11, 517-527
https://www.scirp.org/journal/jmp
ISSN Online: 2153-120X
ISSN Print: 2153-1196

The Mathematical Foundations of Quantum Thermodynamics

Akira Suzuki[1], Hisao Taira[2]

[1]Faculty of Science, Tokyo University of Science, Shinjyuku-Ku, Tokyo, Japan
[2]Faculty of Education, Hokkaido University of Education, Kita-Ku, Sapporo, Japan
Email: asuzuki@rs.tus.ac.jp, taira.hisao@s.hokkyodai.ac.jp

How to cite this paper: Suzuki, A. and Taira, H. (2020) The Mathematical Foundations of Quantum Thermodynamics. *Journal of Modern Physics*, **11**, 517-527.
https://doi.org/10.4236/jmp.2020.114034

Received: February 10, 2020
Accepted: April 5, 2020
Published: April 8, 2020

Abstract

It is proposed a representation of the basic laws (*i.e.* the zeroth, first, second and third laws) in thermodynamics for quantum systems in the pure and mixed ensembles, respectively. We show that the basic laws are represented by parameters that specify respective quantum states. The parameters are the elements of the thermodynamic state space $\mathcal{M}_\theta$ and the state space $\mathcal{M}_\vartheta$ of the mixed ensemble for quantum systems. The introduction of such parameters is based on a probabilistic nature of quantum theory. Consistency between quantum theory and classical thermodynamics is preserved throughout the formulation for the representation of the thermodynamical laws in quantum systems (quantum thermodynamics). The present theory gives the mathematical foundations of quantum thermodynamics.

Keywords

Basic Laws in Thermodynamics, Thermodynamic State Space, Pure and Mixed States, Classical Thermodynamics, Quantum Thermodynamics, Transitive Law, Mixed Ensemble

1. Introduction

Thermodynmics is a universal theory not only for classical but for quantum systems. Classical thermodynamics has been well established by different approaches [1] [2] [3]. Above all, the theoretical importance of thermodynamical consideration in quantum systems (quantum thermodynamics) is emphasized in textbooks [4] [5]. When we consider the thermodynamics for quantum systems, the most important is the change in entropy since entropy is a constant of motion under the unitary transformation generated by a system Hamiltonian [6] [7]. The internal energy of the system plays the same role as temperature [8]. It

should, however, be noticed that in quantum system, thermodynamic equibria cannot be described in terms of a parameter like a temperature as in classical system.

In classical thermodynamics, states of the system are represented by points on a thermodynamic state space. In quantum system, quantum states are expressed by the elements of a complex Hilbert space $\mathscr{H}$. Therefore, in quantum thermodynamics, the Hilbert space itself does *not* play the same role as the state space in classical thermodynamics. In quantum system, thermodynamic equibria cannot be described in terms of a parameter like a temperature as in classical system. To be more precise, respective thermodynamic states are represented by points on a thermodynamic state space $\mathcal{M}_\theta$, and a different point means other thermodynamic states.

In order to gain some insights into the relation between thermodynamic states and quantum states, we have to investigate the structure of thermodynamics (quantum thermodynamics) on the basis of mathematical foundations. Lieb and Yngvason made the mathematical structure of thermodynamics transparent by axiomatic approach [3]. Thermodynamics treats changes of thermodynamical quantities when a system changes from one thermodynamic state to another state. In quantum mechanics, quantum states are expressed by the elements of a complex Hilbert space $\mathscr{H}$. It should be however noted that the Hilbert space itself does *not* play the same role as the thermodynamic state space in classical thermodynamics. In other words, the thermodynamic state space is *not* the same state space. The present authors [9] started with introducing a set $\mathcal{M}_\Psi$ of the state vectors in $\mathscr{H}$ in order to obtain a suitable set which plays the same role as the thermodynamic state space in classical thermodynamics. That is, a set $\mathcal{M}_\theta$, which plays the same role as the thermodynamic state space, is introduced and the correspondence between $\mathcal{M}_\Psi$ and $\mathcal{M}_\theta$ must be derived. In short, we will see this treatment provides an insight into a correspondence between $\mathcal{M}_\Psi$ and $\mathcal{M}_\theta$.

In our previous paper [9], we showed that a representation of the basic laws in thermodynamics for quantum systems in pure states is constructed in terms of the parameters θ's by which respective thermodynamic states corresponding to the respective quantum states of the system are represented. In this paper, we extend the previous theory for the representation of the thermodynamic quantum states applicable to the case for the mixed ensembles in quantum systems. We introduced parameters θ's in $\mathcal{M}_\theta$, which could describe the thermodynamic temperature. The parameters θ's make sense only on existence of the map $\mathcal{M}_\Psi \mapsto \mathcal{M}_\theta$, *i.e.*, $\mathcal{M}_\theta$ is an injection of $\mathcal{M}_\Psi$ valid for a system in pure states.

To extend the range of applicability of the theory is interesting from the viewpoint of fundamental physics. In the previous study [9] we discussed thermodynamics for a system in pure quantum states and constructed the representation of basic laws of quantum thermodynamics in terms of the parameters θs

in $\mathcal{M}_\theta$. In this paper, we extend the theory and construct the formulas representing the basic laws of thermodynamics for a system in a mixed quantum ensemble. The formulation is based on the mathematical foundation by employing axiomatic approach [3].

We will introduce a state space $\mathcal{M}_\vartheta$ in order to take into account a mixed state just like we introduced $\mathcal{M}_\theta$ for a pure state. The parameter ϑ's characterize the state vectors of the mixed states, where fractional population (viz., a probability of occurrence) of the quantum states is naturally introduced for state vectors. It should be noted that the parameters ϑ's are the elements of $\mathcal{M}_\vartheta$ for a system in mixed quantum states and the map $\mathcal{M}_\Psi \mapsto \mathcal{M}_\vartheta$ should hold. We will show that a representation of the basic laws (Zeroth, First, Second and Third laws) in thermodynamics for quantum systems in a mixed state is described by making use of those parameters ϑ's in $\mathcal{M}_\vartheta$.

This paper is organized as follows. In the next section, we present quantum thermodynamics, namely thermodynamics for quantum systems. In subsection 2.1, the zeroth law of quantum thermodynamics is formulated for the case where the quantum systems are in mixed quantum ensembles. We introduce thermodynamic state space $\mathcal{M}_\theta$, $\mathcal{M}_\vartheta$ respectively for pure and mixed quantum ensembles in order to relate $\mathcal{M}_\theta$, $\mathcal{M}_\vartheta$ to the quantum state space $\mathcal{M}_\Psi$. We discuss the connection between the elements in $\mathcal{M}_\Psi$ and those in $\mathcal{M}_\theta$ and $\mathcal{M}_\vartheta$, and formulate the first law of quantum thermodynamics in subsection 2.2. In subsection 2.3, we introduce an entropy function for the system of mixed states as a map on thermodynamic state space $\mathcal{M}_\theta$ and $\mathcal{M}_\vartheta$ for pure and mixed ensembles. We shall see that the entropy function ensures it is defined for all states in terms of θ's ($\in \mathcal{M}_\theta$) and ϑ's ($\in \mathcal{M}_\vartheta$). We will show that thermodynamic temperatures can be defined as a function of θ's and ϑ's for the system of mixed ensembles. In subsection 2.4, the third law of thermodynamics for the quantum systems of mixed states is briefly discussed. The absolute zero temperature is the state that the system is in a single quantum state. Finally, summary and concluding remarks are given in section 3.

2. Thermodynamics for Systems in Mixed Quantum States

In the previous paper [9], we have considered the case where thermodynamic quantum systems are in pure ensembles. The state of quantum systems in a pure ensemble is described by $|\Psi_\alpha\rangle, |\Psi_\beta\rangle$, etc., where subscripts denote the label of respective states of quantum system. The formulation of the present theory can be extended to a case where thermodynamic quantum systems are in mixed ensemble by introducing another parameter in order to describe those mixed ensembles of the quantum system.

Mixed ensembles are defined by

$$\rho := \left(|\Psi_\alpha\rangle, |\Psi_\beta\rangle, |\Psi_\gamma\rangle, \cdots; w_\alpha, w_\beta, w_\gamma, \cdots\right), \tag{1}$$

where fractional populations w_j ($0 < w_j \le 1$ and $\sum w_j = 1$, $j = \alpha, \beta, \gamma, \cdots$)

describes a probability of occurrence corresponding to a state vector $|\Psi_j\rangle$ [10]. This suggests that a mixed ensemble is characterized not only by a probability w_j but also by a probability p which is obtained from $|\Psi\rangle$ as shown in the proof of **L1'** (see Section 2.1). Therefore if we introduce a probability function $Q(\vartheta; y)$ so as to satisfy $Q(\vartheta; y = j) = \omega_j$, a mixed ensemble can be characterized by both $Q(\vartheta; y)$ and $P(\theta; x)$. Thus, a state of the thermodynamic quantum systems can be characterized by these two parameters: ϑ's in $\mathcal{M}_\vartheta$ and θ's in $\mathcal{M}_\theta$. It should be noticed that the origin of θ is a probabilistic nature of quantum mechanics but ϑ is due to the `classical' probability of occurrence ω_j that the state vector is $|\Psi_j\rangle$. In this section, we derive a representation of zeroth, first, second, and third laws of thermodynamics for a quantum system in a mixed ensemble.

At first, we have to introduce the concept of an *ensemble* w_j into the probability amplitude a_i defined by $a_i \equiv \langle i|\Psi\rangle$ where $\langle i| = |i\rangle^\dagger$, $(i = 1, 2, 3, \cdots)$, is complete orthogonal basis. We define the probability amplitude in a mixed ensemble as follows:

$$b_{ij} \equiv \sqrt{w_j}\,\langle i|\Psi_j\rangle. \tag{2}$$

The probability is thus given by

$$p_{ij} = |b_{ij}|^2 = w_j\,|\langle i|\Psi_j\rangle|^2 = p_i w_j. \tag{3}$$

Recall that $|\langle i|\Psi_j\rangle|^2$ is the usual quantum mechanical probability taken with respect to the respective state *i*. Equation (2) tells us that these probabilities must further be weighted by the corresponding fractional populations w_j. Notice how probabilistic concepts enter twice: first in $|\langle i|\Psi_j\rangle|^2$ for the quantum-mechanical probability for the respective state *i* to be found in an eigenstate $|\Psi_j\rangle$, second in the probability factor w_j for finding a quantum-mechanical state characterized by $\langle i|\Psi_j\rangle$ in the ensemble.

In the following subsections, we derive the representation of the basic laws of quantum thermodynamics for a system in mixed ensembles.

2.1. The Zeroth Law of Quantum Thermodynamics

The zeroth law of quantum thermodynamics for a system in mixed ensembles is expressed by making use of the parameter ϑ's in $\mathcal{M}_\vartheta$. In order to represent the zeroth law, we need to introduce the *Lemma* **L1'** as follows:

L1': There exist parameters $\theta_\alpha, \theta_\beta, \cdots$ in $\mathcal{M}_\theta$ for pure quantum states and $\vartheta_\alpha, \vartheta_\beta, \cdots$ in $\mathcal{M}_\vartheta$ for mixed ensembles representing the respective state vectors, $|\Psi_\alpha\rangle, |\Psi_\beta\rangle, \cdots$ in $\mathcal{M}_\Psi$.

Proof of L1': We treat a case for a label α. Other cases, $\beta, \gamma, \cdots$, could be proved in the same way. From Equation (2), one can obtain a sequence $\left\{|b_{1j}^\alpha|^2, |b_{2j}^\alpha|^2, \cdots, |b_{ij}^\alpha|^2, \cdots\right\}$ with an ensemble *j*. By normalizing a state vector $|\Psi_\alpha\rangle$, the sequence satisfies the condition $\sum_{i=1} |b_{ij}^\alpha|^2 = 1$ and it is clear that

$0 \le \left|b_{ij}^{\alpha}\right|^2 \le 1$. Then each element of the sequence describes a definite probability for the respective state *i* and a specific ensemble *j*. Hereafter, we shall omit superscript α for simplicity. Let us introduce a probability function $P(\theta; x)$ so as to satisfy $P(\theta; x = i) = |a_i|^2$ for any *i*. In $P(\theta; x)$, θ is a parameter and *x* is a random variable. We also introduce a probability function so as to satisfy $Q(\vartheta; y = j) = w_j$ for any *j*. Therefore, the parameters θ_k $(k = \alpha, \beta, \gamma, \cdots)$ and ϑ_k $(k = \alpha, \beta, \gamma, \cdots)$, both exist for the representation of a state vector $|\Psi_k\rangle$. ■

We note here that **L1'** ensures the existence of parameters θ_k's and ϑ_k's which correspond to respective state vectors $|\Psi_k\rangle$'s in $\mathcal{M}_\Psi$ through probability functions $P(\theta_k; x)$'s and in $Q(\vartheta_k; y)$'s, respectively.

Now one can compare two quantum states in thermodynamic sense since those parameters θ's and ϑ's can be used to describe two or more systems being equivalent. This leads to the zeroth law of quantum thermodynamics. Let us prepare three systems, $\mathcal{M}_\theta^{\mathrm{A}}$ with $\mathcal{M}_\vartheta^{\mathrm{A}}$, $\mathcal{M}_\theta^{\mathrm{B}}$ with $\mathcal{M}_\vartheta^{\mathrm{B}}$ and $\mathcal{M}_\theta^{\mathrm{C}}$ with $\mathcal{M}_\vartheta^{\mathrm{C}}$, where superscripts indicate labels of respective systems. The zeroth law of quantum thermodynamics (*equivalence relation among quantum states*) is described by the following relation:

Let us first consider the following relation for the system in mixed ensembles:

$$\text{If } \theta_\alpha^{\mathrm{A}} = \theta_\beta^{\mathrm{B}} \text{ and } \vartheta_\alpha^{\mathrm{A}} = \vartheta_\beta^{\mathrm{B}}, \text{ then } |\Psi_\alpha\rangle^{\mathrm{A}} \doteq |\Psi_\beta\rangle^{\mathrm{B}}, \tag{4}$$

where $\theta_\alpha^{\mathrm{A}} \in \mathcal{M}_\theta^{\mathrm{A}}$ and $\theta_\beta^{\mathrm{B}} \in \mathcal{M}_\theta^{\mathrm{B}}$, $\vartheta_\alpha^{\mathrm{A}} \in \mathcal{M}_\vartheta^{\mathrm{A}}$ and $\vartheta_\beta^{\mathrm{B}} \in \mathcal{M}_\vartheta^{\mathrm{B}}$ respectively, and a symbol $\doteq$ here denotes that the state in the left-hand side is *equivalent* to the state in the right-hand side.

Proof of Equation (4): Let $\theta_\alpha^{\mathrm{A}}$ and $\theta_\beta^{\mathrm{B}}$ be the elements of $\mathcal{M}_\theta^{\mathrm{A}}$ and $\mathcal{M}_\theta^{\mathrm{B}}$, respectively. Furthermore, let $\vartheta_\alpha^{\mathrm{A}}$ and $\vartheta_\beta^{\mathrm{B}}$ be the elements of $\mathcal{M}_\vartheta^{\mathrm{A}}$ and $\mathcal{M}_\vartheta^{\mathrm{B}}$, respectively. By **L1'**, it is clear that $\theta_\alpha^{\mathrm{A}} = \theta_\beta^{\mathrm{B}}$ and $\vartheta_\alpha^{\mathrm{A}} = \vartheta_\beta^{\mathrm{B}}$ imply $|\Psi_\alpha\rangle^{\mathrm{A}} \doteq |\Psi_\beta\rangle^{\mathrm{B}}$. ■

The zeroth law: We are now in a position to discuss some consequences obtained by introducing the parameters θ_k and ϑ_k to specify the corresponding thermodynamic states of the systems in mixed quantum ensembles. It is clear from Equation (4) that the *transitive law* holds:

$$\text{If } \theta_\alpha^{\mathrm{A}} = \theta_\beta^{\mathrm{B}} \text{ with } \vartheta_\alpha^{\mathrm{A}} = \vartheta_\beta^{\mathrm{B}} \text{ and } \theta_\beta^{\mathrm{B}} = \theta_\gamma^{\mathrm{C}} \text{ with } \vartheta_\beta^{\mathrm{B}} = \vartheta_\gamma^{\mathrm{C}}, \text{then } |\Psi_\alpha\rangle^{\mathrm{A}} \doteq |\Psi_\gamma\rangle^{\mathrm{C}}. \tag{5}$$

We have established a representation of the zeroth law of quantum thermodynamics (equivalence relation among quantum states). The zeroth law can be expressed in terms of parameters in $\mathcal{M}_\theta$ and $\mathcal{M}_\vartheta$. Equation (5) means that, in the mixed ensemble, the additional condition $\vartheta_\alpha^{\mathrm{A}} = \vartheta_\beta^{\mathrm{B}}$ is required for the equivalence relation among mixed ensembles.

2.2. The First Law of Quantum Thermodynamics

The first law of thermodynamics states that heat is a form of energy, and thermodynamic processes are therefore subject to the principle of conservation of energy, meaning that heat energy cannot be created or destroyed. In order to

discuss the first law and obtain the representation of the first law of quantum thermodynamics, let us consider the internal energy of the system in mixed quantum ensembles.

The internal energy U_{m} of the system in mixed quantum states is given by the expectation value of Hamiltonian $\hat{\mathcal{H}}$:

$$U_{\mathrm{m}} = \left\langle \hat{\mathcal{H}} \right\rangle_{\mathrm{m}} = \sum_{i,j} p_{ij} E_i = \sum_j U_j, \tag{6}$$

where $p_{ij} = p_i w_j$ and $U_j = \sum_i p_{ij} E_i$ is the internal energy of the ensemble *j*. By calculating the total differential of Equation (6), we obtain

$$dU_{\mathrm{m}} = \sum_{i,j} \left(E_i dp_{ij} + p_{ij} dE_i \right) \equiv \sum_j \left(d'Q_j + d'W_j \right). \tag{7}$$

Analogous to the case for a system in a pure ensemble [9], we identify $d'Q_j = \sum_i E_i dp_{ij}$ and $d'W_j = \sum_i p_{ij} dE_i$, respectively, for the heat transferred to the ensemble *j* and for the work done on the ensemble *j*. The variation of the internal energy U_{m}, that is dU_{m} for the mixed ensemble, is obtained by summing up all $d'Q_j$ and $d'W_j$ weighted by w_j since p_{ij} is equal to $p_i w_j$. It is clear that dU_{m} in Equation (7) is reduced to $dU = \sum_i \left(E_i dp_i + p_i dE_i \right)$, which is the case of a quantum system in a pure quantum ensemble since a pure quantum ensemble means $w_j = 1$ only for particular *j* and $w_{j'} = 0$ for $j' \neq j$.

Distinguishing two kinds of transfer of energy, as *heat* and as *thermodynamic work*, adopted for thermodynamic processes, we prove that the equalities $d'W_j = \sum_i p_{ij} dE_i$ and $d'Q_j = \sum_i E_i dp_{ij}$ are true. Let us consider the small change in the outcome is given by

$$dE_i = \frac{\partial E_i(L)}{\partial L} dL, \tag{8}$$

where *L* is the work coordinate related to the work done on the system. Then

$$\sum_i p_{ij} dE_i = \sum_i p_{ij} \frac{\partial E_i}{\partial L} dL, \tag{9}$$

where $p_{ij} = P(\theta; x = i) Q(\vartheta; y = j)$. Note that p_{ij} is a function of the parameters θ and ϑ. The probability p_{ij} does not depend on *L* but the energy E_i of the quantum state *i* does. Thus we can write Equation (9) as

$$\sum_i p_{ij} dE_i = \sum_i \frac{\partial}{\partial L} \left(p_{ij} E_i \right) dL = \frac{\partial}{\partial L} U_j dL. \tag{10}$$

A change in the internal energy of the system in a mixed ensemble is generally related to a *force* defined by

$$F_j \equiv -\frac{\partial U_j(L)}{\partial L}, \tag{11}$$

so that Equation (10) and hence Equation (9) can be expressed as

$$\sum_i p_{ij} dE_i = -F_j dL. \tag{12}$$

Thus, it is clear that the term $\sum_i p_{ij} dE_i$ corresponds to the work $d'W_j$ done

on the system described by ensemble *j* and it is generally expressed by

$$d'W_j = \sum_i p_{ij} dE_i(L) = -F_j dL, \tag{13}$$

where the definite probability p_{ij} can then be replaced by the probability function $P(\theta; x=i)Q(\vartheta; y=j)$. Thereby, from Equations (7) and (13) we have $dU_j = d'Q_j$ when $d'W_j = 0$. Then the term $\sum_i E_i dp_{ij}$ corresponds to the change in the internal energy of the system that occurs when *no* work is done; this is what we understand as *heat* flow.

It should be emphasized that the heat entering the system described by ensemble *j*, $d'Q_j$, is expressed in terms of the variation of $p_{ij} = P(\theta; x=i)Q(\vartheta; y=j)$ while the work is done on the system described by ensemble *j*, $d'W_j$, is expressed in terms of the variation of $E_i(L)$. Since $p_{ij} = P(\theta; x=i)Q(\vartheta; y=j)$, we can write dp_{ij} as

$$dp_{ij} = Q(\vartheta; y=j)\frac{\partial P(\theta; x=i)}{\partial \theta} d\theta + P(\theta; x=i)\frac{\partial Q(\vartheta; y=j)}{\partial \vartheta} d\vartheta. \tag{14}$$

so that $d'Q_j$ is expressed in terms of those parameters θ *and* ϑ:

$$\begin{aligned} d'Q_j &= \sum_i E_i dp_{ij} \\ &= \sum_i E_i \left[Q(\vartheta; y=j)\frac{\partial P(\theta; x=i)}{\partial \theta} d\theta + P(\theta; x=i)\frac{\partial Q(\vartheta; y=j)}{\partial \vartheta} d\vartheta \right]. \end{aligned} \tag{15}$$

We would like to note that Equation (15) reduces to $d'Q = \sum_i E_i dp_i = \sum_i E_i \frac{\partial P(\theta; x=i)}{\partial \theta} d\theta$ for a quantum system in a pure ensemble, where $Q(\vartheta; y=j) = 1$.

2.3. The Second Law of Quantum Thermodynamics

In this subsection, we will give a definition of entropy to describe the entropy principle (viz., the second law of thermodynamics) for quantum system described by a mixed state. The entropy principle states that adiabatic accessibility of any two states is described by an entropy inequality. Here we should refer to the adiabatic process since the second law treated here is defined for the process. The process is characterized by $d'Q_j = 0$ for mixed ensembles. This is ensured when $P(\theta; x)Q(\vartheta; y)$ remains unchanged throughout the process (see **C1'** and argument below). In other words, adiabatic process is a process such that $P(\theta; x)Q(\vartheta; y)$ remains unchanged. It should be noted that adiabatic process allows to change a value of *L* since it affects only the work $d'W_j$. This is consistent with adiabatic processes defined by Lieb and Yngvason [3].

Let us define an entropy function S_{m} for mixed ensembles as a map from the sets $\mathcal{M}_{\theta,L}$ and $\mathcal{M}_{\vartheta,L}$ to a real number $\mathcal{R}$:

$$S_{\mathrm{m}} : \mathcal{M}_{\theta,L}, \mathcal{M}_{\vartheta,L} \mapsto \mathcal{R}. \tag{16}$$

We note that this general definition for entropy can describe all types of entropy functions including well known Boltzmann, Gibbs, and Shannon entro-

pies. The entropy S_{m} defined by the map (16) is clearly a state quantity and ensures that S_{m} can be defined for *all* states (*i.e.* pure and mixed ensembles) in terms of θ and ϑ.

In order to obtain a representation of the second law in terms of θ and ϑ for quantum system, it must be shown that determining parameters θ and ϑ. In order to show this, let us show that U_{m} is specified by θ's, ϑ's and L's (*i.e.*, the elements of $\mathcal{M}_{\theta,L}$ and $\mathcal{M}_{\vartheta,L}$).

First, we show that the following *corollaries*, **C1'** and **C2'**, can be drawn:

C1': The internal energy U_{m} is specified by the respective parameters θ, ϑ and L:

$$U_{\mathrm{m}} = U_{\mathrm{m}}(\theta, \vartheta, L). \tag{17}$$

Proof of C1': Once a maximal test is chosen for a fixed L, respective outcomes E_i $(i = 1, 2, \cdots)$ for the system is uniquely determined and the definite probability p_{ij} is then described as $P(\theta; x = i)Q(\vartheta; y = j)$ by the proof of **L1'**. Therefore, it is clear that the internal energy is specified by the respective parameters θ, ϑ and L. ■

We note that **C1'** states the internal energy U_{m} can be specified by those parameters, θ, ϑ and L. We will omit L in $U_{\mathrm{m}}(\theta, \vartheta, L)$ for simplicity when we consider a fixed L.

C2': $d'Q_j = 0$ implies the consequence of adiabatic equivalence for all ensembles w.r.t. each j.

Proof of C2': By the proof of **L1'**, no change in the probability function implies that the absolute values of the expansion coefficients $|b_{ij}|$'s remain the same. This implies p_{ij} remains constant. Thus $d'Q_j$ is equal to zero throughout the operation (process). ■

In the statement of **C2'**, the consequence of adiabatic equivalence is as follows: if the system were isolated, the absolute values of the expansion coefficients $|b_{ij}|$'s would remain constant. It should be noticed that the notion of heat arises *only* when the state (internal energy) of a system changes, where $dU_j \neq d'W_j$. As in classical thermodynamics, heat in quantum system is also defined as a form of energy flow. Once the internal energy of a quantum system is well defined, heat is also well defined. Thus the following *Lemma* (**L2'**) is established:

L2': There exist U_{m}'s specified by each element of $\mathcal{M}_{\theta,L}$ and $\mathcal{M}_{\vartheta,L}$.

Proof of L2': Without loss of generality, one can consider a fixed maximal test, where outcome of the maximal test is *uniquely* determined: The internal energy for mixed ensembles is thus represented in terms of those parameters θ's and ϑ's:

$$U_{\mathrm{m}} = \sum_{i,j} p_{ij} E_i = \sum_{i,j} P(\theta_\alpha; x = i) Q(\vartheta_\alpha; y = j) E_i, \tag{18}$$

where θ_α and ϑ_α specify the internal energy U_{m}. Therefore, U_{m} can be labeled as $U_{\mathrm{m}\alpha}$. As in the same way, respective internal energies, $U_{\mathrm{m}\beta}, U_{\mathrm{m}\gamma}, \cdots$, can be specified by $\theta_\beta, \theta_\gamma, \cdots$ and $\vartheta_\beta, \vartheta_\gamma, \cdots$. ■

Since the existence of correspondence between an internal energy U_{m} and

parameters θ and ϑ was established by **L2'**, we can obtain one-to-one correspondence between $S_{\mathrm{m}}(X)$ and $S_{\mathrm{m}}(\theta,\vartheta)$. This keeps consistency between an entropy function defined in the entropy principle (see Ref. [9], Section 2) and the statement (16) for a mixed ensemble of the system. We finally obtain a representation of the second law of quantum thermodynamics for a system in a mixed ensemble in terms of θ and ϑ:

$$\theta_\alpha \prec \theta_{\alpha'} \text{ and } \vartheta_\alpha \prec \vartheta_{\alpha'} \text{ if and only if } S_{\mathrm{m}}(\theta_\alpha,\vartheta_\alpha) \le S_{\mathrm{m}}(\theta_{\alpha'},\vartheta_{\alpha'}). \tag{19}$$

This describes the *entropy principle* for quantum systems in mixed quantum ensembles.

For the case where a given arbitrary pair of states represented by $(\theta_\alpha,\theta_\beta)$ and $(\theta_{\alpha'},\theta_{\beta'})$, the following relation holds [9]:

$$(\theta_\alpha,\theta_\beta) \prec (\theta_{\alpha'},\theta_{\beta'}) \text{ if and only if } S(\theta_\alpha)+S(\theta_\beta) \le S(\theta_{\alpha'})+S(\theta_{\beta'}), \tag{20}$$

where θ_j, $j=\alpha,\beta,\cdots$, is the element of the state space $\mathcal{M}_\theta \times \mathcal{M}_\theta$.

From **L2'**, we can immediately obtain the relation for any pairs of states represented by $(\theta_\alpha,\theta_\beta)$, $(\vartheta_\alpha,\vartheta_\beta)$ and $(\theta_{\alpha'},\theta_{\beta'})$, $(\vartheta_{\alpha'},\vartheta_{\beta'})$:

$$\begin{aligned}&(\theta_\alpha,\theta_\beta) \prec (\theta_{\alpha'},\theta_{\beta'}) \text{ and } (\vartheta_\alpha,\vartheta_\beta) \prec (\vartheta_{\alpha'},\vartheta_{\beta'})\\ &\text{if and only if } S(\theta_\alpha,\vartheta_\alpha)+S(\theta_\beta,\vartheta_\beta) \le S(\theta_{\alpha'},\vartheta_{\alpha'})+S(\theta_{\beta'},\vartheta_{\beta'}),\end{aligned} \tag{21}$$

where θ_k and ϑ_k, $k=\alpha,\beta,\cdots$, are the elements of the state space $\mathcal{M}_\theta \times \mathcal{M}_\theta$ and $\mathcal{M}_\vartheta \times \mathcal{M}_\vartheta$, respectively. The statement (21) means that $(\theta_{\alpha'};\vartheta_{\alpha'},\theta_{\beta'};\vartheta_{\beta'})$ is adiabatically accessible from $(\theta_\alpha;\vartheta_\alpha,\theta_\beta;\vartheta_\beta)$.

Since we established S_{m} for the quantum system as a function of parameters θ and ϑ, one can define *thermodynamic temperature* T as a function of θ and ϑ: $T=T(\theta,\vartheta)$.

2.4. The Third Law of Quantum Thermodynamics

Let us briefly discuss the third law of thermodynamics for quantum systems described by mixed ensembles. The probability functions $P(\theta)$ and $Q(\vartheta)$ are found from probability amplitudes (see **L1'**). Accordingly, we can obtain the representation of the third law: The entropy S_{m} is equal to zero only when $P(\theta)$ and $Q(\vartheta)$ satisfy the conditions:

$$P(\theta; x=i)=1 \text{ for arbitrary } i, \tag{22}$$

$$Q(\vartheta; y=j)=1 \text{ for arbitrary } j. \tag{23}$$

At the absolute zero temperature, one can expect a state of quantum system being in a *single* state for each ensemble j such as

$$|\Psi_j\rangle = b_{ij}|i\rangle \quad \text{for arbitrary } i \text{ and } j. \tag{24}$$

The single state here means that only one outcome is obtained with a probability 1 by maximal tests.

3. Summary and Concluding Remarks

In this study, in addition to the parameters θ's in a thermodynamic state space $\mathcal{M}_\theta$ to describe pure quantum ensembles discussed in Ref. [9], parameters ϑ's

in $\mathcal{M}_{\vartheta}$ are newly proposed in order to describe mixed quantum ensembles of quantum systems, where the map $\mathcal{M}_{\Psi} \mapsto \mathcal{M}_{\vartheta}$ is an injection. Therefore, in order to establish the representation of the zeroth law in terms of the elements $\mathcal{M}_{\vartheta}$, it is required to use the *same* maximal tests to obtain the corresponding elements from the respective elements of quantum state vectors Ψ's in the state-vector space $\mathcal{M}_{\Psi}$ for quantum systems. We showed that the *first law* is represented by a state quantity specified in terms of the parameters ϑ's $\in \mathcal{M}_{\vartheta,L}$ along with the parameters θ's $\in \mathcal{M}_{\theta,L}$ for the the systems in mixed ensembles (**C1'**), where L denotes the work coordinate related to the work done on the respective system. We showed that the representation of the *second law* of thermodynamics was also obtained for a system in mixed quantum ensembles by using the parameters in $\mathcal{M}_{\vartheta}$. This representation obtained here could give some insight into the *order relation* in $\mathcal{M}_{\theta,L}$ and $\mathcal{M}_{\vartheta,L}$ for pure and mixed quantum systems. Therefore, the study of the order relation would afford one to investigate thermodynamic structure in a state space characterizing thermodynamics of quantum systems in terms of those parameters in $\mathcal{M}_{\theta,L}$ and $\mathcal{M}_{\vartheta,L}$. Finally, we note on the *third law*. In our representation, when the state is described by $|\Psi_j\rangle = b_{ij}|i\rangle$, where b_{ij} is the probability amplitude in a mixed ensemble, viz. the state of system is characterized by a *single* state for each ensemble *j*, entropy of the system takes the value of zero. Suppose $|i\rangle$ be an energy eigenstate of the system. The state is then described by $|\Psi_j\rangle = b_{ij}|i\rangle$ at the absolute zero temperature. Thus we draw from third law that in our representation the entropy $S \to 0$ as temperature $T \to 0$, where the energy of the system E_i corresponds to the lowest energy quantum state of the system. In summary, based on the mathematical foundation for quantum systems, we have obtained a representation of the basic laws (Zeroth, First, Second and Third Laws) in thermodynamics for quantum systems described by mixed quantum ensembles.

We hope that the present theory affords the mathematical foundation of the basic laws of quantum thermodynamics and the key to treat mixed quantum systems thermodynamically.

Acknowledgements

The authors appreciate unknown reviewers for their comments on the manuscript. One of the authors (H.T.) acknowledges the research grant from Hokkaido University of Education, which partly supported the present research.

Conflicts of Interest

The authors declare no conflicts of interest regarding the publication of this paper.

References

[1] Fermi, E. (1956) Thermodynamics, Dover, New York.

[2] Callen, H.B. (1985) Thermodynamics and an Introduction to Thermostatics. 2nd

Edition, Wiley, New York.

[3] Lieb, E.H. and Yngvason, J. (1999) *Physics Reports*, **310**, 1-96. https://doi.org/10.1016/S0370-1573(98)00082-9

[4] von Neumann, J.L. (1932) Mathematische Grundlagen der Quantenmechanik, Springer, Berlin. In: Beyer, E.T., Ed., (1955) Mathematical Foundations of Quantum Mechanics, Princeton University Press, Princeton.

[5] Peres, A. (1993) Quantum Theory: Concepts and Methods. Kluwer-Academic, Boston.

[6] Wehrl, A. (1978) *Reviews of Modern Physics*, **50**, 221. https://doi.org/10.1103/RevModPhys.50.221

[7] Partovi, M.H. (1989) *Physics Letters A*, **137**, 440-444. https://doi.org/10.1016/0375-9601(89)90221-1

[8] Bender, C.M., Brody, D.C. and Meister, B.K. (2000) *Journal of Physics A*, **33**, 4427-4436. https://doi.org/10.1088/0305-4470/33/24/302

[9] Suzuki, A. and Taira, H. (2018) *Journal of Modern Physics*, **9**, 2420-2436. https://doi.org/10.4236/jmp.2018.914155

[10] Isham, C. J. (1995) Lectures on Quantum Theory: Mathematical and Structural Foundations, Imperial College Press, London. https://doi.org/10.1142/p001

Journal of Modern Physics, 2020, 11, 528-534
https://www.scirp.org/journal/jmp
ISSN Online: 2153-120X
ISSN Print: 2153-1196

The Relativistic Rydberg's Formula in Greater Depth and for Any Atom

Espen Gaarder Haug

Norwegian University of Life Sciences, Ås, Norway
Email: espenhaug@mac.com

How to cite this paper: Haug, E.G. (2020) The Relativistic Rydberg's Formula in Greater Depth and for Any Atom. *Journal of Modern Physics*, **11**, 528-534.
https://doi.org/10.4236/jmp.2020.114035

Received: March 8, 2020
Accepted: April 6, 2020
Published: April 9, 2020

Abstract

K. Suto has recently pointed out an interesting relativistic extension of Rydberg's formula. Here we also discuss Rydberg's formula, and offer additional evidence on how one can easily see that it is non-relativistic and therefore a good approximation, at best, when $v \ll c$. We also extend the Suto formula to hold for any atom and examine the formula in detail.

Keywords

Rydberg's Formula, Relativistic Extension, Compton Wavelength

1. Introduction

Rydberg's [1] formula is given by

$$\frac{1}{\lambda} = R_\infty Z^2 \left(\frac{1}{n_1^2} - \frac{1}{n_2^2} \right) \tag{1}$$

where R_∞ is the Rydberg's constant, which has a value of 10,973,731.568160 (21) m^{-1} (NIST CODATA value). Even though the formula is very simple, the intuition behind the formula is hidden in Rydberg's constant and the way the formula is written. To truly understand what Rydberg's formula represents, we will take a close look at what is embedded in the formula.

Rydberg's constant is given by

$$R_\infty = \frac{m_e e^4}{8\epsilon_0^2 h^3 c}$$

$$R_\infty = \frac{\frac{\hbar}{\lambda_e}\frac{1}{c}\left(\sqrt{\frac{\hbar}{c}}\sqrt{\alpha}\sqrt{10^7}\right)^4}{8\epsilon_0^2 h^3 c}$$

$$R_\infty = \frac{\frac{\hbar^3}{\lambda_e}\frac{1}{c^3}\alpha^2\left(10^7\right)^2}{8\left(\frac{1}{4\pi c^2 10^{-7}}\right)^2 h^3 c}$$

$$R_\infty = \frac{\frac{\hbar^3}{\lambda_e}\frac{1}{c^3}\alpha^2}{8\frac{1}{16\pi^2 c^4}h^3 c}$$

$$R_\infty = \frac{1}{2}\frac{\hbar}{h}\frac{1}{\lambda_e}\alpha^2$$

$$R_\infty = \frac{1}{2}\frac{\frac{h}{2\pi}}{h}\frac{1}{\lambda_e}\alpha^2$$

$$R_\infty = \frac{\alpha^2}{4\pi\lambda_e} \tag{2}$$

Since the Compton [2] wavelength of the electron is given by[1]

$$\lambda_e = \frac{h}{m_e c} \tag{3}$$

This can be rewritten as

$$R_\infty = \frac{\alpha^2}{4\pi\frac{h}{m_e c}} = \frac{\alpha^2 m_e c}{4\pi h} \tag{4}$$

This is well known, so we have shown nothing new so far. Let us now replace this in Rydberg's formula, which gives

$$\frac{1}{\lambda} = \frac{\alpha^2 m_e c}{4\pi h} Z^2\left(\frac{1}{n_1^2} - \frac{1}{n_2^2}\right)$$

$$h\frac{c}{\lambda} = Z^2\left(\frac{1}{2}m_e\frac{\alpha^2 c^2}{n_1^2} - \frac{1}{2}m_e\frac{\alpha^2 c^2}{n_2^2}\right) \tag{5}$$

where $\frac{\alpha^2 c^2}{n_1^2}$ can be seen as v_1^2 and $\frac{\alpha^2 c^2}{n_2^2}$ as v_2^2. In other words, we can write this as

$$h\frac{c}{\lambda} = Z^2\left(\frac{1}{2}m_e v_1^2 - \frac{1}{2}m_e v_2^2\right) \tag{6}$$

and since $h\frac{c}{\lambda}$ is energy, we can write this as

$$E = Z^2\left(\frac{1}{2}m_e v_1^2 - \frac{1}{2}m_e v_2^2\right) \tag{7}$$

Rydberg's formula is thus the difference in the kinetic energy between two

[1]The original Compton derivation actually gives a non-relativistic Compton wave. That is, it is based on the assumption that the electron is standing still before being hit by photons. For more on the relativistic Compton wave, see [3].

electrons (or two states of an electron). However, it is well known that the kinetic energy formula of the form $E_k = \frac{1}{2}mv^2$ is the first order Taylor series approximation to the relativistic version of the formula. This approximation is only valid when $v \ll c$. In other words, Rydberg's formula is an approximation formula that only holds when the electron moves very slowly as compared to the speed of light. However, it may not be completely obvious or clearly acknowledged that Rydberg's formula is a non-relativistic approximation formula. Standard university textbooks on physics, for example, do not comment that the formula is, in reality, a non-relativistic approximation formula, see [4] and [5], for example.

Turning to a specific case, for a hydrogen atom, it is more precise to use the Rydberg constant

$$R_H = R_\infty \frac{m_P}{m_P + m_e} \tag{8}$$

this means we have

$$E = Z^2\left(\frac{1}{2}m_e v_1^2 - \frac{1}{2}m_e v_2^2\right)\frac{m_P}{m_P + m_e} \tag{9}$$

Before we move on to study relativistic effects, it is also worth mentioning that the Rydberg formula can be rewritten as

$$\begin{aligned} h\frac{c}{\bar{\lambda}} &= Z^2\left(\frac{1}{2}m_e\frac{\alpha^2c^2}{n_1^2} - \frac{1}{2}m_e\frac{\alpha^2c^2}{n_2^2}\right) \\ \frac{1}{\bar{\lambda}} &= Z^2\left(\frac{1}{2}\frac{1}{2\pi\bar{\lambda}_e}\frac{\alpha^2}{n_1^2} - \frac{1}{2}\frac{1}{2\pi\bar{\lambda}_e}\frac{\alpha^2}{n_2^2}\right) \\ \frac{1}{\bar{\lambda}} &= Z^2\left(\frac{1}{2}\frac{1}{\lambda}\frac{\alpha^2}{n_1^2} - \frac{1}{2}\frac{1}{\lambda_e}\frac{\alpha^2}{n_2^2}\right) \end{aligned} \tag{10}$$

To set the stage here, all we need to know to obtain the wavelength of the spectra from an atom is the Compton wavelength of the electron, the fine structure constant, and the atomic number. In a recent interesting paper by Suto [6], the author derives a relativistic Rydberg formula that contains the Compton wave of the electron, but he finds it strange that the standard Rydberg formula does not contain the Compton wavelength. In his own words:

> "However, Equation (8) for calculating the wavelength of the spectra of a hydrogen atom is strange because it does not include the Compton wavelength of the electron."

where his Equation (8) is the Rydberg formula, here formula 1. But as we can see by rewriting the standard Rydberg formula, the Compton wave of the electron is hidden inside the Rydberg constant, which is a composite constant consisting of more fundamental constants such as the fine structure constant and the Compton wave of the electron. This is clear from Equation (2), where we see the fine

structure constant and the Compton wave of the electron, as well as π.

2. The Relativistic Rydberg Formula

In the previous section, we observed that Rydberg's formula is a non-relativistic approximation. Recently, Suto [6] has published a relativistic Rydberg formula given by

$$\frac{1}{\bar{\lambda}} = \frac{1}{\bar{\lambda}_e}\left(\left(1-\frac{\alpha^2}{n_1^2}\right)^{-1/2} - \left(1-\frac{\alpha^2}{n_2^2}\right)^{-1/2}\right) \tag{11}$$

He also completes a Taylor series expansion series and gets

$$\frac{1}{\bar{\lambda}} = \frac{1}{\bar{\lambda}_e}\left(\left(1-\frac{\alpha^2}{2n_1^2}-\frac{3\alpha^4}{8n_1^4}+\frac{5\alpha^6}{16n_1^6}\right)-\left(1-\frac{\alpha^2}{2n_2^2}-\frac{3\alpha^4}{8n_2^4}+\frac{5\alpha^6}{16n_2^6}\right)\right) \tag{12}$$

Here may be a small mistake; we suggest that the correct Taylor expansion should be

$$\frac{1}{\bar{\lambda}} = \frac{1}{\bar{\lambda}_e}\left(\left(1-\frac{\alpha^2}{2n_1^2}+\frac{3\alpha^4}{8n_1^4}+\frac{5\alpha^6}{16n_1^6}\right)-\left(1-\frac{\alpha^2}{2n_2^2}+\frac{3\alpha^4}{8n_2^4}+\frac{5\alpha^6}{16n_2^6}\right)\right) \tag{13}$$

In other words, there is a problem with the signs. The error in the Taylor series expansion is likely also the reason the values in the table in his paper are not correct for the prediction of his model. Still, his main result and analysis are correct and we think the relativistic Rydberg formula deserves more attention. For one thing, the Suto formula is only for hydrogen atoms. For a hydrogen atom, the velocity of the electron is very slow, so the difference in predictions between the non-relativistic Rydberg formula and the relativistic formula of Suto is very small and probably not easily evaluated inside the error bounds in measurements.

However, for much heavier elements many of the electrons are moving considerably faster. Here we extend that formula to hold for any element and we get

$$\frac{h}{\lambda}c = \frac{m_e c^2}{\sqrt{1-\left(z^2\alpha^2/n_1^2\right)}} - m_e c^2 - \frac{m_e c^2}{\sqrt{1-\left(z^2\alpha^2/n_2^2\right)}} + m_e c^2$$

$$\frac{h}{\lambda}c = \frac{m_e c^2}{\sqrt{1-\left(z^2\alpha^2/n_1^2\right)}} - \frac{m_e c^2}{\sqrt{1-\left(z^2\alpha^2/n_2^2\right)}}$$

$$\frac{1}{\bar{\lambda}} = \frac{1}{\bar{\lambda}_e}\left(\frac{1}{\sqrt{1-\left(z^2\alpha^2/n_1^2\right)}} - \frac{1}{\sqrt{1-\left(z^2\alpha^2/n_2^2\right)}}\right) \tag{14}$$

where z is the atom/element number. Table 1 shows predictions from both the non-relativistic Rydberg formula and our relativistic formula for element 1 (Hydrogen) and up to element 137 (Feynmanium). Another interesting aspect here is that the Rydberg formula is somewhat linked to the Bohr model, which is obviously only an approximation. In practice, many predictions are done from quantum mechanics, such as results from the Dirac [7] equation. It is therefore

Table 1. The table shows the Rydberg formula predictions and the relativistic predictions for the first 137 elements. As we can see, the difference increases between the two models the higher the element number is. Here we are just looking at the case $n_1 = 1$ and $n_2 = 2$.

Atomic #	Rydberg formula	Relativistic formula	Diff.	Diff. %	Atomic #	Rydberg formula	Relativistic formula	Diff.	Diff. %
1	121.5023	121.4962	−0.0061	−0.0050%	71	0.0241	0.0144	−0.0097	−67.6%
2	30.3756	26.0315	−4.3440	−16.7%	72	0.0234	0.0139	−0.0096	−68.9%
3	13.5003	11.0414	−2.4589	−22.3%	73	0.0228	0.0134	−0.0094	−70.2%
4	7.5939	6.0710	−1.5229	−25.1%	74	0.0222	0.0129	−0.0093	−71.6%
5	4.8601	3.8329	−1.0272	−26.8%	75	0.0216	0.0125	−0.0091	−73.0%
6	3.3751	2.6374	−0.7377	−28.0%	76	0.0210	0.0121	−0.0090	−74.5%
7	2.4796	1.9247	−0.5549	−28.8%	77	0.0205	0.0116	−0.0088	−76.0%
8	1.8985	1.4659	−0.4326	−29.5%	78	0.0200	0.0112	−0.0087	−77.6%
9	1.5000	1.1533	−0.3467	−30.1%	79	0.0195	0.0109	−0.0086	−79.2%
10	1.2150	0.9308	−0.2842	−30.5%	80	0.0190	0.0105	−0.0085	−80.9%
11	1.0042	0.7668	−0.2373	−31.0%	81	0.0185	0.0101	−0.0084	−82.6%
12	0.8438	0.6425	−0.2013	−31.3%	82	0.0181	0.0098	−0.0083	−84.4%
13	0.7189	0.5460	−0.1729	−31.7%	83	0.0176	0.0095	−0.0082	−86.2%
14	0.6199	0.4696	−0.1503	−32.0%	84	0.0172	0.0092	−0.0081	−88.1%
15	0.5400	0.4081	−0.1319	−32.3%	85	0.0168	0.0088	−0.0080	−90.1%
16	0.4746	0.3579	−0.1168	−32.6%	86	0.0164	0.0085	−0.0079	−92.2%
17	0.4204	0.3163	−0.1042	−32.9%	87	0.0161	0.0083	−0.0078	−94.3%
18	0.3750	0.2815	−0.0935	−33.2%	88	0.0157	0.0080	−0.0077	−96.5%
19	0.3366	0.2521	−0.0845	−33.5%	89	0.0153	0.0077	−0.0076	−98.8%
20	0.3038	0.2270	−0.0768	−33.8%	90	0.0150	0.0075	−0.0075	−101.2%
21	0.2755	0.2054	−0.0701	−34.1%	91	0.0147	0.0072	−0.0075	−103.7%
22	0.2510	0.1867	−0.0643	−34.5%	92	0.0144	0.0070	−0.0074	−106.3%
23	0.2297	0.1704	−0.0593	−34.8%	93	0.0140	0.0067	−0.0073	−109.0%
24	0.2109	0.1561	−0.0548	−35.1%	94	0.0138	0.0065	−0.0073	−111.8%
25	0.1944	0.1436	−0.0509	−35.4%	95	0.0135	0.0063	−0.0072	−114.7%
26	0.1797	0.1324	−0.0473	−35.8%	96	0.0132	0.0061	−0.0071	−117.7%
27	0.1667	0.1225	−0.0442	−36.1%	97	0.0129	0.0058	−0.0071	−120.9%
28	0.1550	0.1136	−0.0414	−36.5%	98	0.0127	0.0056	−0.0070	−124.2%
29	0.1445	0.1056	−0.0389	−36.8%	99	0.0124	0.0054	−0.0070	−127.7%
30	0.1350	0.0984	−0.0366	−37.2%	100	0.0122	0.0053	−0.0069	−131.3%
31	0.1264	0.0919	−0.0346	−37.6%	101	0.0119	0.0051	−0.0068	−135.1%
32	0.1187	0.0860	−0.0327	−38.0%	102	0.0117	0.0049	−0.0068	−139.1%
33	0.1116	0.0806	−0.0310	−38.4%	103	0.0115	0.0047	−0.0067	−143.3%
34	0.1051	0.0757	−0.0294	−38.8%	104	0.0112	0.0045	−0.0067	−147.7%

Continued

35	0.0992	0.0712	−0.0280	−39.3%	105	0.0110	0.0044	−0.0067	−152.3%
36	0.0938	0.0671	−0.0267	−39.7%	106	0.0108	0.0042	−0.0066	−157.2%
37	0.0888	0.0633	−0.0254	−40.2%	107	0.0106	0.0040	−0.0066	−162.4%
38	0.0841	0.0598	−0.0243	−40.7%	108	0.0104	0.0039	−0.0065	−167.9%
39	0.0799	0.0566	−0.0233	−41.2%	109	0.0102	0.0037	−0.0065	−173.7%
40	0.0759	0.0536	−0.0223	−41.7%	110	0.0100	0.0036	−0.0065	−179.8%
41	0.0723	0.0508	−0.0214	−42.2%	111	0.0099	0.0034	−0.0064	−186.3%
42	0.0689	0.0483	−0.0206	−42.7%	112	0.0097	0.0033	−0.0064	−193.3%
43	0.0657	0.0459	−0.0199	−43.3%	113	0.0095	0.0032	−0.0064	−200.8%
44	0.0628	0.0436	−0.0191	−43.9%	114	0.0093	0.0030	−0.0063	−208.8%
45	0.0600	0.0415	−0.0185	−44.4%	115	0.0092	0.0029	−0.0063	−217.3%
46	0.0574	0.0396	−0.0178	−45.1%	116	0.0090	0.0028	−0.0063	−226.6%
47	0.0550	0.0378	−0.0172	−45.7%	117	0.0089	0.0026	−0.0062	−236.6%
48	0.0527	0.0360	−0.0167	−46.3%	118	0.0087	0.0025	−0.0062	−247.4%
49	0.0506	0.0344	−0.0162	−47.0%	119	0.0086	0.0024	−0.0062	−259.2%
50	0.0486	0.0329	−0.0157	−47.7%	120	0.0084	0.0023	−0.0062	−272.1%
51	0.0467	0.0315	−0.0152	−48.4%	121	0.0083	0.0021	−0.0062	−286.3%
52	0.0449	0.0301	−0.0148	−49.1%	122	0.0082	0.0020	−0.0061	−302.0%
53	0.0433	0.0289	−0.0144	−49.8%	123	0.0080	0.0019	−0.0061	−319.5%
54	0.0417	0.0277	−0.0140	−50.6%	124	0.0079	0.0018	−0.0061	−339.1%
55	0.0402	0.0265	−0.0136	−51.4%	125	0.0078	0.0017	−0.0061	−361.3%
56	0.0387	0.0255	−0.0133	−52.2%	126	0.0077	0.0016	−0.0061	−386.6%
57	0.0374	0.0244	−0.0130	−53.0%	127	0.0075	0.0015	−0.0061	−415.8%
58	0.0361	0.0235	−0.0126	−53.8%	128	0.0074	0.0013	−0.0061	−450.0%
59	0.0349	0.0226	−0.0123	−54.7%	129	0.0073	0.0012	−0.0061	−490.7%
60	0.0338	0.0217	−0.0121	−55.6%	130	0.0072	0.0011	−0.0061	−540.2%
61	0.0327	0.0209	−0.0118	−56.6%	131	0.0071	0.0010	−0.0061	−602.1%
62	0.0316	0.0201	−0.0115	−57.5%	132	0.0070	0.0009	−0.0061	−682.3%
63	0.0306	0.0193	−0.0113	−58.5%	133	0.0069	0.0008	−0.0061	−791.8%
64	0.0297	0.0186	−0.0111	−59.5%	134	0.0068	0.0006	−0.0061	−953.2%
65	0.0288	0.0179	−0.0108	−60.6%	135	0.0067	0.0005	−0.0062	−1224.9%
66	0.0279	0.0173	−0.0106	−61.7%	136	0.0066	0.0003	−0.0062	−1835.0%
67	0.0271	0.0166	−0.0104	−62.8%	137	0.0065	0.0001	−0.0064	−11273.7%
68	0.0263	0.0160	−0.0102	−63.9%					
69	0.0255	0.0155	−0.0101	−65.1%					
70	0.0248	0.0149	−0.0099	−66.3%					

not clear if the relativistic Rydberg formula has much to offer or not, but it is important for anyone interested in physics to know that it is, at best, a good approximation when the velocity of the electron is $v \ll c$.

3. Conclusion

Suto has recently published an interesting relativistic version of the Rydberg formula. Here we have added additional evidence and insight on how, after some reformulation, one can easily see that the Rydberg formula is simply a non-relativistic approximation. We have also extended the Suto relativistic formula to hold for any element. For those interested in this area of physics, further exploration may yield additional insights.

Conflicts of Interest

The author declares no conflicts of interest regarding the publication of this paper.

References

[1] Rydberg, J.R. (1890) *Philosophical Magazine*, **29**, 331-337. https://doi.org/10.1080/14786449008619945

[2] Compton, A.H. (1923) *Physical Review*, **21**, 210. https://doi.org/10.1103/PhysRev.21.483

[3] Haug, E.G. (2020) Derivation of a Relativistic Compton Wave. https://vixra.org/abs/2002.0523

[4] Walker, J.S. (2010) Physics. 4th Edition, Addison-Wesley, Boston.

[5] Freedman, R.A. and Young, H.D. (2016) University Physics with Modern Physics. 14th Edition, Pearson, London.

[6] Suto, K. (2020) *Journal of Modern Physics*, **11**, 294-303. https://doi.org/10.4236/jmp.2020.112018

[7] Dirac, P.A.M. (1928) The Quantum Theory of the Electron. *Proceedings of the Royal Society London A*, Vol. 117, 610-624. https://doi.org/10.1098/rspa.1928.0023

Journal of Modern Physics, 2020, 11, 535-564
https://www.scirp.org/journal/jmp
ISSN Online: 2153-120X
ISSN Print: 2153-1196

Classification of Relativity

Vu B. Ho

Advanced Study, 9 Adela Court, Mulgrave, Victoria, Australia
Email: vubho@bigpond.net.au

How to cite this paper: Ho, V.B. (2020) Classification of Relativity. *Journal of Modern Physics*, **11**, 535-564.
https://doi.org/10.4236/jmp.2020.114036

Received: March 20, 2020
Accepted: April 7, 2020
Published: April 10, 2020

Abstract

In this work, we discuss the possibility to classify relativity in accordance with the classification of second order partial differential equations that have been applied into the formulation of physical laws in physics. In mathematics, since second order partial differential equations can be classified into hyperbolic, elliptic or parabolic type, therefore we show that it is also possible to classify relativity accordingly into hyperbolic, elliptic or parabolic type by establishing coordinate transformations that preserve the forms of these second order partial differential equations. The coordinate transformation that preserves the form of the hyperbolic equation is the Lorentz transformation and the associated space is the hyperbolic, or pseudo-Euclidean, relativistic spacetime. Typical equations in physics that comply with hyperbolic relativity are Maxwell and Dirac equations. The coordinate transformation that preserves the form of the elliptic equation is the modified Lorentz transformation that we have formulated in our work on Euclidean relativity and the associated space is the elliptic, or Euclidean, relativistic spacetime. As we will show in this work, equations that comply with elliptic relativity are the equations that describe the subfields of Maxwell and Dirac field. And the coordinate transformation that preserves the form of the parabolic equation is the Euclidean transformation consisting of the translation and rotation in the spatial space and the associated space is the parabolic relativistic spacetime, which is a Euclidean space with a universal time. Typical equations in physics that comply with parabolic relativity are the diffusion equation, the Schrödinger equation and in particular the diffusion equations that are derived from the four-current defined in terms of the differentiable structures of the spacetime manifold, and the Ricci flow.

Keywords

Special Relativity, Elliptic Equation, Hyperbolic Equation, Parabolic Equation, Elliptic Relativity, Hyperbolic Relativity, Parabolic Relativity, Classification of Relativity, Maxwell and Dirac Field, Maxwell and Dirac Subfield

1. Introduction

In physics, it appears that physical objects are endowed with many different physical properties each of which couples to a physical field that obeys a specific physical law that can be described by a particular system of partial differential equations. It is also conventionally assumed, due to our ability of observing and perceiving of the natural environment, that physical events occur in a three-dimensional space and progress forward in one-dimensional time, even though it is conceivable to speculate that physical events may also progress backwards in time and occur in a higher dimensional space. From the physical laws that are derived and formulated from observation, a mathematical structure of space and time can be constructed to conform to the corresponding observed physical occurrences. In Newton physics since the established dynamical laws that describe the dynamics of material particles seem to obey the Galilean transformation of space and time therefore it is reasonable to assume that time is absolute. On the other hand, in Einstein physics, space and time are relative since it is established that Maxwell field equations of the electromagnetic field comply with the Lorentz transformation. Maxwell field equations are wave equations that describe the dynamics of a wave motion rather than that of a material particle. Until the quantum mechanics was invented which embraces the wave-particle dual characteristics of a material particle, it had been regarded that Newton and Maxwell dynamics are two different dynamics that describe physical systems that have completely different physical compositions, even though Newton himself speculated that the electromagnetic field is also composed of particles. The difficulty associated with the wave-particle duality may be due to the assumption that an elementary particle such as an electron is simply a mass-point with no internal structure. In fact, we have shown that it is possible to describe mathematically an elementary particle as a three-dimensional differentiable manifold whose mathematical structure can be expressed in terms of a Schrödinger wavefunction. Therefore, from the superposition principle associated with the wave motion and the assumption of internal structures of an elementary particle, we may assume that a physical property endowed to an elementary particle does not have to satisfy the requirements that are imposed on other physical properties of the particle but rather follows its own physical law that obeys its own type of relativity. For example, in quantum mechanics the time-independent Schrödinger wave equation describes the structure of atoms and it has been shown that atoms are stable and their physical structures are invariant with respect to translation and rotation, and we have also shown that the spin dynamics can be formulated by the Schrödinger equation in terms of intrinsic coordinates rather than the Dirac relativistic equation, therefore the Schrödinger equation should not be considered as a non-relativistic limit of Dirac relativistic equation but rather a physical formulation that follows its own relativity and as we will show later that the relativity that the Schrödinger equation obeys is the parabolic relativity, in the same way as Maxwell and Dirac field to comply with the pseudo-Euclidean

relativity.

In this work, we discuss a classification of relativity in which the spacetime manifold in which physical phenomena occur are classified into hyperbolic, elliptic or parabolic relativistic spacetime. Since the classification of relativity is closely related to the classification of second order partial differential equations therefore for reference we first outline the classification of the second order partial differential equations in Section 2, and the classification of relativity will be given in Section 4. A hyperbolic relativistic spacetime is a pseudo-Euclidean space that was formulated by Minkowski to establish a mathematical foundation for Einstein's theory of special relativity. That is a four-dimensional differentiable manifold which possesses a fundamental quadratic form of Lorentz signature that makes the wave equation invariant under Lorentz transformation [1]. On the other hand, we have shown in our work on the Euclidean relativity that quantum particles may possess physical properties that comply with the Euclidean relativity rather than the pseudo-Euclidean relativity. Since this type of relativity is associated with the elliptic equation therefore we will refer to the spacetime continuum whose mathematical structure complies with the Euclidean relativity an elliptic relativistic spacetime. And we have also shown in our work on Euclidean relativity that the elliptic equations are invariant under a modified Lorentz transformation, which is a rotation in spacetime [2] [3]. The two types of relativistic spacetime that we have considered depend essentially on the corresponding second order partial differential equations that are used to describe possible physical properties associated with a quantum particle. In fact, in Section 3 we show that the Euclidean relativity is the spacetime structure that is associated with the subfields of the Maxwell and Dirac field, in which the dynamics of the subfields is described by elliptic equations. In addition to the elliptic and hyperbolic relativity, in Section 4 we also discuss the parabolic relativity. As it is well-known that second order partial differential equations can be classified into three distinctive types of equations therefore it seems appropriate also to classify relativistic spacetime into three different types, and the third type of relativistic spacetime that we introduce in this work is the parabolic relativistic spacetime. Therefore, by definition, a parabolic relativistic spacetime is a space whose mathematical structure is determined by the invariance of a parabolic equation such as the diffusion equation and the Schrödinger wave equation in quantum mechanics. Overall, we assume that a quantum particle may have different physical properties which are described by different physical laws each of which is formulated independently in either the hyperbolic or the elliptic or the parabolic relativistic spacetime. All of these relativistic spaces can be regarded as different fibres of the fibre bundle of the spacetime continuum.

2. A Classification of Second Order Partial Differential Equations

A general second order partial differential equation can be written in the form:

$$\sum_{i=1}^{n}\sum_{j=1}^{n} a_{ij}\frac{\partial^2\psi}{\partial x_i \partial x_j} + \sum_{i=1}^{n} b_i \frac{\partial\psi}{\partial x_i} + c\psi + d = 0 \tag{1}$$

If the matrix $A = \left(a_{ij}\right)$ is symmetric then it can be transformed into a diagonal matrix by applying a diagonalising matrix M

$$M^{\mathrm{T}} AM = \begin{pmatrix} \lambda_1 & \cdots & 0 \\ \vdots & \ddots & \vdots \\ 0 & \cdots & \lambda_n \end{pmatrix} \tag{2}$$

Then the second order partial differential equation given in Equation (1) can be classified into three different types of partial differential equations as follows [4].

- If all eigenvalues λ_i are non-zero and have the same sign then Equation (1) is elliptic.
- If all eigenvalues λ_i are non-zero and have the same sign except for one of the eigenvalues then Equation (1) is hyperbolic.
- If exactly one of the eigenvalues is zero and all the others have the same sign then Equation (1) is parabolic. In this case, the matrix A is singular.

In this work, we consider the second order partial differential equations, and classify relativity accordingly, in the spacetime continuum in which space has three dimensions and time has one dimension therefore we only need to present the case of the partial differential equations in the four-dimensional space whose coordinates are specified by three spatial coordinates (x, y, z) and one temporal coordinate t. With this specification, the three different types of second order partial differential equations are given as follows:

- Elliptic equation can be written in the form

$$\frac{\partial^2\psi}{\partial t^2} + \frac{\partial^2\psi}{\partial x^2} + \frac{\partial^2\psi}{\partial y^2} + \frac{\partial^2\psi}{\partial z^2} = a\frac{\partial\psi}{\partial t} + b\frac{\partial\psi}{\partial x} + c\frac{\partial\psi}{\partial y} + d\frac{\partial\psi}{\partial z} + e\psi + f \tag{3}$$

We will show in the next section that elliptic equations in the four-dimensional spacetime manifold play an important role in the determination of the dynamics of the subfields of Maxwell and Dirac field [5]. Therefore, the subfields of Maxwell and Dirac field comply with the Euclidean relativity which we will classify as elliptic relativity in this work.

- Hyperbolic equation can be written in the form

$$\frac{\partial^2\psi}{\partial t^2} - \frac{\partial^2\psi}{\partial x^2} - \frac{\partial^2\psi}{\partial y^2} - \frac{\partial^2\psi}{\partial z^2} = a\frac{\partial\psi}{\partial t} + b\frac{\partial\psi}{\partial x} + c\frac{\partial\psi}{\partial y} + d\frac{\partial\psi}{\partial z} + e\psi + f \tag{4}$$

Hyperbolic equations play an important role in physics with Maxwell theory of the electromagnetic field and Dirac theory of quantum particles [6] [7]. In particular, the invariance of the hyperbolic equations under Lorentz transformation led Einstein to develop his theories of special and general relativity. We will classify Einstein relativity as hyperbolic relativity in this work.

- Parabolic equation can be written in the form

$$\frac{\partial^2\psi}{\partial x^2} + \frac{\partial^2\psi}{\partial y^2} + \frac{\partial^2\psi}{\partial z^2} = a\frac{\partial\psi}{\partial t} + b\frac{\partial\psi}{\partial x} + c\frac{\partial\psi}{\partial y} + d\frac{\partial\psi}{\partial z} + e\psi + f \tag{5}$$

We will classify as parabolic relativity for the mathematical structure of the spacetime manifold that makes the parabolic equations invariant. The important parabolic equations in physics are the diffusion equation, the Schrödinger equation, and diffusion equations that are derived from the four-current associated with the differentiable structure of the spacetime manifold and the Ricci flow. The parabolic relativity complies with the Euclidean transformation which consists of translation and rotation in the spatial space.

3. Subfield Structure of Maxwell and Dirac Field

In this section, we will discuss possible physical fields that comply with the elliptic equation given in Equation (3). We have shown in our previous works that both Maxwell field equations of the electromagnetic field and Dirac equation of massive quantum particles can be formulated from a general system of linear first order partial differential equations, and, as a consequence, the field equations of the two physical fields have many common features that specify characteristics that are not typical in classical physics [8] [9] [10] [11]. In the following, we further show the similarity between the Maxwell and Dirac field by examining the subfields that are coupled to form either of these two physical fields. We show that the subfields have the mathematical structures and physical properties that are essentially different from the coupled field of Maxwell, and that of Dirac. In particular, we show that the subfields of both Maxwell and Dirac field satisfy elliptic equations rather than hyperbolic equations therefore while Maxwell and Dirac field are described by wave equations therefore they comply with the laws of the pseudo-Euclidean relativity, the Maxwell and Dirac subfields are described by elliptic equations therefore they comply with those of the Euclidean relativity instead [12]. The fact that the subfields of Maxwell and Dirac fields are Euclidean relativistic has profound implications, such as they can be used to explain the stability of elementary particles because if elementary particles are represented by subfields which are described by elliptic equations then since elliptic equations are used to describe equilibrium states of physical systems therefore elementary particles associated with those subfields are also stable. Furthermore, if quantum particles possess physical properties that are represented by subfields which are described by elliptic equations, hence acting in accordance with the Euclidean relativity, then they can be used to explain physical phenomena that require physical transmissions with speeds greater than the speed of light in vacuum, such as the Einstein-Podosky-Rosen paradox in quantum entanglement [13] [14] [15].

The system of linear first order partial differential equations that we need to use in this work is given as follows [16] [17]

$$\sum_{i=1}^{n}\sum_{j=1}^{n} a_{ij}^{r}\frac{\partial \psi_i}{\partial x_j} = k_1\sum_{l=1}^{n} b_l^r \psi_l + k_2 c^r, \quad r = 1,2,\cdots,n \tag{6}$$

Equation (6) can be rewritten in a matrix form as:

$$\left(\sum_{i=1}^{n} A_i \frac{\partial}{\partial x_i}\right)\psi = k_1\sigma\psi + k_2 J \tag{7}$$

where $\psi = (\psi_1, \psi_2, \cdots, \psi_n)^{\mathrm{T}}$, $\partial\psi/\partial x_i = (\partial\psi_1/\partial x_i, \partial\psi_2/\partial x_i, \cdots, \partial\psi_n/\partial x_i)^{\mathrm{T}}$, A_i, σ and J are matrices representing the quantities a_{ij}^k, b_l^r and c^r, and k_1 and k_2 are undetermined constants. Now, if we apply the operator $\sum_{i=1}^{n} A_i \partial/\partial x_i$ on the left on both sides of Equation (7) then we obtain

$$\left(\sum_{i=1}^{n} A_i \frac{\partial}{\partial x_i}\right)\left(\sum_{j=1}^{n} A_j \frac{\partial}{\partial x_j}\right)\psi = \left(\sum_{i=1}^{n} A_i \frac{\partial}{\partial x_i}\right)\left(k_1\sigma\psi + k_2 J\right) \tag{8}$$

If we assume further that the coefficients a_{ij}^k and b_l^r are constants and $A_i\sigma = \sigma A_i$, then Equation (8) can be rewritten in the following form

$$\begin{aligned}&\left(\sum_{i=1}^{n} A_i^2 \frac{\partial^2}{\partial x_i^2} + \sum_{i=1}^{n}\sum_{j>i}^{n}\left(A_iA_j + A_jA_i\right)\frac{\partial^2}{\partial x_i \partial x_j}\right)\psi \\ &= k_1^2\sigma^2\psi + k_1k_2\sigma J + k_2\sum_{i=1}^{n} A_i \frac{\partial J}{\partial x_i}\end{aligned} \tag{9}$$

In order for the above systems of partial differential equations to be applied to physical phenomena, the matrices A_i must be determined. For the case of Maxwell and Dirac field, the matrices A_i must take a form so that Equation (9) reduces to a wave equation

$$\left(\sum_{i=1}^{n} A_i^2 \frac{\partial^2}{\partial x_i^2}\right)\psi = k_1^2\sigma^2\psi + k_1k_2\sigma J + k_2\sum_{i=1}^{n} A_i \frac{\partial J}{\partial x_i} \tag{10}$$

From Equation (9), for Dirac field, we simply require the matrices A_i to satisfy the conditions $A_iA_j + A_jA_i = 0$ and $A_i^2 = \pm 1$. However, for the case of Maxwell field, the conditions required for the matrices A_i can be determined from the classical form of Maxwell field equations [3] [18]. Furthermore, as shown in the next subsection, in order to reduce Equation (9) to Equation (10) for the case of Maxwell field, we will also need an extra condition on the components of the wavefuction ψ in the form of a divergence or Gauss's law

$$\sum_{i=1}^{n} \frac{\partial\psi_i}{\partial x_i} = \rho \tag{11}$$

In this work, we will discuss only Maxwell and Dirac field therefore we will set $\sigma = 1$.

3.1. Maxwell Field as a Coupling of Two Elliptic Fields

In this subsection, we show that Maxwell field of electromagnetism is a coupled field that is formed from the coupling of two subfields that satisfy an elliptic equation. In order to distinguish a field that satisfies an elliptic equation from a field that satisfies a hyperbolic equation, or wave equation, we refer to the former as an elliptic field and the latter as a hyperbolic field. From the general equation given in Equation (7), the two subfields that are coupled to form the Maxwell field can be rewritten in the following simple form:

$$\left(A_0 \frac{\partial}{\partial t} + A_1 \frac{\partial}{\partial x_1} + A_2 \frac{\partial}{\partial x_2} + A_3 \frac{\partial}{\partial x_3} \right) \psi = k_1 \psi + k_2 J \tag{12}$$

where $\psi = (\psi_1, \psi_2, \psi_3)^{\mathrm{T}}$ and $J = (j_1, j_2, j_3)^{\mathrm{T}}$, and the matrices A_i are given as follows

$$\begin{aligned} A_0 &= \mp \begin{pmatrix} 1 & 0 & 0 \\ 0 & 1 & 0 \\ 0 & 0 & 1 \end{pmatrix}, \; A_1 = \begin{pmatrix} 0 & 0 & 0 \\ 0 & 0 & -1 \\ 0 & 1 & 0 \end{pmatrix}, \\ A_2 &= \begin{pmatrix} 0 & 0 & 1 \\ 0 & 0 & 0 \\ -1 & 0 & 0 \end{pmatrix}, \; A_3 = \begin{pmatrix} 0 & -1 & 0 \\ 1 & 0 & 0 \\ 0 & 0 & 0 \end{pmatrix} \end{aligned} \tag{13}$$

In Equation (13), the negative sign, or negative time, in front of the matrix A_0 together with other matrices form one subfield and the positive sign, or positive time, in front of the matrix A_0 together with other matrices form another subfield. Then we obtain the following results

$$\begin{aligned} A_0^2 &= \begin{pmatrix} 1 & 0 & 0 \\ 0 & 1 & 0 \\ 0 & 0 & 1 \end{pmatrix}, \; A_1^2 = \begin{pmatrix} 0 & 0 & 0 \\ 0 & -1 & 0 \\ 0 & 0 & -1 \end{pmatrix}, \\ A_2^2 &= \begin{pmatrix} -1 & 0 & 0 \\ 0 & 0 & 0 \\ 0 & 0 & -1 \end{pmatrix}, \; A_3^2 = \begin{pmatrix} -1 & 0 & 0 \\ 0 & -1 & 0 \\ 0 & 0 & 0 \end{pmatrix} \end{aligned} \tag{14}$$

$$A_0 A_i + A_i A_0 = \mp 2 A_i \quad \text{for } i = 1, 2, 3 \tag{15}$$

$$\begin{aligned} A_1 A_2 + A_2 A_1 &= \begin{pmatrix} 0 & 1 & 0 \\ 1 & 0 & 0 \\ 0 & 0 & 0 \end{pmatrix}, \; A_1 A_3 + A_3 A_1 = \begin{pmatrix} 0 & 0 & 1 \\ 0 & 0 & 0 \\ 1 & 0 & 0 \end{pmatrix}, \\ A_2 A_3 + A_3 A_2 &= \begin{pmatrix} 0 & 0 & 0 \\ 0 & 0 & 1 \\ 0 & 1 & 0 \end{pmatrix} \end{aligned} \tag{16}$$

Using the matrices A_i given in Equation (13) with the negative sign for the matrix A_0 we obtain the following system of differential equations from Equation (12)

$$-\frac{\partial \psi_1}{\partial t} + \frac{\partial \psi_3}{\partial x_2} - \frac{\partial \psi_2}{\partial x_3} = k_1 \psi_1 + k_2 j_1 \tag{17}$$

$$-\frac{\partial \psi_2}{\partial t} - \frac{\partial \psi_3}{\partial x_1} + \frac{\partial \psi_1}{\partial x_3} = k_1 \psi_2 + k_2 j_2 \tag{18}$$

$$-\frac{\partial \psi_3}{\partial t} + \frac{\partial \psi_2}{\partial x_1} - \frac{\partial \psi_1}{\partial x_2} = k_1 \psi_3 + k_2 j_3 \tag{19}$$

Similarly, using the matrices A_i given in Equation (13) with the positive sign for the matrix A_0 we obtain the following system of differential equations from Equation (12)

$$\frac{\partial \psi_4}{\partial t}+\frac{\partial \psi_6}{\partial x_2}-\frac{\partial \psi_5}{\partial x_3}=k_1\psi_4+k_2 j_4 \tag{20}$$

$$\frac{\partial \psi_5}{\partial t}-\frac{\partial \psi_6}{\partial x_1}+\frac{\partial \psi_4}{\partial x_3}=k_1\psi_5+k_2 j_5 \tag{21}$$

$$\frac{\partial \psi_6}{\partial t}+\frac{\partial \psi_5}{\partial x_1}-\frac{\partial \psi_4}{\partial x_2}=k_1\psi_6+k_2 j_6 \tag{22}$$

In Equations (20)-(22), we have used different subscripts for the field components ψ_i because it is a different field from the field given in Equations (17)-(19). However, for simplicity, we have used the same k_1 and k_2 for the system of equations given in Equations (20)-(22) even though they may have different dimensional values from those given in Equations (17)-(19).

On the other hand, using the matrices A_i given in Equation (13) with negative sign for the matrix A_0 we obtain the following system of differential equations from Equation (9).

$$\begin{aligned}&\frac{\partial^2 \psi_1}{\partial t^2}-\frac{\partial^2 \psi_1}{\partial x_2^2}-\frac{\partial^2 \psi_1}{\partial x_3^2}-2\frac{\partial}{\partial t}\left(\frac{\partial \psi_3}{\partial x_2}-\frac{\partial \psi_2}{\partial x_3}\right)+\frac{\partial}{\partial x_1}\left(\frac{\partial \psi_2}{\partial x_2}+\frac{\partial \psi_3}{\partial x_3}\right)\\&=k_1^2\psi_1+k_1k_2 j_1+k_2\left(-\frac{\partial j_1}{\partial t}+\frac{\partial j_3}{\partial x_2}-\frac{\partial j_2}{\partial x_3}\right)\end{aligned} \tag{23}$$

$$\begin{aligned}&\frac{\partial^2 \psi_2}{\partial t^2}-\frac{\partial^2 \psi_2}{\partial x_1^2}-\frac{\partial^2 \psi_2}{\partial x_3^2}+2\frac{\partial}{\partial t}\left(\frac{\partial \psi_3}{\partial x_1}-\frac{\partial \psi_1}{\partial x_3}\right)+\frac{\partial}{\partial x_2}\left(\frac{\partial \psi_1}{\partial x_1}+\frac{\partial \psi_3}{\partial x_3}\right)\\&=k_1^2\psi_2+k_1k_2 j_2+k_2\left(-\frac{\partial j_2}{\partial t}+\frac{\partial j_1}{\partial x_3}-\frac{\partial j_3}{\partial x_1}\right)\end{aligned} \tag{24}$$

$$\begin{aligned}&\frac{\partial^2 \psi_3}{\partial t^2}-\frac{\partial^2 \psi_3}{\partial x_1^2}-\frac{\partial^2 \psi_3}{\partial x_2^2}-2\frac{\partial}{\partial t}\left(\frac{\partial \psi_2}{\partial x_1}-\frac{\partial \psi_1}{\partial x_2}\right)+\frac{\partial}{\partial x_3}\left(\frac{\partial \psi_1}{\partial x_1}+\frac{\partial \psi_2}{\partial x_2}\right)\\&=k_1^2\psi_3+k_1k_2 j_3+k_2\left(-\frac{\partial j_3}{\partial t}+\frac{\partial j_2}{\partial x_1}-\frac{\partial j_1}{\partial x_2}\right)\end{aligned} \tag{25}$$

Similarly, using the matrices A_i given in Equation (13) with positive sign for the matrix A_0 we obtain the following system of differential equations also from Equation (9).

$$\begin{aligned}&\frac{\partial^2 \psi_4}{\partial t^2}-\frac{\partial^2 \psi_4}{\partial x_2^2}-\frac{\partial^2 \psi_4}{\partial x_3^2}+2\frac{\partial}{\partial t}\left(\frac{\partial \psi_6}{\partial x_2}-\frac{\partial \psi_5}{\partial x_3}\right)+\frac{\partial}{\partial x_1}\left(\frac{\partial \psi_5}{\partial x_2}+\frac{\partial \psi_6}{\partial x_3}\right)\\&=k_1^2\psi_4+k_1k_2 j_4+k_2\left(\frac{\partial j_4}{\partial t}+\frac{\partial j_6}{\partial x_2}-\frac{\partial j_5}{\partial x_3}\right)\end{aligned} \tag{26}$$

$$\begin{aligned}&\frac{\partial^2 \psi_5}{\partial t^2}-\frac{\partial^2 \psi_5}{\partial x_1^2}-\frac{\partial^2 \psi_5}{\partial x_3^2}-2\frac{\partial}{\partial t}\left(\frac{\partial \psi_6}{\partial x_1}-\frac{\partial \psi_4}{\partial x_3}\right)+\frac{\partial}{\partial x_2}\left(\frac{\partial \psi_4}{\partial x_1}+\frac{\partial \psi_6}{\partial x_3}\right)\\&=k_1^2\psi_5+k_1k_2 j_5+k_2\left(\frac{\partial j_5}{\partial t}+\frac{\partial j_6}{\partial x_2}-\frac{\partial j_4}{\partial x_3}\right)\end{aligned} \tag{27}$$

$$\begin{aligned}&\frac{\partial^2 \psi_6}{\partial t^2}-\frac{\partial^2 \psi_6}{\partial x_1^2}-\frac{\partial^2 \psi_6}{\partial x_2^2}+2\frac{\partial}{\partial t}\left(\frac{\partial \psi_5}{\partial x_1}-\frac{\partial \psi_4}{\partial x_2}\right)+\frac{\partial}{\partial x_3}\left(\frac{\partial \psi_4}{\partial x_1}+\frac{\partial \psi_5}{\partial x_2}\right)\\&=k_1^2\psi_6+k_1k_2 j_6+k_2\left(\frac{\partial j_6}{\partial t}+\frac{\partial j_5}{\partial x_1}-\frac{\partial j_4}{\partial x_2}\right)\end{aligned} \tag{28}$$

The equations given in Equations (23)-(28) contain cross derivatives that involve both space and time. Even though the cross derivatives that involve the time coordinate can be removed by using the system of equations given in Equations (17)-(19) and Equations (20)-(22), the cross derivatives that involve the spatial coordinates can only be removed by imposing on the wave function ψ an additional condition that is commonly known as the divergence of a vector field as given in Equation (11). The divergence of a field in fact endows the field with a physical character and gives a direct relationship between a mathematical object and a physical entity. Using Equation (11), Gauss's laws for the field $\psi = \left(\psi_1, \psi_2, \psi_3\right)^{\mathrm{T}}$ and the field $\psi = \left(\psi_4, \psi_5, \psi_6\right)^{\mathrm{T}}$ are written as follows:

$$\frac{\partial \psi_1}{\partial x_1} + \frac{\partial \psi_2}{\partial x_2} + \frac{\partial \psi_3}{\partial x_3} = \rho_1 \tag{29}$$

$$\frac{\partial \psi_4}{\partial x_1} + \frac{\partial \psi_5}{\partial x_2} + \frac{\partial \psi_6}{\partial x_3} = \rho_2 \tag{30}$$

where ρ_1 and ρ_2 are physical quantities that can be identified with the electric and magnetic charge density. Using Equation (29) and Equations (17)-(19) then from Equations (23)-(25) we obtain the following system of equations:

$$\begin{aligned} &\frac{\partial^2 \psi_1}{\partial t^2} + \frac{\partial^2 \psi_1}{\partial x_1^2} + \frac{\partial^2 \psi_1}{\partial x_2^2} + \frac{\partial^2 \psi_1}{\partial x_3^2} + 2k_1 \frac{\partial \psi_1}{\partial t} \\ &= -k_1^2 \psi_1 - k_1 k_2 j_1 - k_2 \left(\frac{\partial j_1}{\partial t} + \frac{\partial j_3}{\partial x_2} - \frac{\partial j_2}{\partial x_3} \right) + \frac{\partial \rho_1}{\partial x_1} \end{aligned} \tag{31}$$

$$\begin{aligned} &\frac{\partial^2 \psi_2}{\partial t^2} + \frac{\partial^2 \psi_2}{\partial x_1^2} + \frac{\partial^2 \psi_2}{\partial x_2^2} + \frac{\partial^2 \psi_2}{\partial x_3^2} + 2k_1 \frac{\partial \psi_2}{\partial t} \\ &= -k_1^2 \psi_2 - k_1 k_2 j_2 - k_2 \left(\frac{\partial j_2}{\partial t} + \frac{\partial j_3}{\partial x_2} - \frac{\partial j_1}{\partial x_3} \right) + \frac{\partial \rho_1}{\partial x_2} \end{aligned} \tag{32}$$

$$\begin{aligned} &\frac{\partial^2 \psi_3}{\partial t^2} + \frac{\partial^2 \psi_3}{\partial x_1^2} + \frac{\partial^2 \psi_3}{\partial x_2^2} + \frac{\partial^2 \psi_3}{\partial x_1^2} + 2k_1 \frac{\partial \psi_3}{\partial t} \\ &= -k_1^2 \psi_3 - k_1 k_2 j_3 - k_2 \left(\frac{\partial j_3}{\partial t} + \frac{\partial j_2}{\partial x_1} - \frac{\partial j_1}{\partial x_2} \right) + \frac{\partial \rho_1}{\partial x_3} \end{aligned} \tag{33}$$

In order to obtain a system of differential equations that can be applied to the electromagnetic field we set $k_1 = 0$. Then Equations (31)-(33) reduce to the following system of equations:

$$\frac{\partial^2 \psi_1}{\partial t^2} + \frac{\partial^2 \psi_1}{\partial x_1^2} + \frac{\partial^2 \psi_1}{\partial x_2^2} + \frac{\partial^2 \psi_1}{\partial x_3^2} = -k_2 \left(\frac{\partial j_1}{\partial t} + \frac{\partial j_3}{\partial x_2} - \frac{\partial j_2}{\partial x_3} \right) + \frac{\partial \rho_1}{\partial x_1} \tag{34}$$

$$\frac{\partial^2 \psi_2}{\partial t^2} + \frac{\partial^2 \psi_2}{\partial x_1^2} + \frac{\partial^2 \psi_2}{\partial x_2^2} + \frac{\partial^2 \psi_2}{\partial x_3^2} = -k_2 \left(\frac{\partial j_2}{\partial t} + \frac{\partial j_3}{\partial x_2} - \frac{\partial j_1}{\partial x_3} \right) + \frac{\partial \rho_1}{\partial x_2} \tag{35}$$

$$\frac{\partial^2 \psi_3}{\partial t^2} + \frac{\partial^2 \psi_3}{\partial x_1^2} + \frac{\partial^2 \psi_3}{\partial x_2^2} + \frac{\partial^2 \psi_3}{\partial x_1^2} = -k_2 \left(\frac{\partial j_3}{\partial t} + \frac{\partial j_2}{\partial x_1} - \frac{\partial j_1}{\partial x_2} \right) + \frac{\partial \rho_1}{\partial x_3} \tag{36}$$

The equations given in Equations (34)-(36) are elliptic equations rather than hyperbolic or wave equations therefore these subfields are more suitable to rep-

resent stable quantum particles with invariant physical properties. Moreover, since elliptic equations comply with the Euclidean relativity instead of the pseudo-Euclidean relativity therefore there may exist some physical properties associated with quantum particles that can travel with speeds greater than the speed of light in vacuum, which is a speed limit of transmission for physical events that comply with the pseudo-Euclidean relativity.

Similarly, by using the matrices A_i given in Equation (13), Equations (26)-(28), Gauss's laws given in Equation (30), and $k_1 = 0$, a system of equations with the positive sign for the matrix A_0 can be obtained and given as follows:

$$\frac{\partial^2 \psi_4}{\partial t^2} + \frac{\partial^2 \psi_4}{\partial x_1^2} + \frac{\partial^2 \psi_4}{\partial x_2^2} + \frac{\partial^2 \psi_4}{\partial x_3^2} = -k_2 \left(-\frac{\partial j_4}{\partial t} + \frac{\partial j_6}{\partial x_2} - \frac{\partial j_5}{\partial x_3} \right) + \frac{\partial \rho_2}{\partial x_1} \tag{37}$$

$$\frac{\partial^2 \psi_5}{\partial t^2} + \frac{\partial^2 \psi_5}{\partial x_1^2} + \frac{\partial^2 \psi_5}{\partial x_2^2} + \frac{\partial^2 \psi_5}{\partial x_3^2} = -k_2 \left(-\frac{\partial j_5}{\partial t} + \frac{\partial j_6}{\partial x_2} - \frac{\partial j_4}{\partial x_3} \right) + \frac{\partial \rho_2}{\partial x_2} \tag{38}$$

$$\frac{\partial^2 \psi_6}{\partial t^2} + \frac{\partial^2 \psi_6}{\partial x_1^2} + \frac{\partial^2 \psi_6}{\partial x_2^2} + \frac{\partial^2 \psi_6}{\partial x_1^2} = -k_2 \left(-\frac{\partial j_6}{\partial t} + \frac{\partial j_5}{\partial x_1} - \frac{\partial j_4}{\partial x_2} \right) + \frac{\partial \rho_2}{\partial x_3} \tag{39}$$

The equations of the subfield with the positive sign for the matrix A_0 also satisfy elliptic equations rather than wave equations therefore they are also suitable to represent quantum particles with stable properties that accompany the stable properties associated with the field equations given in Equations (37)-(39).

Having shown the basic equations for the two subfields by using the matrices A_i with negative and positive time, each of which can be used to represent stable properties of quantum particles due to the fact that they satisfy elliptic equations rather than wave equations, we now show that a coupling of these two subfields can give rise to a coupled field that satisfies wave equations such as Maxwell field equations of the electromagnetic field. A coupled field from the two subfields with the matrices given in Equation (13) can be formulated by using the following coupled matrices.

$$\begin{aligned} A_0 &= \begin{pmatrix} -1 & 0 & 0 & 0 & 0 & 0 \\ 0 & -1 & 0 & 0 & 0 & 0 \\ 0 & 0 & -1 & 0 & 0 & 0 \\ 0 & 0 & 0 & 1 & 0 & 0 \\ 0 & 0 & 0 & 0 & 1 & 0 \\ 0 & 0 & 0 & 0 & 0 & 1 \end{pmatrix}, \quad A_1 = \begin{pmatrix} 0 & 0 & 0 & 0 & 0 & 0 \\ 0 & 0 & 0 & 0 & 0 & -1 \\ 0 & 0 & 0 & 0 & 1 & 0 \\ 0 & 0 & 0 & 0 & 0 & 0 \\ 0 & 0 & -1 & 0 & 0 & 0 \\ 0 & 1 & 0 & 0 & 0 & 0 \end{pmatrix}, \\ A_2 &= \begin{pmatrix} 0 & 0 & 0 & 0 & 0 & 1 \\ 0 & 0 & 0 & 0 & 0 & 0 \\ 0 & 0 & 0 & -1 & 0 & 0 \\ 0 & 0 & 1 & 0 & 0 & 0 \\ 0 & 0 & 0 & 0 & 0 & 0 \\ -1 & 0 & 0 & 0 & 0 & 0 \end{pmatrix}, \quad A_3 = \begin{pmatrix} 0 & 0 & 0 & 0 & -1 & 0 \\ 0 & 0 & 0 & 1 & 0 & 0 \\ 0 & 0 & 0 & 0 & 0 & 0 \\ 0 & -1 & 0 & 0 & 0 & 0 \\ 1 & 0 & 0 & 0 & 0 & 0 \\ 0 & 0 & 0 & 0 & 0 & 0 \end{pmatrix} \end{aligned} \tag{40}$$

Then we obtain the following results:

$$A_0^2=\begin{pmatrix}1&0&0&0&0&0\\0&1&0&0&0&0\\0&0&1&0&0&0\\0&0&0&1&0&0\\0&0&0&0&1&0\\0&0&0&0&0&1\end{pmatrix},\quad A_1^2=\begin{pmatrix}0&0&0&0&0&0\\0&-1&0&0&0&0\\0&0&-1&0&0&0\\0&0&0&0&0&0\\0&0&0&0&-1&0\\0&0&0&0&0&-1\end{pmatrix}$$

$$A_2^2=\begin{pmatrix}-1&0&0&0&0&0\\0&0&0&0&0&0\\0&0&-1&0&0&0\\0&0&0&-1&0&0\\0&0&0&0&0&0\\0&0&0&0&0&-1\end{pmatrix},\quad A_3^2=\begin{pmatrix}-1&0&0&0&0&0\\0&-1&0&0&0&0\\0&0&0&0&0&0\\0&0&0&-1&0&0\\0&0&0&0&-1&0\\0&0&0&0&0&0\end{pmatrix}$$

$$A_1A_2+A_2A_1=\begin{pmatrix}0&1&0&0&0&0\\1&0&0&0&0&0\\0&0&0&0&0&0\\0&0&0&0&1&0\\0&0&0&1&0&0\\0&0&0&0&0&0\end{pmatrix},\quad A_1A_3+A_3A_1=\begin{pmatrix}0&0&1&0&0&0\\0&0&0&0&0&0\\1&0&0&0&0&0\\0&0&0&0&0&1\\0&0&0&0&0&0\\0&0&0&1&0&0\end{pmatrix}$$

$$A_2A_3+A_3A_2=\begin{pmatrix}0&0&0&0&0&0\\0&0&1&0&0&0\\0&1&0&0&0&0\\0&0&0&0&0&0\\0&0&0&0&0&1\\0&0&0&0&1&0\end{pmatrix},\quad A_0A_i+A_iA_0=0\ \text{ for } i=1,2,3 \tag{41}$$

It is noticed from the results obtained in Equation (41) that by coupling the two subfields with negative and positive time the cross derivatives that involve time are automatically removed. This shows that the electromagnetic field may be considered as a resonant field which is formed from the superposition of two physical fields that flow in opposite temporal directions. Similar to the case of subfields, we also rewrite Equation (7) for the coupled field in the following simple form:

$$\left(A_0\frac{\partial}{\partial t}+A_1\frac{\partial}{\partial x_1}+A_2\frac{\partial}{\partial x_2}+A_3\frac{\partial}{\partial x_3}\right)\psi=k_1\psi+k_2J \tag{42}$$

where $\psi=\left(\psi_1,\psi_2,\psi_3,\psi_4,\psi_5,\psi_6\right)^{\mathrm{T}}$ and $J=\left(j_1,j_2,j_3,j_4,j_5,j_6\right)^{\mathrm{T}}$. Using the matrices given in Equation (40) we obtain the following system of equations for the coupled field from Equation (42):

$$-\frac{\partial\psi_1}{\partial t}+\frac{\partial\psi_6}{\partial x_2}-\frac{\partial\psi_5}{\partial x_3}=k_1\psi_1+k_2j_1 \tag{43}$$

$$-\frac{\partial\psi_2}{\partial t}+\frac{\partial\psi_4}{\partial x_3}-\frac{\partial\psi_6}{\partial x_1}=k_1\psi_2+k_2j_2 \tag{44}$$

$$-\frac{\partial \psi_3}{\partial t}+\frac{\partial \psi_5}{\partial x_1}-\frac{\partial \psi_4}{\partial x_2}=k_1\psi_3+k_2 j_3 \tag{45}$$

$$\frac{\partial \psi_4}{\partial t}+\frac{\partial \psi_3}{\partial x_2}-\frac{\partial \psi_2}{\partial x_3}=k_1\psi_4+k_2 j_4 \tag{46}$$

$$\frac{\partial \psi_5}{\partial t}+\frac{\partial \psi_1}{\partial x_3}-\frac{\partial \psi_3}{\partial x_1}=k_1\psi_5+k_2 j_5 \tag{47}$$

$$\frac{\partial \psi_6}{\partial t}+\frac{\partial \psi_2}{\partial x_1}-\frac{\partial \psi_1}{\partial x_2}=k_1\psi_6+k_2 j_6 \tag{48}$$

Using the results obtained for the matrices A_i given in Equation (41) we obtain the following system of equations for the coupled field from Equation (9):

$$\begin{aligned}&\frac{\partial^2\psi_1}{\partial t^2}-\frac{\partial^2\psi_1}{\partial x_2^2}-\frac{\partial^2\psi_1}{\partial x_3^2}+\frac{\partial}{\partial x_1}\left(\frac{\partial \psi_2}{\partial x_2}+\frac{\partial \psi_3}{\partial x_3}\right)\\&=k_1^2\psi_1+k_1k_2 j_1+k_2\left(-\frac{\partial j_1}{\partial t}+\frac{\partial j_6}{\partial x_2}-\frac{\partial j_5}{\partial x_3}\right)\end{aligned} \tag{49}$$

$$\begin{aligned}&\frac{\partial^2\psi_2}{\partial t^2}-\frac{\partial^2\psi_2}{\partial x_1^2}-\frac{\partial^2\psi_2}{\partial x_3^2}+\frac{\partial}{\partial x_2}\left(\frac{\partial \psi_1}{\partial x_1}+\frac{\partial \psi_3}{\partial x_3}\right)\\&=k_1^2\psi_2+k_1k_2 j_2+k_2\left(-\frac{\partial j_2}{\partial t}+\frac{\partial j_4}{\partial x_3}-\frac{\partial j_6}{\partial x_1}\right)\end{aligned} \tag{50}$$

$$\begin{aligned}&\frac{\partial^2\psi_3}{\partial t^2}-\frac{\partial^2\psi_3}{\partial x_1^2}-\frac{\partial^2\psi_3}{\partial x_2^2}+\frac{\partial}{\partial x_3}\left(\frac{\partial \psi_1}{\partial x_1}+\frac{\partial \psi_2}{\partial x_2}\right)\\&=k_1^2\psi_3+k_1k_2 j_3+k_2\left(-\frac{\partial j_3}{\partial t}+\frac{\partial j_5}{\partial x_1}-\frac{\partial j_4}{\partial x_2}\right)\end{aligned} \tag{51}$$

$$\begin{aligned}&\frac{\partial^2\psi_4}{\partial t^2}-\frac{\partial^2\psi_4}{\partial x_2^2}-\frac{\partial^2\psi_4}{\partial x_3^2}+\frac{\partial}{\partial x_1}\left(\frac{\partial \psi_5}{\partial x_2}+\frac{\partial \psi_6}{\partial x_3}\right)\\&=k_1^2\psi_4+k_1k_2 j_4+k_2\left(\frac{\partial j_4}{\partial t}+\frac{\partial j_3}{\partial x_2}-\frac{\partial j_2}{\partial x_3}\right)\end{aligned} \tag{52}$$

$$\begin{aligned}&\frac{\partial^2\psi_5}{\partial t^2}-\frac{\partial^2\psi_5}{\partial x_1^2}-\frac{\partial^2\psi_5}{\partial x_3^2}+\frac{\partial}{\partial x_2}\left(\frac{\partial \psi_4}{\partial x_1}+\frac{\partial \psi_6}{\partial x_3}\right)\\&=k_1^2\psi_5+k_1k_2 j_5+k_2\left(\frac{\partial j_5}{\partial t}+\frac{\partial j_1}{\partial x_3}-\frac{\partial j_3}{\partial x_1}\right)\end{aligned} \tag{53}$$

$$\begin{aligned}&\frac{\partial^2\psi_6}{\partial t^2}-\frac{\partial^2\psi_6}{\partial x_1^2}-\frac{\partial^2\psi_6}{\partial x_2^2}+\frac{\partial}{\partial x_3}\left(\frac{\partial \psi_4}{\partial x_1}+\frac{\partial \psi_5}{\partial x_2}\right)\\&=k_1^2\psi_6+k_1k_2 j_6+k_2\left(\frac{\partial j_6}{\partial t}+\frac{\partial j_2}{\partial x_1}-\frac{\partial j_1}{\partial x_2}\right)\end{aligned} \tag{54}$$

Using the divergence conditions or Gauss's laws given in Equations ((29), (30)) the system of equations given in Equations (49)-(54) reduces to the following system of equations:

$$\frac{\partial^2\psi_1}{\partial t^2}-\frac{\partial^2\psi_1}{\partial x_1^2}-\frac{\partial^2\psi_1}{\partial x_2^2}-\frac{\partial^2\psi_1}{\partial x_3^2}$$
$$=k_1^2\psi_1+k_1k_2j_1+k_2\left(-\frac{\partial j_1}{\partial t}+\frac{\partial j_6}{\partial x_2}-\frac{\partial j_5}{\partial x_3}\right)-\frac{\partial\rho_1}{\partial x_1} \quad (55)$$

$$\frac{\partial^2\psi_2}{\partial t^2}-\frac{\partial^2\psi_2}{\partial x_1^2}-\frac{\partial^2\psi_2}{\partial x_2^2}-\frac{\partial^2\psi_2}{\partial x_3^2}$$
$$=k_1^2\psi_2+k_1k_2j_2+k_2\left(-\frac{\partial j_2}{\partial t}+\frac{\partial j_4}{\partial x_3}-\frac{\partial j_6}{\partial x_1}\right)-\frac{\partial\rho_1}{\partial x_2} \quad (56)$$

$$\frac{\partial^2\psi_3}{\partial t^2}-\frac{\partial^2\psi_3}{\partial x_1^2}-\frac{\partial^2\psi_3}{\partial x_2^2}-\frac{\partial^2\psi_3}{\partial x_3^2}$$
$$=k_1^2\psi_3+k_1k_2j_3+k_2\left(-\frac{\partial j_3}{\partial t}+\frac{\partial j_5}{\partial x_1}-\frac{\partial j_4}{\partial x_2}\right)-\frac{\partial\rho_1}{\partial x_3} \quad (57)$$

$$\frac{\partial^2\psi_4}{\partial t^2}-\frac{\partial^2\psi_4}{\partial x_1^2}-\frac{\partial^2\psi_4}{\partial x_2^2}-\frac{\partial^2\psi_4}{\partial x_3^2}$$
$$=k_1^2\psi_4+k_1k_2j_4+k_2\left(\frac{\partial j_4}{\partial t}+\frac{\partial j_3}{\partial x_2}-\frac{\partial j_2}{\partial x_3}\right)-\frac{\partial\rho_2}{\partial x_1} \quad (58)$$

$$\frac{\partial^2\psi_5}{\partial t^2}-\frac{\partial^2\psi_5}{\partial x_1^2}-\frac{\partial^2\psi_5}{\partial x_2^2}-\frac{\partial^2\psi_5}{\partial x_3^2}$$
$$=k_1^2\psi_5+k_1k_2j_5+k_2\left(\frac{\partial j_5}{\partial t}+\frac{\partial j_1}{\partial x_3}-\frac{\partial j_3}{\partial x_1}\right)-\frac{\partial\rho_2}{\partial x_2} \quad (59)$$

$$\frac{\partial^2\psi_6}{\partial t^2}-\frac{\partial^2\psi_6}{\partial x_1^2}-\frac{\partial^2\psi_6}{\partial x_2^2}-\frac{\partial^2\psi_6}{\partial x_3^2}$$
$$=k_1^2\psi_6+k_1k_2j_6+k_2\left(\frac{\partial j_6}{\partial t}+\frac{\partial j_2}{\partial x_1}-\frac{\partial j_1}{\partial x_2}\right)-\frac{\partial\rho_2}{\partial x_3} \quad (60)$$

Now, to obtain Maxwell field equations of the electromagnetic field we set $k_1=0$ and the system of equations given in Equations (43)-(48) reduces to:

$$-\frac{\partial\psi_1}{\partial t}+\frac{\partial\psi_6}{\partial x_2}-\frac{\partial\psi_5}{\partial x_3}=k_2j_1 \quad (61)$$

$$-\frac{\partial\psi_2}{\partial t}+\frac{\partial\psi_4}{\partial x_3}-\frac{\partial\psi_6}{\partial x_1}=k_2j_2 \quad (62)$$

$$-\frac{\partial\psi_3}{\partial t}+\frac{\partial\psi_5}{\partial x_1}-\frac{\partial\psi_4}{\partial x_2}=k_2j_3 \quad (63)$$

$$\frac{\partial\psi_4}{\partial t}+\frac{\partial\psi_3}{\partial x_2}-\frac{\partial\psi_2}{\partial x_3}=k_2j_4 \quad (64)$$

$$\frac{\partial\psi_5}{\partial t}+\frac{\partial\psi_1}{\partial x_3}-\frac{\partial\psi_3}{\partial x_1}=k_2j_5 \quad (65)$$

$$\frac{\partial\psi_6}{\partial t}+\frac{\partial\psi_2}{\partial x_1}-\frac{\partial\psi_1}{\partial x_2}=k_2j_6 \quad (66)$$

By identifying $\boldsymbol{E}=(\psi_1,\psi_2,\psi_3)$, $\boldsymbol{B}=(\psi_4,\psi_5,\psi_6)$, $\boldsymbol{j}_1=(j_1,j_2,j_3)$ and $\boldsymbol{j}_2=(j_4,j_5,j_6)$ the system of equations given in Equations (61)-(66), together with Gauss's laws given in Equations ((29), (30)), can be rewritten in the familiar form in classical electrodynamics:

$$\nabla\cdot\boldsymbol{E}=\rho_1 \tag{67}$$

$$\nabla\cdot\boldsymbol{B}=\rho_2 \tag{68}$$

$$\nabla\times\boldsymbol{E}+\frac{\partial\boldsymbol{B}}{\partial t}=k_2\boldsymbol{j}_2 \tag{69}$$

$$\nabla\times\boldsymbol{B}-\frac{\partial\boldsymbol{E}}{\partial t}=k_2\boldsymbol{j}_1 \tag{70}$$

With $k_1=0$ we also obtain the following system of equations from Equations (55)-(60):

$$\frac{\partial^2\psi_1}{\partial t^2}-\frac{\partial^2\psi_1}{\partial x_1^2}-\frac{\partial^2\psi_1}{\partial x_2^2}-\frac{\partial^2\psi_1}{\partial x_3^2}=k_2\left(-\frac{\partial j_1}{\partial t}+\frac{\partial j_6}{\partial x_2}-\frac{\partial j_5}{\partial x_3}\right)-\frac{\partial\rho_1}{\partial x_1} \tag{71}$$

$$\frac{\partial^2\psi_2}{\partial t^2}-\frac{\partial^2\psi_2}{\partial x_1^2}-\frac{\partial^2\psi_2}{\partial x_2^2}-\frac{\partial^2\psi_2}{\partial x_3^2}=k_2\left(-\frac{\partial j_2}{\partial t}+\frac{\partial j_4}{\partial x_3}-\frac{\partial j_6}{\partial x_1}\right)-\frac{\partial\rho_1}{\partial x_2} \tag{72}$$

$$\frac{\partial^2\psi_3}{\partial t^2}-\frac{\partial^2\psi_3}{\partial x_1^2}-\frac{\partial^2\psi_3}{\partial x_2^2}-\frac{\partial^2\psi_3}{\partial x_3^2}=k_2\left(-\frac{\partial j_3}{\partial t}+\frac{\partial j_5}{\partial x_1}-\frac{\partial j_4}{\partial x_2}\right)-\frac{\partial\rho_1}{\partial x_3} \tag{73}$$

$$\frac{\partial^2\psi_4}{\partial t^2}-\frac{\partial^2\psi_4}{\partial x_1^2}-\frac{\partial^2\psi_4}{\partial x_2^2}-\frac{\partial^2\psi_4}{\partial x_3^2}=k_2\left(\frac{\partial j_4}{\partial t}+\frac{\partial j_3}{\partial x_2}-\frac{\partial j_2}{\partial x_3}\right)-\frac{\partial\rho_2}{\partial x_1} \tag{74}$$

$$\frac{\partial^2\psi_5}{\partial t^2}-\frac{\partial^2\psi_5}{\partial x_1^2}-\frac{\partial^2\psi_5}{\partial x_2^2}-\frac{\partial^2\psi_5}{\partial x_3^2}=k_2\left(\frac{\partial j_5}{\partial t}+\frac{\partial j_1}{\partial x_3}-\frac{\partial j_3}{\partial x_1}\right)-\frac{\partial\rho_2}{\partial x_2} \tag{75}$$

$$\frac{\partial^2\psi_6}{\partial t^2}-\frac{\partial^2\psi_6}{\partial x_1^2}-\frac{\partial^2\psi_6}{\partial x_2^2}-\frac{\partial^2\psi_6}{\partial x_3^2}=k_2\left(\frac{\partial j_6}{\partial t}+\frac{\partial j_2}{\partial x_1}-\frac{\partial j_1}{\partial x_2}\right)-\frac{\partial\rho_2}{\partial x_3} \tag{76}$$

Equations (71)-(76) can be rewritten in a vector form as a system of two equations as in classical electrodynamics:

$$\frac{\partial^2\boldsymbol{E}}{\partial t^2}-\nabla^2\boldsymbol{E}=\nabla(\rho_1)-k_2\frac{\partial\boldsymbol{J}_e}{\partial t}+k_2\nabla\times\boldsymbol{J}_2 \tag{77}$$

$$\frac{\partial^2\boldsymbol{B}}{\partial t^2}-\nabla^2\boldsymbol{B}=\nabla(\rho_2)-k_2\frac{\partial\boldsymbol{J}_b}{\partial t}+k_2\nabla\times\boldsymbol{J}_1 \tag{78}$$

where the charge density ρ_i and the current density $\boldsymbol{j}_i$ satisfy the conservation law

$$\nabla\cdot\boldsymbol{j}_i+\frac{\partial\rho_i}{\partial t}=0. \tag{79}$$

3.2. Dirac Field as a Coupling of Two Elliptic Fields

In this subsection, we will formulate Dirac field and subfields using the same procedure that we have applied to the Maxwell field of electromagnetism in the previous subsection. We have shown that Maxwell field is represented by matri-

ces of rank six but the two subfields that are coupled to form Maxwell field are represented by matrices of rank three. Now, as it has been known that Dirac equation is formulated with matrices of rank four which are built upon Pauli matrices therefore we will simply use Pauli matrices as the required matrices for the two subfields. The Dirac equation then can be seen as a coupling of two systems of field equations similar to the case of Maxwell field equations of the electromagnetic field. Although the formulation of Dirac equation we consider in this work is straightforward from the known results there are new features that emerge with regard to the nature of the subfields that are coupled to form the Dirac field, such as the subfields also satisfy elliptic equations and therefore comply with the Euclidean relativity instead of wave equations and the pseudo-Euclidean relativity. Except for the dimensions, these characteristics show that the quantum behaviours of both Maxwell and Dirac are similar when they are represented by the subfields. The Pauli matrices $A_i = \sigma_i$ that we use for Dirac subfields are given as follows:

$$\begin{aligned} A_0 &= \mp\begin{pmatrix} 1 & 0 \\ 0 & 1 \end{pmatrix},\ A_1 = \begin{pmatrix} 0 & 1 \\ 1 & 0 \end{pmatrix}, \\ A_2 &= \begin{pmatrix} 0 & -i \\ i & 0 \end{pmatrix},\ A_3 = \begin{pmatrix} 1 & 0 \\ 0 & -1 \end{pmatrix} \end{aligned} \tag{80}$$

We then obtain the following results:

$$A_i^2 = 1 \text{ and } A_i A_j + A_j A_i = 0 \text{ for } i, j = 0,1,2,3 \tag{81}$$

Using the Pauli matrices A_i given in Equation (80) with negative time we obtain the following system of differential equations from Equation (7):

$$-\frac{\partial \psi_1}{\partial t} + \frac{\partial \psi_2}{\partial x_1} - i\frac{\partial \psi_2}{\partial x_2} + \frac{\partial \psi_1}{\partial x_3} = k_1 \psi_1 + k_2 j_1 \tag{82}$$

$$-\frac{\partial \psi_2}{\partial t} + \frac{\partial \psi_1}{\partial x_1} + i\frac{\partial \psi_1}{\partial x_2} - \frac{\partial \psi_2}{\partial x_3} = k_1 \psi_2 + k_2 j_2 \tag{83}$$

Using the Pauli matrices A_i given in Equation (80) with positive time we obtain the following system of differential equations from Equation (7):

$$\frac{\partial \psi_3}{\partial t} + \frac{\partial \psi_4}{\partial x_1} - i\frac{\partial \psi_4}{\partial x_2} + \frac{\partial \psi_3}{\partial x_3} = k_1 \psi_3 + k_2 j_1 \tag{84}$$

$$\frac{\partial \psi_4}{\partial t} + \frac{\partial \psi_3}{\partial x_1} + i\frac{\partial \psi_3}{\partial x_2} - \frac{\partial \psi_4}{\partial x_3} = k_1 \psi_4 + k_2 j_2 \tag{85}$$

On the other hand, using the results obtained in Equation (81) with negative time we obtain the following equation for the components of the function $\psi = \left(\psi_1, \psi_2\right)^{\mathrm{T}}$ from Equation (9):

$$\begin{aligned} &\frac{\partial^2 \psi_1}{\partial t^2} + \frac{\partial^2 \psi_1}{\partial x_1^2} + \frac{\partial^2 \psi_1}{\partial x_2^2} + \frac{\partial^2 \psi_1}{\partial x_3^2} \\ &= k_1^2 \psi_1 + k_1 k_2 j_1 + k_2 \left(-\frac{\partial j_1}{\partial t} + \frac{\partial j_2}{\partial x_1} - i\frac{\partial j_2}{\partial x_2} + \frac{\partial j_1}{\partial x_3} \right) \end{aligned} \tag{86}$$

$$\begin{aligned}&\frac{\partial^2\psi_2}{\partial t^2}+\frac{\partial^2\psi_2}{\partial x_1^2}+\frac{\partial^2\psi_2}{\partial x_2^2}+\frac{\partial^2\psi_2}{\partial x_3^2}\\&=k_1^2\psi_2+k_1k_2j_2+k_2\left(-\frac{\partial j_2}{\partial t}+\frac{\partial j_1}{\partial x_1}+i\frac{\partial j_1}{\partial x_2}-\frac{\partial j_2}{\partial x_3}\right)\end{aligned}\tag{87}$$

Similarly, using the results obtained in Equation (81) with positive time we obtain the following equation for the components of the function $\psi=(\psi_3,\psi_4)^{\mathrm{T}}$ from Equation (9):

$$\begin{aligned}&\frac{\partial^2\psi_3}{\partial t^2}+\frac{\partial^2\psi_3}{\partial x_1^2}+\frac{\partial^2\psi_3}{\partial x_2^2}+\frac{\partial^2\psi_3}{\partial x_3^2}\\&=k_1^2\psi_3+k_1k_2j_3+k_2\left(\frac{\partial j_3}{\partial t}+\frac{\partial j_4}{\partial x_1}-i\frac{\partial j_4}{\partial x_2}+\frac{\partial j_3}{\partial x_3}\right)\end{aligned}\tag{88}$$

$$\begin{aligned}&\frac{\partial^2\psi_4}{\partial t^2}+\frac{\partial^2\psi_4}{\partial x_1^2}+\frac{\partial^2\psi_4}{\partial x_2^2}+\frac{\partial^2\psi_4}{\partial x_3^2}\\&=k_1^2\psi_4+k_1k_2j_4+k_2\left(\frac{\partial j_4}{\partial t}+\frac{\partial j_3}{\partial x_1}+i\frac{\partial j_3}{\partial x_2}-\frac{\partial j_4}{\partial x_3}\right)\end{aligned}\tag{89}$$

As in the case of the subfields of Maxwell field of the electromagnetic field, the equations given in Equations (86)-(89) are elliptic equations therefore they can be used to describe the steady states of physical systems, in particular they can be used to explain the stability of elementary particles. Furthermore, if quantum particles possess physical properties that are represented by subfields which are described by elliptic equations, hence complying with the Euclidean relativity, then they can be used to explain physical phenomena that require physical transmissions with speeds greater than the speed of light in vacuum, such as the Einstein-Podosky-Rosen paradox in quantum entanglement.

Now, as being well-known the coupled field which can be used to represent Dirac field is formulated by using the familiar gamma matrices γ^μ written in terms of the Pauli and unit matrices as:

$$\gamma_0=\begin{pmatrix}I&0\\0&-I\end{pmatrix},\ \gamma_i=\begin{pmatrix}0&\sigma_i\\-\sigma_i&0\end{pmatrix}\tag{90}$$

$$\begin{aligned}&\gamma_0=\begin{pmatrix}1&0&0&0\\0&1&0&0\\0&0&-1&0\\0&0&0&-1\end{pmatrix},\ \gamma_1=\begin{pmatrix}0&0&0&1\\0&0&1&0\\0&-1&0&0\\-1&0&0&0\end{pmatrix},\\&\gamma_2=\begin{pmatrix}0&0&0&-i\\0&0&i&0\\0&i&0&0\\-i&0&0&0\end{pmatrix},\ \gamma_3=\begin{pmatrix}0&0&1&0\\0&0&0&-1\\-1&0&0&0\\0&1&0&0\end{pmatrix}\end{aligned}\tag{91}$$

With $k_2=0$, Equation (7) reduces to Dirac equation for a free particle which is written in the form:

$$\gamma^\mu\partial_\mu\psi=-im\psi\tag{92}$$

Using the gamma matrices given in Equation (91), Dirac equation given in Equation (92) can be written out for the wavefunction $\psi = \left(\psi_1, \psi_2, \psi_3, \psi_4\right)^{\mathrm{T}}$ as

$$\frac{\partial \psi_1}{\partial t} + im\psi_1 = -\frac{\partial \psi_3}{\partial z} - \left(\frac{\partial}{\partial x} + i\frac{\partial}{\partial y}\right)\psi_4 \tag{93}$$

$$\frac{\partial \psi_2}{\partial t} + im\psi_2 = -\left(\frac{\partial}{\partial x} + i\frac{\partial}{\partial y}\right)\psi_3 + \frac{\partial \psi_4}{\partial z} \tag{94}$$

$$\frac{\partial \psi_3}{\partial t} - im\psi_3 = -\frac{\partial \psi_1}{\partial z} - \left(\frac{\partial}{\partial x} - i\frac{\partial}{\partial y}\right)\psi_2 \tag{95}$$

$$\frac{\partial \psi_4}{\partial t} - im\psi_4 = -\left(\frac{\partial}{\partial x} + i\frac{\partial}{\partial y}\right)\psi_1 - \frac{\partial \psi_2}{\partial z} \tag{96}$$

Dirac equation written as a system of linear first order partial differential equations given in Equations (93)-(96) suggests that matter wave can be interpreted as a coupling of two different physical subfields represented by the field $\left(\psi_1, \psi_2\right)$ and the field $\left(\psi_3, \psi_4\right)$ whose temporal rates of change will convert one field to the other. From the gamma matrices given in Equation (91) we obtain the following relations:

$$\gamma_0^2 = 1,\ \gamma_i^2 = -1 \text{ for } i = 1,2,3 \text{ and } \gamma_i\gamma_j + \gamma_j\gamma_i = 0 \text{ for } i \neq j \tag{97}$$

With the relations obtained in Equation (97), it can be shown that all components of Dirac wavefunction $\psi = \left(\psi_1, \psi_2, \psi_3, \psi_4\right)^{\mathrm{T}}$ satisfy the Klein-Gordon equation:

$$\frac{\partial^2 \psi_\mu}{\partial t^2} - \frac{\partial^2 \psi_\mu}{\partial x^2} - \frac{\partial^2 \psi_\mu}{\partial y^2} - \frac{\partial^2 \psi_\mu}{\partial z^2} = -m^2\psi_\mu \tag{98}$$

The Klein-Gordon equation is a wave equation that is Lorentz invariant in the pseudo-Euclidean space which was proposed and developed by Minkowski based on Einstein's theory of special relativity.

In fact, it is possible to formulate a coupled field that is similar to Dirac field from the subfields represented by the Pauli matrices but instead satisfies an elliptic equation rather than a wave equation. Such field therefore will be Euclidean invariant. Consider a coupled field that is formed from the subfields represented by Pauli matrices with the coupled matrices given as follows:

$$A_0 = \begin{pmatrix} -I & 0 \\ 0 & I \end{pmatrix},\ A_i = \begin{pmatrix} 0 & \sigma_i \\ \sigma_i & 0 \end{pmatrix} \tag{99}$$

Then we obtain the following results:

$$\gamma_0^2 = 1,\ \gamma_i^2 = 1 \text{ for } i = 1,2,3 \text{ and } \gamma_i\gamma_j + \gamma_j\gamma_i = 0 \text{ for } i \neq j \tag{100}$$

From the relations obtained in Equation (100), then it can be shown that all components of the wavefunction $\psi = \left(\psi_1, \psi_2, \psi_3, \psi_4\right)^{\mathrm{T}}$ satisfy the following elliptic equation:

$$\frac{\partial^2 \psi_\mu}{\partial t^2} + \frac{\partial^2 \psi_\mu}{\partial x^2} + \frac{\partial^2 \psi_\mu}{\partial y^2} + \frac{\partial^2 \psi_\mu}{\partial z^2} = -m^2\psi_\mu \tag{101}$$

As a further remark, we would like to mention here that we have formulated Maxwell and Dirac field essentially from a general system of linear first order partial differential equations which is a purely mathematical framework that can be used to formulate any physical theory that requires such mathematical structure, similar to the case of Laplace or Poisson's equation. Nonetheless, with such perspective, it has been suggested that they should be referred to as Maxwell-like and Dirac-like field equations instead of Maxwell and Dirac. The approach that we have used to formulate Maxwell and Dirac field is quite different from other mathematical methods such as gauge theories whose formulation is based on the variational principle [19] [20]. However, as we have shown in our work on the principle of least action that the variational principle with quantum objects may not lead to the least action as the principle is supposed to provide but only complies with Feynman's integral method of random paths or random surfaces, which itself is not related to the principle of least action [21]. Therefore, physical theories such as gauge theories that rely on the variational principle with a Lagrangian function to establish a deterministic least action should not be regarded as statistical theories therefore they are not in accordance with the current interpretation of the quantum theory which relies on the probability view for their interpretation of experimental results.

4. A Classification of Relativity

In this section, we show that relativity can be classified into three different types that are determined by the mathematical structures given to the spactime continuum so that it can manifest as three different types of relativistic spaces associated with the types of second order partial differential equations that are classified in Section 2. We call the spacetime continuum with the mathematical structure associated with the hyperbolic or wave equation a hyperbolic relativistic space and the corresponding relativity is the hyperbolic relativity. Similarly, we also define the elliptic and parabolic relativity. The problem that we address in this section is similar to our discussion on the fibre bundle structure of the spacetime continuum in which the spacetime continuum is the base space and all other physical events occur on different types of fibres and manifest in different physical forms that can be described by different mathematical structures [22]. We have shown that the spacetime structures result from different relationships between space and time and the apparent geometric and topological structures of the total spatiotemporal manifold are due to the dynamics and the geometric interactions of the decomposed cells from the base space of the total spatiotemporal manifold. The decomposed cells can form different types of fibres which may also geometrically interact with each other. In a more general context, we also discussed in detail a spacetime which has the mathematical structure of a 6-sphere bundle in which the dynamics of the fibres result from the geometric interactions of different types of decomposed cells that give rise to various relationships between space and time. In this case, it is assumed that we

can only perceive within our physical ability the appearance of the grown intrinsic geometric structures on the base space of the total spatiotemporal manifold and the base space itself may not be observable with a reasonable assumption that a physical object is not observable if it does not have any form of geometric interactions. It could be that the base space of the spatiotemporal manifold at the beginning was only a six-dimensional Euclidean spatiotemporal continuum R^6 which had no non-trivial geometric structures therefore contained no physical objects. As we have shown in our work on Maxwell and Dirac field with three-dimensional time [23], we can assume that the spatiotemporal manifold is described by a six-dimensional differentiable manifold M which is composed of a three-dimensional spatial manifold and a three-dimensional temporal manifold, in which all physical objects are embedded, then the manifold M can be decomposed in the form $M = M \# S_S^3 \# S_T^3$, where S_S^3 and S_T^3 are the spatial and temporal 3-sphere, respectively. It is expected that the mathematical formulation of possible fibres of the spatiotemporal manifold should be derived from a general line element $\mathrm{d}s^2 = g_{\alpha\beta}\mathrm{d}x^\alpha \mathrm{d}x^\beta$. In the following, however, we propose that the three types of relativity are classified in accordance with the classification of their corresponding coordinate transformations.

4.1. Hyperbolic Relativity

Hyperbolic relativity refers to the relativistic spacetime continuum with the mathematical structure of a pseudo-Euclidean space that associates with the hyperbolic type of the second order partial differential equations. In physics, the concept of a pseudo-Euclidean spacetime, or relativistic hyperbolic spacetime, was introduced by Minkowski in order to accommodate Einstein's theory of special relativity in which the coordinate transformation between the inertial frame S with spacetime coordinates (ct, x, y, z) and the inertial frame S' with coordinates (ct', x', y', z') are derived from the principle of relativity and the postulate of a universal speed c, which is assumed to be the speed of light in vacuum. The coordinate transformation is the Lorentz transformation:

$$\begin{aligned} &x' = \gamma(x - \beta ct), \quad y' = y, \quad z' = z, \\ &ct' = \gamma(-\beta x + ct) \end{aligned} \tag{102}$$

where $\beta = v/c$ and $\gamma = 1/\sqrt{1-\beta^2}$. It can be shown that the Minkowski spacetime interval $c^2t^2 - x^2 - y^2 - z^2$ is invariant under Lorentz transformation given in Equation (102). Now, in order to show that the hyperbolic equations are associated with the hyperbolic relativity, we need to show that the part that composes of the second order derivatives of the hyperbolic equation given in Equation (4) is invariant under Lorentz transformation. The Lorentz transformation and its inverse can be rewritten in the following forms:

$$x'^\mu = \Lambda^\mu{}_\nu x^\nu \quad \text{and} \quad x^\nu = \Lambda_\mu{}^\nu x'^\mu \tag{103}$$

where $x^\mu = (ct, x, y, z)$ and the Lorentz matrix $\Lambda^\mu{}_\nu$ and its inverse $\Lambda_\mu{}^\nu$ are given as:

$$\Lambda^{\mu}{}_{\nu}=\begin{pmatrix}\gamma & -\beta\gamma & 0 & 0\\ -\beta\gamma & \gamma & 0 & 0\\ 0 & 0 & 1 & 0\\ 0 & 0 & 0 & 1\end{pmatrix} \text{ and } \Lambda_{\mu}{}^{\nu}=\begin{pmatrix}\gamma & \beta\gamma & 0 & 0\\ \beta\gamma & \gamma & 0 & 0\\ 0 & 0 & 1 & 0\\ 0 & 0 & 0 & 1\end{pmatrix} \tag{104}$$

In order to show that the hyperbolic relativity associates with the hyperbolic type of second order partial differential equations we only need to show that the d'Alembert operator $\partial_{\mu}\partial^{\mu}=\partial^2/c^2\partial t^2-\nabla^2$ is invariant under Lorentz transformation, where the differential operators ∂_{μ} and ∂^{μ} are defined as $\partial_{\mu}=\left(\partial/c\partial t,\partial/\partial x,\partial/\partial y,\partial/\partial z\right)$ and $\partial^{\mu}=g^{\mu\nu}\partial_{\nu}=\left(-\partial/c\partial t,\partial/\partial x,\partial/\partial y,\partial/\partial z\right)^{\mathrm{T}}$. This can be seen by the fact that the differential operators ∂_{μ} and ∂^{μ} are vectors therefore by using the transformations $\partial'_{\mu}=\Lambda_{\mu}{}^{\nu}\partial_{\nu}$ and $\partial'^{\mu}=g^{\mu\nu}\partial'_{\nu}$ we then obtain $\partial'_{\mu}\partial'^{\mu}=\partial_{\mu}\partial^{\mu}$.

Now, it is remarkable that even though the concept of a relativistic hyperbolic spacetime originates from the invariance of Maxwell field equations under Lorentz transformation, Einstein was able to generalise it into a more general structure utilising the mathematics of differentiable manifold and the resulted theory has only been applied into the description of the gravitational field in which the electromagnetic field can only act as a source. And the only invariance that is required is the transformation of general coordinates. Einstein general relativity that complies with the hyperbolic relativity in curved spaces is represented in tensor form as $T_{\mu\nu}=k\left(R_{\mu\nu}-\frac{1}{2}Rg_{\mu\nu}+\Lambda g_{\mu\nu}\right)$. Then using the centrally symmetric gravitational field with Schwarzschild metric:

$$\mathrm{d}s^2=\mathrm{e}^{\psi}c^2\mathrm{d}t^2-\mathrm{e}^{\chi}\mathrm{d}r^2-r^2\left(\mathrm{d}\theta^2+\sin^2\theta\mathrm{d}\phi^2\right) \tag{105}$$

Schwarzschild solution can be found as:

$$\mathrm{d}s^2=\left(1-\frac{C}{r}\right)c^2\mathrm{d}t^2-\left(1-\frac{C}{r}\right)^{-1}\mathrm{d}r^2-r^2\left(\mathrm{d}\theta^2+\sin^2\theta\mathrm{d}\phi^2\right) \tag{106}$$

where $C=2MG/c^2$. From the Schwarzschild solution, Newton law of gravity can be obtained as an approximation. We show in the next subsection on the elliptic relativistic spacetime that this result can also be obtained from the elliptic or Euclidean relativity.

4.2. Elliptic Relativity

Elliptic relativity refers to the relativistic spacetime continuum with the mathematical structure of a Euclidean space that associates with the elliptic type of the second order partial differential equations. We have also shown in our work on Euclidean relativity that it is possible to construct a special relativistic transformation that will make the four-dimensional spacetime continuum a Euclidean space rather than a pseudo-Euclidean space as in the case of Einstein's theory of special relativity. Consider the following modified Lorentz transformation:

$$x'=\gamma_E\left(x-\beta ct\right),\ \ y'=y,\ \ z'=z,\ \ ct'=\gamma_E\left(\beta x+ct\right) \tag{107}$$

where $\beta = v/c$ and γ_E will be determined from the principle of relativity and the postulate of a universal speed. If we now assume the invariance of the Euclidean interval $c^2t^2 + x^2 + y^2 + z^2 = c^2t'^2 + x'^2 + y'^2 + z'^2$ then from the modified Lorentz transformation given in Equation (107), we obtain $\gamma_E = 1/\sqrt{1+\beta^2}$. It is seen from this expression for γ_E that there is no upper limit in the relative speed v between inertial frames. The value of γ_E at the universal speed $v = c$ is $\gamma_E = 1/\sqrt{2}$. For the values of $v \ll c$, the modified Lorentz transformation also reduces to the Galilean transformation. However, it is interesting to observe that when $v \to \infty$ we have $\gamma_E \to 0$ and $\beta\gamma_E \to 1$, and in this case, we have $x' \to -ct$ and $ct' \to x$. This result shows that there is a conversion between space and time when $v \to \infty$. We can also derive the relativistic kinematics from the modified Lorentz transformation, such as the transformation of a length, the transformation of a time interval and the transformation of velocities. Let L_0 be the proper length and Δt_0 is the proper time interval then the length and the time interval transformations can be found as $L = \sqrt{1+\beta^2}L_0$ and $\Delta t = \Delta t_0/\sqrt{1+\beta^2}$. It is observed from the length transformation that the length of a moving object is expanding rather than contracting as in Einstein theory of special relativity. It is also observed from the time interval transformation that the proper time interval is longer than the same time interval measured by a moving observer. With the modified Lorentz transformation, the transformation of velocities can be found as:

$$v_x' = \frac{v_x - \beta c}{1+\beta v_x/c},\quad v_y' = \frac{v_y}{\gamma_E\left(1+\beta v_x/c\right)},\quad v_z' = \frac{v_z}{\gamma_E\left(1+\beta v_x/c\right)} \tag{108}$$

From Equation (108), if we let $v_x = c$ then we obtain $v_x' = \left((c-v)/(c+v)\right)c$. Therefore in this case $v_x' = c$ only when the relative speed v between two inertial frames vanishes. In other words, the universal speed c is not the common speed of any moving physical object or physical field in inertial reference frames. In order to specify the nature of the assumed universal speed, we observe that in Einstein theory of special relativity it is assumed that spatial space of an inertial frame remains steady and this assumption is contradicted to Einstein theory of general relativity that shows that spatial space is actually expanding. Therefore it seems reasonable to suggest that the universal speed c in the modified Lorentz transformation is the universal speed of expansion of the spatial space of all inertial frames. The modified Lorentz transformation and its inverse can be rewritten in the following forms:

$$x'^{\mu} = \Lambda^{\mu}{}_{\nu}x^{\nu} \quad \text{and} \quad x^{\nu} = \Lambda_{\mu}{}^{\nu}x'^{\mu} \tag{109}$$

where $x^{\mu} = (ct, x, y, z)$ and the modified Lorentz matrix $\Lambda^{\mu}{}_{\nu}$ and its inverse $\Lambda_{\mu}{}^{\nu}$ are given as:

$$\Lambda^{\mu}{}_{\nu} = \begin{pmatrix} \gamma_E & \beta\gamma_E & 0 & 0 \\ -\beta\gamma_E & \gamma_E & 0 & 0 \\ 0 & 0 & 1 & 0 \\ 0 & 0 & 0 & 1 \end{pmatrix} \text{ and } \Lambda_{\mu}{}^{\nu} = \begin{pmatrix} \gamma_E & -\beta\gamma_E & 0 & 0 \\ \beta\gamma_E & \gamma_E & 0 & 0 \\ 0 & 0 & 1 & 0 \\ 0 & 0 & 0 & 1 \end{pmatrix} \tag{110}$$

In order to show that the elliptic relativity associates with the elliptic type of second order partial differential equations we only need to show that the Euclidean differential operator $\partial_\mu \partial^\mu = \partial^2/c^2\partial t^2 + \nabla^2$ is invariant under the modified Lorentz transformation given in Equation (20), where the differential operators ∂_μ and ∂^μ are defined as $\partial_\mu = (\partial/c\partial t, \partial/\partial x, \partial/\partial y, \partial/\partial z)$ and $\partial^\mu = g^{\mu\nu}\partial_\nu = (\partial/c\partial t, \partial/\partial x, \partial/\partial y, \partial/\partial z)^{\mathrm{T}}$. Since the differential operators ∂_μ and ∂^μ are vectors therefore by using the transformations $\partial'_\mu = \Lambda_\mu{}^\nu \partial_\nu$ and $\partial'^\mu = g^{\mu\nu}\partial'_\nu$ we then obtain $\partial'_\mu \partial'^\mu = \partial_\mu \partial^\mu$.

We assume that a general relativity that complies with the elliptic relativity in curved spaces can also be represented in tensor form as $T_{\mu\nu} = k\left(R_{\mu\nu} - \frac{1}{2}Rg_{\mu\nu} + \Lambda g_{\mu\nu}\right)$. Then using the centrally symmetric gravitational field with Schwarzschild-like metric:

$$\mathrm{d}s^2 = \mathrm{e}^{\psi}c^2\mathrm{d}t^2 + \mathrm{e}^{\chi}\mathrm{d}r^2 + r^2\left(\mathrm{d}\theta^2 + \sin^2\theta\mathrm{d}\phi^2\right) \tag{111}$$

Schwarzschild-like vacuum solution is found as:

$$\mathrm{d}s^2 = \left(1-\frac{C}{r}\right)c^2\mathrm{d}t^2 + \left(1-\frac{C}{r}\right)^{-1}\mathrm{d}r^2 + r^2\left(\mathrm{d}\theta^2 + \sin^2\theta\mathrm{d}\phi^2\right) \tag{112}$$

where $C = 2MG/c^2$. It can also be shown from the Schwarzschild-like solution given in Equation (112) that Newton law of gravity is obtained as an approximation [2].

4.3. Parabolic Relativity

We have shown that the hyperbolic and elliptic relativity are classified according to the mathematical structure of the second order derivatives of the second order partial differential equations $\sum_{i=1}^{n}\sum_{j=1}^{n} a_{ij}\,\partial^2\psi/\partial x_i\partial x_j$. For the hyperbolic relativity associated with the four-dimensional spacetime manifold we have $\sum_{i=1}^{n}\sum_{j=1}^{n} a_{ij}\,\partial^2\psi/\partial x_i\partial x_j = \partial^2\psi/\partial t^2 - \partial^2\psi/\partial x^2 - \partial^2\psi/\partial y^2 - \partial^2\psi/\partial z^2$. On the other hand, for the elliptic relativity we have $\sum_{i=1}^{n}\sum_{j=1}^{n} a_{ij}\,\partial^2\psi/\partial x_i\partial x_j = \partial^2\psi/\partial t^2 + \partial^2\psi/\partial x^2 + \partial^2\psi/\partial y^2 + \partial^2\psi/\partial z^2$. Now, for the case of the parabolic equation, because there are only three spatial components of second order derivatives for the four-dimensional spacetime continuum therefore as a consequence we consider the invariance of the parabolic equation only for these components under a parabolic coordinate transformation. Parabolic relativity refers to the relativistic spacetime continuum with the mathematical structure of a Euclidean space that associates with the parabolic type of the second order partial differential equations. There are many physical events that are described by the second order partial differential equations that involve only the spatial components of the second order derivatives therefore these physical events can be regarded as being associated with the parabolic relativity. In particular, the physical events that can be described by the diffusion equation and the Schrödinger equation that can be written generically as follows:

$$\frac{\partial^2\psi}{\partial x^2}+\frac{\partial^2\psi}{\partial y^2}+\frac{\partial^2\psi}{\partial z^2}=a\frac{\partial\psi}{\partial t} \tag{113}$$

In Equation (113), we obtain the diffusion equation if $a\partial\psi/\partial t\neq 0$ and the Schrödinger equation by setting $a\partial\psi/\partial t=-\left(i2m/\hbar\right)\partial\psi/\partial t$. As in the case of the hyperbolic and elliptic relativity in which the Lorentz and modified Lorentz transformation involve only the second order derivatives of the differential equations, therefore to discuss coordinate transformation for the parabolic equation we should also consider the second order derivatives which form the Laplace operator. Therefore the corresponding transformations for the parabolic equation that leave the Laplace operator unchanged, that is in the parabolic relativity we only consider the invariance of the Euclidean spatial interval $x^2+y^2+z^2=x'^2+y'^2+z'^2$. The time in parabolic relativity is therefore a universal time which is assumed to flow uniformly with the same rate in all reference systems. In general, the parabolic relativity is invariant with respect to the translation and rotation given as follows:

$$x_i'=x_i+a_i \quad \text{and} \quad x_i'=\sum_{j=1}^{n}b_{ij}x_j \tag{114}$$

where $\boldsymbol{x}=\left(x_1,x_2,\cdots,x_n\right)^{\mathrm{T}}$, and $A=\left\{a_i\right\}$ is a matrix for the translation and $B=\left\{b_{ij}\right\}$ is an orthogonal matrix for the rotation. If the matrix $B=\left\{b_{ij}\right\}$ is an orthogonal matrix then we have $\sum_{k=1}^{n}b_{ik}b_{jk}=\delta_i^j$, therefore we obtain the following result:

$$\nabla_x^2=\sum_{i=1}^{n}\left(\sum_{j,k=1}^{n}b_{ji}b_{ki}\frac{\partial^2}{\partial x_j'\partial x_k'}\right)=\sum_{j,k=1}^{n}\left(\sum_{i=1}^{n}b_{ji}b_{ki}\right)\frac{\partial^2}{\partial x_j'\partial x_k'}=\nabla_{x'}^2 \tag{115}$$

We now extend our discussion to a particular parabolic equation that is related to the curved structure of the spacetime manifold. We have shown in our work on the spacetime structure of quantum particles that they can be endowed with geometric and topological structures of differentiable manifolds and their motion should be described as isometric embeddings in higher Euclidean space that involve the diffusion equation. Fundamentally, we show that the three main dynamical descriptions of physical events in classical physics, namely Newton mechanics, Maxwell electromagnetism and Einstein gravitation, can be formulated in the same general covariant form and they can be represented by the general equation [8] [9]:

$$\nabla_\beta M=kJ \tag{116}$$

where M is a mathematical object that represents the corresponding physical system and ∇_β is a covariant derivative. For Newton mechanics, $M=\frac{1}{2}m\sum_{\mu=1}^{3}\left(\mathrm{d}x^\mu/\mathrm{d}t\right)^2+V$ and $J=0$. For Maxwell electromagnetism, $M=F^{\alpha\beta}=\partial^\mu A^\nu-\partial^\nu A^\mu$, with the four-vector potential $A^\mu\equiv\left(V,\boldsymbol{A}\right)$ and J can be identified with the electric and magnetic currents. And for Einstein gravitation, $M=R^{\alpha\beta}$ and J can be defined in terms of a metric $g_{\alpha\beta}$ and the Ricci

scalar curvature using the Bianchi identities $\nabla_\beta R^{\alpha\beta} = \frac{1}{2} g^{\alpha\beta} \nabla_\beta R$, that is, $J = \frac{1}{2} g^{\alpha\beta} \nabla_\beta R$. If we use the Bianchi identities as field equations for the gravitational field then Einstein field equations $T_{\mu\nu} = k\left(R_{\mu\nu} - \frac{1}{2} R g_{\mu\nu} + \Lambda g_{\mu\nu} \right)$, as in the case of the electromagnetic field, should be regarded as a definition for the energy-momentum tensor $T_{\mu\nu}$ for the gravitational field. From the definition of the four-current $j^\alpha = (\rho, \boldsymbol{j}_i) = \frac{1}{2} g^{\alpha\beta} \nabla_\beta R$ for the gravitational field, by comparing with the Poisson equation for a potential V in classical physics, $\nabla^2 V = 4\pi\rho$, we can identify the scalar potential V with the Ricci scalar curvature R and then obtain a diffusion equation:

$$\frac{\partial R}{\partial t} = k\left(\frac{\partial^2 R}{\partial x^2} + \frac{\partial^2 R}{\partial y^2} + \frac{\partial^2 R}{\partial z^2} \right) \tag{117}$$

whose solutions can be found to take the form:

$$R(x, y, z, t) = \left(\frac{M}{\left(\sqrt{4\pi k t}\right)^3} \right) \exp\left(-\frac{x^2 + y^2 + z^2}{4kt} \right) \tag{118}$$

which determines the probabilistic distribution of an amount of geometrical substance M which is defined via the Ricci scalar curvature R and manifests as observable matter. We have also shown that the Ricci scalar curvature R associated with a differentiable manifold can be expressed in terms of the Schrödinger wavefunction ψ in quantum mechanics. Now, instead of deriving a diffusion equation for the Ricci scalar curvature from the four-current we can also derive a diffusion equation for the Ricci scalar curvature from the Ricci flow by considering the case in which $J = \frac{1}{2} g^{\alpha\beta} \nabla_\beta R = 0$. Then we obtain the equation:

$$\nabla_\beta R^{\alpha\beta} = 0 \tag{119}$$

Since $\nabla_\mu g^{\alpha\beta} \equiv 0$ for a given metric tensor $g^{\alpha\beta}$, Equation (119) implies $R^{\alpha\beta} = \Lambda g^{\alpha\beta}$ which can be written in a covariant form as:

$$R_{\alpha\beta} = \Lambda g_{\alpha\beta} \tag{120}$$

where Λ is an undetermined constant. Using the identities $g_{\alpha\beta} g^{\alpha\beta} = 4$ and $g_{\alpha\beta} R^{\alpha\beta} = R$, we obtain $\Lambda = R/4$.

The Ricci flow can be derived from the field equation given in Equation (119) as follows [24] [25]. In differential geometry, the covariant derivative of a contravariant tensor of second rank $A^{\alpha\beta}$ is given by:

$$\nabla_\gamma A^{\alpha\beta} = \partial_\gamma A^{\alpha\beta} + \Gamma^\alpha_{\sigma\gamma} A^{\sigma\beta} + \Gamma^\beta_{\sigma\gamma} A^{\alpha\sigma} \tag{121}$$

The partial time derivative of Equation (121) is given as:

$$\begin{aligned} \partial_t \left(\nabla_\gamma A^{\alpha\beta} \right) = {} & \partial_t \left(\partial_\gamma A^{\alpha\beta} \right) + \left(\partial_t \Gamma^\alpha_{\sigma\gamma} \right) A^{\sigma\beta} + \Gamma^\alpha_{\sigma\gamma} \left(\partial_t A^{\sigma\beta} \right) \\ & + \left(\partial_t \Gamma^\beta_{\sigma\gamma} \right) A^{\alpha\sigma} + \Gamma^\beta_{\sigma\gamma} \left(\partial_t A^{\alpha\sigma} \right) \end{aligned} \tag{122}$$

Under the coordinate transformation $x'^{\alpha} = f^{\alpha}\left(x^{\beta}\right)$, the tensor $A^{\alpha\beta}$ is transformed as

$$A'^{\alpha\beta} = \frac{\partial x'^{\alpha}}{\partial x^{\rho}} \frac{\partial x'^{\beta}}{\partial x^{\sigma}} A^{\rho\sigma} \tag{123}$$

If the coordinate transformation is time-independent then the partial time derivative of the tensor $A^{\alpha\beta}$ is also a tensor which is transformed according to the rule:

$$\frac{\partial A'^{\alpha\beta}}{\partial t} = \frac{\partial x'^{\alpha}}{\partial x^{\rho}} \frac{\partial x'^{\beta}}{\partial x^{\sigma}} \frac{\partial A^{\rho\sigma}}{\partial t} \tag{124}$$

In this case, we have:

$$\nabla_{\gamma}\left(\partial_t A^{\alpha\beta}\right) = \partial_{\gamma}\left(\partial_t A^{\alpha\beta}\right) + \Gamma^{\alpha}_{\sigma\gamma}\left(\partial_t A^{\sigma\beta}\right) + \Gamma^{\beta}_{\sigma\gamma}\left(\partial_t A^{\alpha\sigma}\right) \tag{125}$$

It is observed from Equations (122) and (125) that if we impose the following condition on Equation (122):

$$\left(\partial_t \Gamma^{\alpha}_{\sigma\gamma}\right) A^{\sigma\beta} + \left(\partial_t \Gamma^{\beta}_{\sigma\gamma}\right) A^{\alpha\sigma} = 0 \tag{126}$$

then we obtain the identity:

$$\nabla_{\gamma}\left(\partial_t A^{\alpha\beta}\right) = \partial_t\left(\nabla_{\gamma} A^{\alpha\beta}\right) \tag{127}$$

In the case of a metric tensor $g^{\alpha\beta}$ then we have $\nabla_{\gamma}\left(\partial_t g^{\alpha\beta}\right) = \partial_t\left(\nabla_{\gamma} g^{\alpha\beta}\right) \equiv 0$, and from the field equations $\nabla_{\beta} R^{\alpha\beta} = 0$ we arrive at the Ricci flow:

$$\frac{\partial g_{\alpha\beta}}{\partial t} = kR_{\alpha\beta} \tag{128}$$

From Equation (128) we can obtain a diffusion equation for the Ricci scalar curvature as follows [26] [27]:

$$\frac{\partial R}{\partial t} = \Delta R + 2g^{\alpha\beta} g^{\gamma\sigma} R_{\alpha\sigma} R_{\beta\gamma} \tag{129}$$

As a further remark, it should be mentioned here that it has been shown that parabolic equations have associated invariants that may be related to physical properties of physical objects. For example, consider a linear second order parabolic partial differential equation in two independent variables x and t:

$$\frac{\partial \psi}{\partial t} + a(x,t)\frac{\partial^2 \psi}{\partial x^2} + b(x,t)\frac{\partial \psi}{\partial x} + c(x,t)\psi = 0 \tag{130}$$

It is shown that the form of the parabolic equation given in Equation (130) is invariant under the group of equivalence transformations which consists of the linear transformation of the dependent variable and the invertible transformations of the independent variables as follows:

$$\chi = \sigma(x,t)\psi, \quad t' = \varphi(t), \quad x' = \rho(x,t) \tag{131}$$

where $\sigma(x,t)$, $\varphi(t)$ and $\rho(x,t)$ are arbitrary functions [28] [29] [30]. The transformed equation of the equation given in Equation (131) then takes the form:

$$\frac{\partial \chi}{\partial t'} + a'(x',t')\frac{\partial^2 \chi}{\partial x'^2} + b'(x',t')\frac{\partial \chi}{\partial x'} + c'(x',t')\chi = 0 \tag{132}$$

Then an invariant of the parabolic equation given in Equation (130) is a function of the form

$$J = J\left(a, b, c, \frac{\partial a}{\partial t}, \frac{\partial a}{\partial x}, \frac{\partial b}{\partial t}, \frac{\partial b}{\partial x}, \frac{\partial c}{\partial t}, \frac{\partial c}{\partial x}, \frac{\partial^2 a}{\partial t^2}, \frac{\partial^2 a}{\partial t \partial x}, \frac{\partial^2 a}{\partial x^2}, \cdots\right). \tag{133}$$

4.4. Simultaneous Relativities

We have shown in previous subsections that the mathematical structure of the spacetime manifold can be classified in accordance with the classification of second order partial differential equations into hyperbolic, elliptic or parabolic relativistic space. On the other hand, normally a complex physical system such as an atom has various physical properties that involve different physical processes described by different types of second order partial differential equations in different relativities. If the physical properties associated with the physical system remain invariant then we can assume that they can be described independently by different second order partial differential equations, and hence their corresponding relativistic spaces should also exist independently from each other. As we have discussed in the introduction, these relativistic spaces may be considered as independent fibres of the spatiotemporal fibre bundle. Then in order to describe independent physical properties, we simply express all corresponding physical equations in all relativistic spaces simultaneously. For example, we assume that a physical system that possesses physical properties that can be described in the parabolic relativity and elliptic relativity respectively. If the parabolic property is massive and the elliptic property is massless then we have a simultaneous system of two equations that take the forms similar to the massive Schrödinger equation and massless Klein-Gordon equation as follows:

$$\frac{\partial^2 \psi_p}{\partial x^2} + \frac{\partial^2 \psi_p}{\partial y^2} + \frac{\partial^2 \psi_p}{\partial z^2} = -i\frac{2m}{\hbar}\frac{\partial \psi_p}{\partial t} \tag{134}$$

$$\frac{\partial^2 \psi_e}{c_e^2 \partial t^2} + \frac{\partial^2 \psi_e}{\partial x_1^2} + \frac{\partial^2 \psi_e}{\partial x_2^2} + \frac{\partial^2 \psi_e}{\partial x_3^2} = 0 \tag{135}$$

where ψ_p and ψ_e are wavefunctions in the parabolic and elliptic relativistic space respectively. We have also written c_e to indicate that, unlike the universal speed c in the hyperbolic relativity, the speed c_e may be very large according to the elliptic relativity. In an n-dimensional space, solutions to Laplace equation can be expressed by the Green function as $G = k\Big/\left(x_1^2 + x_2^2 + \cdots + x_n^2\right)^{\frac{n-2}{2}}$, hence for the Laplace equation given in Equation (135) with $n = 4$, we obtain the solution:

$$\psi_e = \frac{k}{c_e^2 t^2 + x^2 + y^2 + z^2} \tag{136}$$

It is seen that if c_e is very large then while other parabolic relativistic proper-

ties of a quantum particle remain the same the elliptic properties vanish quickly with time, and in particular this result may be invoked to explain the EPR paradox in quantum mechanics. However, if different physical properties belong to the same type of relativity then we can express the total equation as a sum of different equations in the same relativistic space, as in the case we have shown in our work on spin dynamics that a total Schrödinger equation can be written as a sum of two separate Schrödinger equations in two different coordinate systems, one of them can be considered as intrinsic. This can be outlined as follows. Instead of introducing a spin operator, we introduce a differential operator that depends on an intrinsic coordinate system and can be used to formulate a spin dynamics. Since spin angular momentum and orbital angular momentum are similar in nature therefore it is possible to suggest that the spin operator in the intrinsic coordinate system should also have similar form to that of the orbital angular momentum operator. From this perspective, we can write a Schrödinger wave equation that is used to describe both the orbital and spin dynamics as follows [31]:

$$\begin{aligned} &-\frac{\hbar^2}{2\mu}\nabla^2\Psi\left(\boldsymbol{r},\boldsymbol{r}_s\right)+V\left(\boldsymbol{r}\right)\Psi\left(\boldsymbol{r},\boldsymbol{r}_s\right)-\frac{\hbar^2}{2\mu_s}\nabla_s^2\Psi\left(\boldsymbol{r},\boldsymbol{r}_s\right) \\ &+V_s\left(\boldsymbol{r}_s\right)\Psi\left(\boldsymbol{r},\boldsymbol{r}_s\right)=E\Psi\left(\boldsymbol{r},\boldsymbol{r}_s\right) \end{aligned} \tag{137}$$

The quantity μ can be identified with a reduced mass. However, since we are treating spin angular momentum as a particular case of angular momentum therefore we retain the Planck constant and the quantity μ_s also retains the dimension of mass. We call the quantity μ_s an intrinsic mass and it could be related to the curvature that determines the differential geometric and topological structure of a quantum particle, as in the case of Bohr model, or charge. On the other hand, the quantity $V\left(\boldsymbol{r}\right)$ can be identified with normal potential, such as Coulomb potential but the quantity $V_s\left(\boldsymbol{r}_s\right)$ represents an intrinsic potential that depends on physical intrinsic properties associated with the spin angular momentum of a quantum particle. Since the two dynamics are independent, the wave equation given in Equation (137) is separable and the total wavefunction $\Psi\left(\boldsymbol{r},\boldsymbol{r}_s\right)$ can be written as a product of two wavefunctions as $\Psi\left(\boldsymbol{r},\boldsymbol{r}_s\right)=\psi\left(\boldsymbol{r}\right)\chi\left(\boldsymbol{r}_s\right)$. Then Equation (137) is separated into two equations as follows:

$$-\frac{\hbar^2}{2\mu}\nabla^2\psi\left(\boldsymbol{r}\right)+V\left(\boldsymbol{r}\right)\psi\left(\boldsymbol{r}\right)=E_0\psi\left(\boldsymbol{r}\right) \tag{138}$$

$$-\frac{\hbar^2}{2\mu_s}\nabla_s^2\chi\left(\boldsymbol{r}_s\right)+V_s\left(\boldsymbol{r}_s\right)\chi\left(\boldsymbol{r}_s\right)=E_1\chi\left(\boldsymbol{r}_s\right) \tag{139}$$

where $E_0+E_1=E$. For the case of the hydrogen atom then the total energy spectrum can be found as the sum of two energy spectra as:

$$E\left(n,n_s,m_s\right)=-\frac{\mu}{2\hbar^2}\left(\frac{Zq^2}{4\pi\varepsilon_0}\right)^2\frac{1}{n^2}-\frac{A_s\mu_s}{2\hbar^2\left(n_s+m_s+\frac{1}{2}\right)^2} \tag{140}$$

It is seen that the total energy spectrum has a fine structure depending on the

intrinsic quantum numbers n_s and m_s. Furthermore, the total energy spectrum also depends on the undetermined physical quantities μ_s and A_s that define the intrinsic properties of a quantum particle, which is the electron in this case. Without restriction, the quantity μ_s can take zero, positive or negative values. Similarly, it is also possible to explain the wave-particle duality by writing simultaneous equations for a quantum particle in the parabolic and hyperbolic relativistic space respectively. If an experiment is designed to detect an invariance associated with a quantum particle which is invariant in the parabolic relativity then it appears as a particle, but if it is invariant in the hyperbolic relativity then it appears as a wave. The formulation of dual properties of particle and wave in two coexisting relativistic spaces may be viewed as a representation of the hidden variable theory and de Broglie theory of double solution in wave mechanics [32] [33].

5. Conclusion

We have shown in this work the possibility to classify relativity in accordance with the classification of second order partial differential equations that have been applied into the formulation of physical laws in physics. Based on the classification of second order partial differential equations into hyperbolic, elliptic or parabolic type, we suggested that relativity should also be classified accordingly into hyperbolic, elliptic or parabolic type by establishing coordinate transformations that preserve the forms of the second order partial differential equations. The coordinate transformation that preserves the form of the hyperbolic equation is the Lorentz transformation and the associated space is the hyperbolic, or pseudo-Euclidean, relativistic spacetime. The coordinate transformation that preserves the form of the elliptic equation is the modified Lorentz transformation, or rotation in spacetime, that we have formulated in our work on Euclidean relativity and the associated space is the elliptic, or Euclidean, relativistic spacetime. And the coordinate transformation that preserves the form of the parabolic equation is the Euclidean transformation consisting of the translation and rotation in the spatial space and the associated space is the parabolic relativistic spacetime, which is a Euclidean space with a universal time. Besides the typical equations in physics that comply with hyperbolic relativity such as Maxwell and Dirac equations, we have also established equations that comply with elliptic relativity and these equations can be used to describe the subfields of Maxwell and Dirac field. On the other hand, apart from the typical equations in physics that comply with parabolic relativity such as the diffusion equation, the Schrödinger equation, we have shown that the diffusion equations that are derived from the four-current defined in terms of the differentiable structures of the spacetime manifold and the Ricci flow also belong to parabolic relativity.

Acknowledgements

We would like to thank the reviewers for their constructive comments and we

would also like to thank Jane Gao of the administration of JMP for her editorial advice during the preparation of this work.

Conflicts of Interest

The author declares no conflicts of interest regarding the publication of this paper.

References

[1] Einstein, A. (1952) The Principle of Relativity. Dover Publications, New York.

[2] Ho, V.B. (2017) Euclidean Relativity.

[3] Schliewe, J. (2019) *Open Physics*, **17**, 731-742. https://doi.org/10.1515/phys-2019-0077

[4] Strauss, W.A. (1992) Partial Differential Equation. John Wiley & Sons, Inc., New York.

[5] Ho, V.B. (2019) On the Nature of Maxwell and Dirac Field.

[6] Jackson, J.D. (1975) Classical Electrodynamics. John Wiley & Sons, New York.

[7] Dirac, P.A.M. (1928) *Proceedings of the Royal Society A*: *Mathematical*, *Physical and Engineering Sciences*, **117**, 610-624. https://doi.org/10.1098/rspa.1928.0023

[8] Ho, V.B. (2018) *International Journal of Physics*, **6**, 105-115. https://doi.org/10.12691/ijp-6-4-2

[9] Ho, V.B. (2018) *GJSFR-A*, **18**, 37-58.

[10] Ho, V.B. (2018) *Journal of Modern Physics*, **9**, 2402-2419. https://doi.org/10.4236/jmp.2018.914154

[11] Ho, V.B. (2018) Fluid State of the Electromagnetic Field.

[12] Ho, V.B. (2017) On the Motion of Quantum Particles and Euclidean Relativity.

[13] Einstein, A., Podolsky, B. and Rosen, N. (1935) *Physical Review*, **47**, 777-780. https://doi.org/10.1103/PhysRev.47.777

[14] Bell, J.S. (1964) *Physics*, **1**, 195-290. https://doi.org/10.1103/PhysicsPhysiqueFizika.1.195

[15] Rosenfeld, W., Burchardt, D., Garthoff, R., Redeker, K., Ortegel, N., Rau, M. and Weinfurter, H. (2017) *Physical Review Letters*, **119**, Article ID: 010402. https://doi.org/10.1103/PhysRevLett.119.010402

[16] Melshko, S.V. (2005) Methods for Constructing Exact Solutions of Partial Differential Equations. Springer Science & Business Media, Berlin.

[17] Sobolev, S.L. (1964) Partial Differential Equations of Mathematical Physics. Dover Publications, Inc., New York.

[18] Landau, L.D. and Lifshitz, E.M. (1987) The Classical Theory of Fields. Pergamon Press, Sydney.

[19] Lopes, J.L. (2011) Gauge Field Theories: An Introduction. Pergamon Press, Sydney.

[20] Lim Zheng Liang (2019) Aspects of Newton Cartan Gauge Theory. National University of Singapore, Singapore.

[21] Ho, V.B. (2018) *International Journal of Physics*, **6**, 47-52. https://doi.org/10.12691/ijp-6-2-4

[22] Ho, V.B. (2018) On the Geometric Structure of the Spatiotemporal Manifold.

[23] Ho, V.B. (2019) Maxwell and Dirac Field with Three-Dimensional Time.

[24] Ho, V.B. (2017) A Derivation of the Ricci Flow.

[25] Ho, V.B. (2017) A Covariant Ricci Flow.

[26] Richard, S. and Hamilton, R.S. (1982) *Journal of Differential Geometry*, **17**, 255-306. https://doi.org/10.4310/jdg/1214436922

[27] Cao, H.-D. and Zhu, X.-P. (2006) *The Asian Journal of Mathematics*, **10**, 165-492. https://doi.org/10.4310/AJM.2006.v10.n2.a2

[28] Ibragimov, N.H., Meleshko, S.V. and Thailert, E. (2008) *Communications in Nonlinear Science and Numerical Simulation*, **13**, 277-284. https://doi.org/10.1016/j.cnsns.2006.03.017

[29] Ibragimov, N.H. (2009) *Communications in Nonlinear Science and Numerical Simulation*, **14**, 1157-1168. https://doi.org/10.1016/j.cnsns.2008.04.010

[30] Ibragimov, N.H. and Meleshko, S.V. (2009) *Communications in Nonlinear Science and Numerical Simulation*, **14**, 2551-2558. https://doi.org/10.1016/j.cnsns.2008.10.007

[31] Ho, V.B. (2019) *Journal of Modern Physics*, **10**, 1374-1393. https://doi.org/10.4236/jmp.2019.1011091

[32] de Broglie, L. (1925) *Annales de Physique*, **10**, 22-128. https://doi.org/10.1051/anphys/192510030022

[33] Bohm, D. (1952) *Physical Review*, **85**, 180-193. https://doi.org/10.1103/PhysRev.85.180

Journal of Modern Physics, 2020, 11, 565-580
https://www.scirp.org/journal/jmp
ISSN Online: 2153-120X
ISSN Print: 2153-1196

Recent QFT of Einstein's Gravity Simplified via Ultrahyperfunctions

A. Plastino[1,2,3*], M. C. Rocca[1,2,4]

[1]Departamento de Física, Universidad Nacional de La Plata, La Plata, Argentina
[2]Consejo Nacional de Investigaciones Cientícas y Tecnológicas, La Plata, Argentina
[3](IFLP-CCT-CONICET)-C. C., La Plata, Argentina
[4]Departamento de Matemática, Universidad Nacional de La Plata, La Plata, Argentina
Email: *angeloplastino@gmail.com

How to cite this paper: Plastino, A. and Rocca, M.C. (2020) Recent QFT of Einstein's Gravity Simplified via Ultrahyperfunctions. *Journal of Modern Physics*, **11**, 565-580.
https://doi.org/10.4236/jmp.2020.114037

Received: March 22, 2020
Accepted: April 11, 2020
Published: April 14, 2020

Abstract

Previously published treatment is rather involved. Here we present a useful approximation to the concomitant derivation that yields a simpler way of handling things and still obtains results quite similar to those yielded by the exact treatment. Our approximation consists of giving the graviton field a simpler, but still quite good approximate form.

Keywords

Quantum Field Theory, Einstein Gravity, Non-Renormalizable Theories, Unitarity

1. Introduction

Previous attempts to quantize Einstein gravity (EG) have failed because of 1) they utilize a Rigged Hilber Space (RHS) with undefined metric, 2) non-unitarity troubles, and 3) non-renormalizablity problems. These problems were successfully bypassed in [1] [2], yielding a viable quantification procedure for Einstein's gravity. One used two kinds of tools. Some are of physical nature and were developed in [3] [4] [5]. Others are of a purely mathematical character, and concern the nature and properties of a generalization of Schwartz's distributions made in the 1960s. The generalized entities were called Ultrahyperfuntions (UHF). The existence and uniqueness of their convolution, whcih yields another UHF, were demonstrated in the 1990s [6]-[10]. Such convolutions are finite. Since quantum propagators can be seen to be UHFs, and their convolution is finite, all Feynman diagrams also turn out to be finite. There is no longer a need for renormalization. These important mathematical advanced were founded on the efforts

of A. Grothendieck [11] and J. S. Silva (JSS) [12]. The concomitant mathematical apparatus was specifically devised so as to quantify non-renormalizable field theories. For a detailed discussion of it, see [10]. One ends up facing a theory similar to QED, endowed with unitarity at all finite orders of power expansions in the gravitation constant G of the EG Lagrangian. This feat was previously attempted, but without success, by Gupta and by Feynman (in his celebrated Acta Physica Polonica paper [13]).

Our paper is structured as indicated below:

1) Section 2 deals with preliminary materials.

2) Section 3 treats the QFT Lagrangian for EG and introduces our approximation that consists of setting the graviton field $\phi^{\mu\nu} = \gamma^{\mu\nu}\phi$, where $\gamma^{\mu\nu}$ is a constant tensor and ϕ a scalar (graviton) field.

3) Section 4 quantizes the ensuing theory.

4) Section 5 evaluates the graviton's self-energy up to second order.

5) Section 6 introduces axions into our scenario and considers the axions-gravitons interaction.

6) Section 7 calculates the graviton's self-energy in the presence of axions.

7) Section 8 evaluates the axion's self-energy, up to second order.

8) Finally, some conclusions are drawn in Section 9.

2. Preliminary Materials

The most general quantification approach is based upon Schwinger-Feynman's variational principle [14] and can successfully deal even with high order supersymmetric (HOS) theories (see [15] [16]). It is important to emphasize, for QFT experts, that HOS theories cannot be quantized by appeal to the customary Dirac-brackets approach.

Consider now the action for a set of fields $\phi_A(x)$ written in the fashion

$$\begin{aligned} &\mathcal{S}\left[\sigma(x),\sigma_0,\phi_A(x)\right] \\ &= \int_{\sigma_0}^{\sigma(x)} L\left[\phi_A(\xi),\partial_\mu\phi_A(\xi),\xi\right]\mathrm{d}\xi, \end{aligned} \tag{2.1}$$

where $\sigma(x)$ if a space-like surface passing through the point x. σ_0 is that surface (at the remote past), for which all field variations vanish. The Schwinger-Feynman variational principle asserts then that:

> "Any Hermitian infinitesimal variation $\delta\mathcal{S}$ of the action induces a canonical transformation of the vector space in which the quantum system is defined, and the generator of this transformation is this same operator $\delta\mathcal{S}$".

In such circumstances, this equality is seen to hold

$$\delta\phi_A = i\left[\delta\mathcal{S},\phi_A\right]. \tag{2.2}$$

Accordingly, for a Poincare transformation one has

$$\delta \mathcal{S} = a^{\mu} \mathcal{P}_{\mu} + \frac{1}{2} a^{\mu\nu} \mathcal{M}_{\mu\nu}, \tag{2.3}$$

where a^{μ} and $a^{\mu\nu}$ are variational constants, the first for displacement and the second for rotation, $\mathcal{P}_{\mu}$ refers to linear momentum, and $\mathcal{M}_{\mu\nu}$ to complete angular momentum. For the field variation the last two quantities are represented by $\hat{P}_{\mu}$ and $\hat{M}_{\mu\nu}$, respectively. One has

$$\delta \phi_a = a^{\mu} \hat{P}_{\mu} \phi_A + \frac{1}{2} a^{\mu\nu} \hat{M}_{\mu\nu} \phi_A. \tag{2.4}$$

From (2.2) one can now ascertain that

$$\partial_{\mu} \phi_A = i \left[\mathcal{P}_{\mu}, \phi_A \right]. \tag{2.5}$$

More to the point,

$$\partial_0 \phi_A = i \left[\mathcal{P}_0, \phi_A \right]. \tag{2.6}$$

Equation (2.6) will be used below for quantizing EG.

3. The Convolution of Two Lorentz Invariant Tempered Ultradistributions

In [7] we have obtained a conceptually simple but rather lengthy expression for the convolution of two Lorentz invariant tempered ultradistributions. ρ and Λ are defined there. Θ is the Heaviside function and $\Im$ stands for imaginary part. We have then

$$\begin{aligned}
&H_{\lambda}(\rho,\Lambda) \\
&= \frac{1}{8\pi^2 \rho} \int\int_{\Gamma_1 \Gamma_2} F(\rho_1) G(\rho_2) \rho_1^{\lambda} \rho_2^{\lambda} \left\{ \Theta\left[\Im(\rho)\right] \right\} \left\{ \left[\ln(-\rho_1 + \Lambda) - \ln(-\rho_1 - \Lambda) \right] \right. \\
&\times \left[\ln(-\rho_2 + \Lambda) - \ln(-\rho_2 - \Lambda) \right] \sqrt{4(\rho_1 + \Lambda)(\rho_2 + \Lambda) - (\rho - \rho_1 - \rho_2 - 2\Lambda)^2} \\
&\times \ln \left[\frac{\sqrt{4(\rho_1 + \Lambda)(\rho_2 + \Lambda) - (\rho - \rho_1 - \rho_2 - 2\Lambda)^2} - i(\rho - \rho_1 - \rho_2 - 2\Lambda)}{2\sqrt{(\rho_1 + \Lambda)(\rho_2 + \Lambda)}} \right] \\
&+ \left[\ln(\rho_1 + \Lambda) - \ln(\rho_1 - \Lambda) \right] \left[\ln(\rho_2 + \Lambda) - \ln(\rho_2 - \Lambda) \right] \\
&\times \sqrt{4(\rho_1 - \Lambda)(\rho_2 - \Lambda) - (\rho - \rho_1 - \rho_2 + 2\Lambda)^2} \\
&\times \ln \left[\frac{\sqrt{4(\rho_1 - \Lambda)(\rho_2 - \Lambda) - (\rho - \rho_1 - \rho_2 + 2\Lambda)^2} - i(\rho - \rho_1 - \rho_2 + 2\Lambda)}{2\sqrt{(\rho_1 - \Lambda)(\rho_2 - \Lambda)}} \right] \\
&+ \left[\ln(\rho_1 + \Lambda) - \ln(\rho_1 - \Lambda) \right] \left[\ln(-\rho_2 + \Lambda) - \ln(-\rho_2 - \Lambda) \right] \\
&\times \left\{ \frac{i\pi}{2} \left[\sqrt{4(\rho_1 + \Lambda)(\rho_2 - \Lambda) - (\rho - \rho_1 - \rho_2)^2} - i(\rho - \rho_1 - \rho_2) \right] \right. \\
&+ \sqrt{4(\rho_1 + \Lambda)(\rho_2 - \Lambda) - (\rho - \rho_1 - \rho_2)^2}
\end{aligned}$$

$$\times\ln\left[\frac{\sqrt{4(\rho_1+\Lambda)(\rho_2-\Lambda)-(\rho-\rho_1-\rho_2)^2}-i(\rho-\rho_1-\rho_2)}{2i\sqrt{-(\rho_1+\Lambda)(\rho_2-\Lambda)}}\right]\Bigg\}$$
$$+\left[\ln(-\rho_1+\Lambda)-\ln(-\rho_1-\Lambda)\right]\left[\ln(\rho_2+\Lambda)-\ln(\rho_2-\Lambda)\right]$$
$$\times\Bigg\{\frac{i\pi}{2}\left[\sqrt{4(\rho_1-\Lambda)(\rho_2+\Lambda)-(\rho-\rho_1-\rho_2)^2}-i(\rho-\rho_1-\rho_2)\right]$$
$$+\sqrt{4(\rho_1-\Lambda)(\rho_2+\Lambda)-(\rho-\rho_1-\rho_2)^2}$$
$$\times\ln\left[\frac{\sqrt{4(\rho_1-\Lambda)(\rho_2+\Lambda)-(\rho-\rho_1-\rho_2)^2}-i(\rho-\rho_1-\rho_2)}{2i\sqrt{-(\rho_1-\Lambda)(\rho_2+\Lambda)}}\right]\Bigg\}\Bigg\}$$

$$-\Theta\left[-\Im(\rho)\right]\Bigg\{\left[\ln(-\rho_1+\Lambda)-\ln(-\rho_1-\Lambda)\right]\left[\ln(-\rho_2+\Lambda)-\ln(-\rho_2-\Lambda)\right]$$
$$\times\sqrt{4(\rho_1-\Lambda)(\rho_2-\Lambda)-(\rho-\rho_1-\rho_2+2\Lambda)^2}$$
$$\times\ln\left[\frac{\sqrt{4(\rho_1-\Lambda)(\rho_2-\Lambda)-(\rho-\rho_1-\rho_2+2\Lambda)^2}-i(\rho-\rho_1-\rho_2+2\Lambda)}{2\sqrt{(\rho_1-\Lambda)(\rho_2-\Lambda)}}\right]$$
$$+\left[\ln(\rho_1+\Lambda)-\ln(\rho_1-\Lambda)\right]\left[\ln(\rho_2+\Lambda)-\ln(\rho_2-\Lambda)\right]$$
$$\times\sqrt{4(\rho_1+\Lambda)(\rho_2+\Lambda)-(\rho-\rho_1-\rho_2-2\Lambda)^2}$$
$$\times\ln\left[\frac{\sqrt{4(\rho_1+\Lambda)(\rho_2+\Lambda)-(\rho-\rho_1-\rho_2-2\Lambda)^2}-i(\rho-\rho_1-\rho_2-2\Lambda)}{2\sqrt{(\rho_1+\Lambda)(\rho_2+\Lambda)}}\right]$$
$$+\left[\ln(\rho_1+\Lambda)-\ln(\rho_1-\Lambda)\right]\left[\ln(-\rho_2+\Lambda)-\ln(-\rho_2-\Lambda)\right]$$
$$\times\Bigg\{\frac{i\pi}{2}\left[\sqrt{4(\rho_1-\Lambda)(\rho_2+\Lambda)-(\rho-\rho_1-\rho_2)^2}-i(\rho-\rho_1-\rho_2)\right]$$
$$+\sqrt{4(\rho_1-\Lambda)(\rho_2+\Lambda)-(\rho-\rho_1-\rho_2)^2}$$
$$\times\ln\left[\frac{\sqrt{4(\rho_1-\Lambda)(\rho_2+\Lambda)-(\rho-\rho_1-\rho_2)^2}-i(\rho-\rho_1-\rho_2)}{2i\sqrt{-(\rho_1-\Lambda)(\rho_2+\Lambda)}}\right]\Bigg\}$$
$$+\left[\ln(-\rho_1+\Lambda)-\ln(-\rho_1-\Lambda)\right]\left[\ln(\rho_2+\Lambda)-\ln(\rho_2-\Lambda)\right]$$
$$\times\Bigg\{\frac{i\pi}{2}\left[\sqrt{4(\rho_1+\Lambda)(\rho_2-\Lambda)-(\rho-\rho_1-\rho_2)^2}-i(\rho-\rho_1-\rho_2)\right]$$
$$+\sqrt{4(\rho_1+\Lambda)(\rho_2-\Lambda)-(\rho-\rho_1-\rho_2)^2}$$
$$\times\ln\left[\frac{\sqrt{4(\rho_1+\Lambda)(\rho_2-\Lambda)-(\rho-\rho_1-\rho_2)^2}-i(\rho-\rho_1-\rho_2)}{2i\sqrt{-(\rho_1+\Lambda)(\rho_2-\Lambda)}}\right]\Bigg\}\Bigg\}$$
$$-\frac{i}{2}\Big\{\left[\ln(-\rho_1+\Lambda)-\ln(-\rho_1-\Lambda)\right]\left[\ln(-\rho_2+\Lambda)-\ln(-\rho_2-\Lambda)\right]$$

$$
\begin{aligned}
&\times(\rho_1-\rho_2)\left[\ln\left(i\sqrt{\frac{\rho_1+\Lambda}{\rho_2+\Lambda}}\right)+\ln\left(-i\sqrt{\frac{\rho_1-\Lambda}{\rho_2-\Lambda}}\right)\right]\\
&+\left[\ln(\rho_1+\Lambda)-\ln(\rho_1-\Lambda)\right]\left[\ln(\rho_2+\Lambda)-\ln(\rho_2-\Lambda)\right]\\
&\times(\rho_1-\rho_2)\left[\ln\left(-i\sqrt{\frac{\Lambda-\rho_1}{\Lambda-\rho_2}}\right)+\ln\left(i\sqrt{\frac{\Lambda+\rho_1}{\Lambda+\rho_2}}\right)\right]\\
&+\left[\ln(\rho_1+\Lambda)-\ln(\rho_1-\Lambda)\right]\left[\ln(-\rho_2+\Lambda)-\ln(-\rho_2-\Lambda)\right]\\
&\times\left\{(\rho_1-\rho_2)\left[\ln\left(\sqrt{\frac{\Lambda+\rho_1}{\Lambda-\rho_2}}\right)+\ln\left(\sqrt{\frac{\Lambda-\rho_1}{\Lambda+\rho_2}}\right)\right]\right.\\
&+\frac{\rho_1-\rho_2}{2}\left[\ln(-\rho_1-\rho_2+\Lambda)-\ln(-\rho_1-\rho_2-\Lambda)\right.\\
&\left.-\ln(\rho_1+\rho_2+\Lambda)+\ln(\rho_1+\rho_2-\Lambda)\right]+\rho_2\left[\ln(-\rho_1-\rho_2+\Lambda)\right.\\
&\left.\left.-\ln(-\rho_1-\rho_2-\Lambda)\right]+\rho_1\left[\ln(\rho_1+\rho_2+\Lambda)-\ln(\rho_1+\rho_2-\Lambda)\right]\right\}\\
&\left[\ln(-\rho_1+\Lambda)-\ln(-\rho_1-\Lambda)\right]\left[\ln(\rho_2+\Lambda)-\ln(\rho_2-\Lambda)\right]\\
&\times\left\{(\rho_1-\rho_2)\left[\ln\left(\sqrt{\frac{\Lambda-\rho_1}{\Lambda+\rho_2}}\right)+\ln\left(\sqrt{\frac{\Lambda+\rho_1}{\Lambda-\rho_2}}\right)\right]\right.\\
&+\frac{\rho_1-\rho_2}{2}\left[\ln(\rho_1+\rho_2+\Lambda)-\ln(\rho_1+\rho_2-\Lambda)\right.\\
&\left.-\ln(-\rho_1-\rho_2+\Lambda)+\ln(-\rho_1-\rho_2-\Lambda)\right]+\rho_1\left[\ln(-\rho_1-\rho_2+\Lambda)\right.\\
&\left.\left.\left.\left.-\ln(-\rho_1-\rho_2-\Lambda)\right]+\rho_2\left[\ln(\rho_1+\rho_2+\Lambda)-\ln(\rho_1+\rho_2-\Lambda)\right]\right\}\right\}\right\}\mathrm{d}\rho_1\mathrm{d}\rho_2
\end{aligned}
\tag{3.1}
$$

This defines an ultradistribution in the variables ρ and Λ for

$$\left|\Im(\rho)\right|>\Im(\Lambda)>\left|\Im(\rho_1)\right|+\left|\Im(\rho_2)\right|$$

Let $\mathfrak{B}$ be a vertical band contained in the complex λ-plane $\mathfrak{P}$. Integral (3.1) is an analytic function of λ defined in the domain $\mathfrak{B}$. Moreover, it is bounded by a power of $\left|\rho\Lambda\right|$. Then, $H_\lambda(\rho,\Lambda)$ can be analytically continued to other parts of $\mathfrak{P}$. Thus, we define

$$H(\rho)=H^{(0)}\left(\rho,i0^+\right) \tag{3.2}$$

$$H_\lambda\left(\rho,i0^+\right)=\sum_{-m}^{\infty}H^{(n)}\left(\rho,i0^+\right)\lambda^n \tag{3.3}$$

As in the other cases, we define now

$$\{F*G\}(\rho)=H(\rho) \tag{3.4}$$

as the convolution of two Lorentz invariant tempered ultradistributions.

The Feynman propagators corresponding to a massless particle F and a massive particle G (mass m) are, respectively, the following ultrahyperfunctions:

$$F(\rho) = -\Theta\left[-\Im(\rho)\right]\rho^{-1}$$

$$G(\rho) = -\Theta\left[-\Im(\rho)\right]\left(\rho + m^2\right)^{-1} \tag{3.5}$$

where ρ is the complex variable, such that on the real axis one has $\rho = k_1^2 + k_2^2 + k_3^2 - k_0^2$. For them, the following equalities are satisfied

$$\rho^{\lambda} F(\rho) = -\Theta\left[-\Im(\rho)\right]\rho^{\lambda-1}$$

$$\rho^{\lambda} G(\rho) = -\Theta\left[-\Im(\rho)\right]\left(\rho + m^2\right)^{\lambda-1} \tag{3.6}$$

where we have used: $\left(\rho + m^2\right)^{\lambda} \simeq \rho^{\lambda}$, since we have chosen m to be very small. On the real axis, the previously defined propagators are given by:

$$f(\rho) = F(\rho + i0) - F(\rho - i0) = (\rho - i0)^{-1}$$

$$g(\rho) = G(\rho + i0) - G(\rho - i0) = \left(\rho + m^2 - i0\right)^{-1} \tag{3.7}$$

These are the usual expressions for Feynman propagators.

Consider first the convolution of two massless propagators. We use (3.6), since here the corresponding ultrahyperfunctions do not have singularities in the complex plane. We obtain from (3.1) a simplified expression for the convolution:

$$h_{\lambda}(\rho) = \frac{\pi}{2\rho}\iint_{-\infty}^{\infty}(\rho_1 - i0)^{\lambda-1}(\rho_2 - i0)^{\lambda-1}\left[(\rho - \rho_1 - \rho_2)^2 - 4\rho_1\rho_2\right]_{+}^{\frac{1}{2}}\mathrm{d}\rho_1\mathrm{d}\rho_2 \tag{3.8}$$

This expression is nothing other than the usual convolution:

$$h_{\lambda}(\rho) = (\rho - i0)^{\lambda-1} * (\rho - i0)^{\lambda-1} \tag{3.9}$$

In the same way, we obtain for massive propagators:

$$h_{\lambda}(\rho) = \left(\rho + m^2 - i0\right)^{\lambda-1} * \left(\rho - m^2 - i0\right)^{\lambda-1} \tag{3.10}$$

These last two expressions are the ones we will use later to evaluate the graviton's self-energy.

4. The Lagrangian of Einstein's QFT

The EG Lagrangian is [3] [4] [5], for curvature $\boldsymbol{R}$ and κ^2 the gravitation's constant,

$$\mathcal{L}_{\mathrm{G}} = \frac{1}{\kappa^2}\boldsymbol{R}\sqrt{|g|} - \frac{1}{2}\eta_{\mu\nu}\partial_{\alpha}h^{\mu\alpha}\partial_{\beta}h^{\nu\beta}, \tag{4.1}$$

where Minkowski's $\eta^{\mu\nu} = diag(1,1,1,-1)$, while $h^{\mu\nu} = \sqrt{|g|}g^{\mu\nu}$, with $g^{\mu\nu}$ the metric tensor. The second term in (4.1) establishes the gauge fixing. We reach here a critical stage. At it, we will proceed to perform a crucial linear approximation. This will be immediately seen to be an approximation to the graviton field. We will write

$$h^{\mu\nu} = \eta^{\mu\nu} + \kappa\phi^{\mu\nu}, \tag{4.2}$$

where κ^2 is the gravitation's constant and $\phi^{\mu\nu}$ the graviton field. Our ap-

proximation, based on [1], reads

$$\phi^{\mu\nu} = \gamma^{\mu\nu}\phi, \tag{4.3}$$

with ϕ a scalar field and where $\gamma^{\mu\nu}$ is a constant tensor which satisfies

$$\gamma^{\mu}_{\mu} = 0 \tag{4.4}$$

This approximate casting of $\phi^{\mu\nu}$ considerably simplifies the handling of matters without sacrifice of rigor. We write now the Lagrangian as a sum of a non-perturbative component plus an interactive one, *i.e.*,

$$\mathcal{L}_G = \mathcal{L}_L + \mathcal{L}_I, \tag{4.5}$$

where

$$\mathcal{L}_L = -\frac{1}{4}\gamma_{\mu\nu}\gamma^{\mu\nu}\partial_\lambda\phi\partial^\lambda\phi, \tag{4.6}$$

and, up to 2nd order, one has [3] [4] [5]

$$\mathcal{L}_I = -\frac{1}{2}\kappa\gamma^{\mu\nu}\phi\left[\frac{1}{2}\gamma_{\rho\lambda}\gamma^{\rho\lambda}\partial_\mu\phi\partial_\nu\phi + \gamma_{\mu\beta}\gamma_{\lambda\nu}\partial^\lambda\phi\partial^\beta\phi - \gamma_{\mu\rho}\gamma^{\rho}_{\nu}\partial_\lambda\phi\partial^\lambda\phi\right], \tag{4.7}$$

having made use of the constraint (4). This constraint is required in order to satisfy gauge invariance [17] For the field ϕ. We have then, as can also be seen to happen for the considerations made in [10],

$$\Box\phi = 0, \tag{4.8}$$

whose solution is

$$\phi(x) = \frac{1}{(2\pi)^{\frac{3}{2}}}\int\left[\frac{a(\boldsymbol{k})}{\sqrt{2k_0}}\mathrm{e}^{ik_\mu x^\mu} + \frac{a^+(\boldsymbol{k})}{\sqrt{2k_0}}\mathrm{e}^{-ik_\mu x^\mu}\right]\mathrm{d}^3k, \tag{4.9}$$

with $k_0 = |\boldsymbol{k}|$. Above, $a(\boldsymbol{k})$ and $a^+(\boldsymbol{k})$ stand for Fourier coefficients. Up to this point, we were using Einstein's Lagrangian. Its quantization begins next.

5. Quantization of the Theory

As usual in QFT (see for instance Visconti' celebrated book [14]), the quantum energy-momentum tensor T^λ_ρ is cast as

$$T^\lambda_\rho = \frac{\partial L}{\partial\partial^\rho\phi^{\mu\nu}}\partial^\lambda\phi^{\mu\nu} - \delta^\lambda_\rho L, \tag{5.1}$$

and the time-component of the four-momentum is now the quantum operator

$$\mathcal{P}_0 = \int T^0_0\mathrm{d}^3x. \tag{5.2}$$

Using (4) we have

$$T^0_0 = -\frac{1}{4}\gamma_{\mu\nu}\gamma^{\mu\nu}\left[\partial_0\phi\partial^0\phi - \partial_j\phi\partial^j\phi\right]. \tag{5.3}$$

Consequently,

$$\mathcal{P}_0 = \frac{1}{4}\gamma_{\mu\nu}\gamma^{\mu\nu}\int|\boldsymbol{k}|\left[a(\boldsymbol{k})a^+(\boldsymbol{k}) + a^+(\boldsymbol{k})a(\boldsymbol{k})\right]\mathrm{d}^3k. \tag{5.4}$$

Appeal to (2.6) leads now to

$$\left[\mathcal{P}_0, a(\boldsymbol{k})\right] = -k_0 a(\boldsymbol{k})$$

$$\left[\mathcal{P}_0, a^+(\boldsymbol{k})\right] = k_0 a^+(\boldsymbol{k}). \tag{5.5}$$

From the last relation in (5.5) one gathers that

$$|\boldsymbol{k}| a^+(\boldsymbol{k}') = \frac{\gamma_{\mu\nu}\gamma^{\mu\nu}}{2}\int |\boldsymbol{k}|\left[a(\boldsymbol{k}), a^+(\boldsymbol{k}')\right] a^+(\boldsymbol{k}) \mathrm{d}^3 k. \tag{5.6}$$

The solution of this integral equation is

$$\left[a(\boldsymbol{k}), a^+(\boldsymbol{k}')\right] = \frac{2}{\gamma_{\mu\nu}\gamma^{\mu\nu}}\delta(\boldsymbol{k}-\boldsymbol{k}'). \tag{5.7}$$

We use now the usual definition

$$\Delta(x-y) = \langle 0 | T\left[\phi(x)\phi(y)\right] | 0\rangle. \tag{5.8}$$

The graviton's propagator then turns out to be

$$\Delta(x-y) = \frac{i}{(2\pi)^4}\frac{2}{\gamma_{\mu\nu}\gamma^{\mu\nu}}\int \frac{\mathrm{e}^{ik_\mu\left(x^\mu - y^\mu\right)}}{k^2 - i0}\mathrm{d}^4 k. \tag{5.9}$$

As a consequence, we can write

$$\mathcal{P}_0 = \frac{\gamma_{\mu\nu}\gamma^{\mu\nu}}{4}\int |\boldsymbol{k}|\left[a(\boldsymbol{k})a^+(\boldsymbol{k}') + a^+(\boldsymbol{k}')a(\boldsymbol{k})\right]\delta(\boldsymbol{k}-\boldsymbol{k}')\mathrm{d}^3 k \mathrm{d}^3 k', \tag{5.10}$$

or

$$\mathcal{P}_0 = \frac{\gamma_{\mu\nu}\gamma^{\mu\nu}}{4}\int |\boldsymbol{k}|\left[2a^+(\boldsymbol{k}')a(\boldsymbol{k}) + \frac{2}{\gamma_{\rho\lambda}\gamma^{\rho\lambda}}\delta(\boldsymbol{k}-\boldsymbol{k}')\right]\delta(\boldsymbol{k}-\boldsymbol{k}')\mathrm{d}^3 k \mathrm{d}^3 k'. \tag{5.11}$$

Thus, we obtain

$$\mathcal{P}_0 = \frac{\gamma_{\mu\nu}\gamma^{\mu\nu}}{2}\int |\boldsymbol{k}| a^+(\boldsymbol{k})a(\boldsymbol{k})\mathrm{d}^3 k, \tag{5.12}$$

where we have used the fact that the product of two deltas with the same argument vanishes [6], *i.e.*, $\delta(\boldsymbol{k}-\boldsymbol{k}')\delta(\boldsymbol{k}-\boldsymbol{k}') = 0$. This illustrates the fact that using Ultrahyperfunctions is here equivalent to adopting the normal order in the definition of the time-component of the four-momentum

$$\mathcal{P}_0 = \frac{\gamma_{\mu\nu}\gamma^{\mu\nu}}{4}\int |\boldsymbol{k}| :\left[a(\boldsymbol{k})a^+(\boldsymbol{k}) + a^+(\boldsymbol{k})a(\boldsymbol{k})\right]: \mathrm{d}^3 k. \tag{5.13}$$

Now, we must insist on the fact that the physical state should satisfy the relation (see [3] [4] [5])

$$\gamma^{\mu\nu}\partial_\mu \phi |\psi\rangle = 0. \tag{5.14}$$

The ensuing theory is similar to the QED-one obtained via the quantization approach of Gupta-Bleuler. This implies that the theory is unitary for any finite perturbative order. In this theory, just one type of graviton arises, ϕ^{12}, while in Gupta's treatment two sorts of graviton emerge. Of course, this happens for a non-interacting theory, as pointed out by Gupta.

6. Graviton's Self Energy

So as to compute the graviton's self-energy (SF) we begin with the interaction Hamiltonian $\mathcal{H}_I$. Remark that the Lagrangian has derivative interaction terms.

$$\mathcal{H}_I = \frac{\partial \mathcal{L}_I}{\partial \partial^0 \phi^{\mu\nu}} \partial^0 \phi^{\mu\nu} - \mathcal{L}_I. \tag{6.1}$$

A typical term reads

$$\Sigma_{G\alpha_1\alpha_2\alpha_3\alpha_4}(k) = k_{\alpha_1}k_{\alpha_2}(\rho - i0)^{-1} * k_{\alpha_3}k_{\alpha_4}(\rho - i0)^{-1}, \tag{6.2}$$

where $\rho = k_1^2 + k_2^2 + k_3^2 - k_0^2$.

The Fourier transform of (2) becomes

$$\begin{aligned}
&\mathcal{F}\left[k_{\alpha_1}k_{\alpha_2}(\rho - i0)^{\lambda-1} * k_{\alpha_3}k_{\alpha_4}(\rho - i0)^{\lambda-1}\right] \\
&= -\frac{2^{4(\lambda+1)}\left[\Gamma(2+\lambda)^2\right]}{4\Gamma(1-\lambda)^2}\eta_{\alpha_1\alpha_2}\eta_{\alpha_3\alpha_4}(x+i0)^{-2\lambda-4} \\
&+ \frac{2^{4(\lambda+1)}\Gamma(2+\lambda)\Gamma(3+\lambda)}{2\Gamma(1-\lambda)^2}\left(\eta_{\alpha_1\alpha_2}x_{\alpha_3}x_{\alpha_4} + \eta_{\alpha_3\alpha_4}x_{\alpha_1}x_{\alpha_2}\right)(x+i0)^{-2\lambda-5} \\
&- \frac{2^{4(\lambda+1)}\Gamma(3+\lambda)^2}{\Gamma(1-\lambda)}x_{\alpha_1}x_{\alpha_2}x_{\alpha_3}x_{\alpha_4}(x+i0)^{-\nu-2}
\end{aligned} \tag{6.3}$$

where $x = x_1^2 + x_2^2 + x_3^2 - x_0^2$.

Anti-transforming the above equation one has

$$\begin{aligned}
&k_{\alpha_1}k_{\alpha_2}(\rho - i0)^{\lambda-1} * k_{\alpha_3}k_{\alpha_4}(\rho - i0)^{\lambda-1} \\
&= \frac{i\pi^2}{4\Gamma(1-\lambda)^2}\left\{\Gamma(\lambda+2)\left[\frac{\Gamma(2+\lambda)}{\Gamma(2\lambda+4)} - 2\frac{\Gamma(3+\lambda)}{\Gamma(2\lambda+5)}\right]\eta_{\alpha_1\alpha_2}\eta_{\alpha_3\alpha_4}\right. \\
&\left. + \frac{\Gamma(\lambda+3)^2}{\Gamma(2\lambda+6)}\left(\eta_{\alpha_1\alpha_2}\eta_{\alpha_3\alpha_4} + \eta_{\alpha_2\alpha_3}\eta_{\alpha_1\alpha_4} + \eta_{\alpha_2\alpha_4}\eta_{\alpha_1\alpha_3}\right)\right\}\Gamma(-2\lambda-2)(\rho - i0)^{2\lambda+2} \\
&+ \frac{i\pi^2\Gamma(\lambda+3)}{2\Gamma(1-\lambda)^2}\left\{\frac{\Gamma(2+\lambda)}{\Gamma(2\lambda+5)}\Gamma(\nu+1)\left(\eta_{\alpha_1\alpha_2}k_{\alpha_3}k_{\alpha_4} + \eta_{\alpha_3\alpha_4}k_{\alpha_1}k_{\alpha_2}\right)\right. \\
&- \frac{\Gamma(\lambda+3)}{\Gamma(2\lambda+6)}\left(\eta_{\alpha_1\alpha_2}k_{\alpha_3}k_{\alpha_4} + \eta_{\alpha_1\alpha_3}k_{\alpha_2}k_{\alpha_4} + \eta_{\alpha_1\alpha_4}k_{\alpha_2}k_{\alpha_3} + \eta_{\alpha_3\alpha_4}k_{\alpha_1}k_{\alpha_2}\right. \\
&\left.\left. + \eta_{\alpha_2\alpha_3}k_{\alpha_1}k_{\alpha_4} + \eta_{\alpha_2\alpha_4}k_{\alpha_1}k_{\alpha_3}\right)\right\}\Gamma(-2\lambda-1)(\rho - i0)^{2\lambda+1} \\
&+ \frac{i\pi^2\Gamma(\lambda+3)^2}{\Gamma(1-\lambda)^2\Gamma(2\lambda+6)}k_{\alpha_1}k_{\alpha_2}k_{\alpha_3}k_{\alpha_4}\Gamma(-2\lambda)(\rho - i0)^{2\lambda}
\end{aligned} \tag{6.4}$$

Computing the Self-Energy

We proceed here to perform a λ-Laurent expansion, keeping from it just the λ independent term [10]. We Laurent-expand (4) around $\lambda = 0$ and encounter:

$$
\begin{aligned}
&k_{\alpha_1}k_{\alpha_2}\left(\rho-i0\right)^{\lambda-1}*k_{\alpha_3}k_{\alpha_4}\left(\rho-i0\right)^{\lambda-1}\\
&=-i\frac{\pi^2}{4\lambda}\left\{\frac{1}{5!}\left(\eta_{\alpha_1\alpha_2}\eta_{\alpha_3\alpha_4}+\eta_{\alpha_2\alpha_3}\eta_{\alpha_1\alpha_4}+\eta_{\alpha_2\alpha_4}\eta_{\alpha_1\alpha_3}\right)\rho^2\right.\\
&-\left[\frac{2}{4!}\left(\eta_{\alpha_1\alpha_2}k_{\alpha_3}k_{\alpha_4}+\eta_{\alpha_3\alpha_4}k_{\alpha_1}k_{\alpha_2}\right)-\frac{1}{6!}\left(\eta_{\alpha_1\alpha_2}k_{\alpha_3}k_{\alpha_4}\right.\right.\\
&+\eta_{\alpha_3\alpha_4}k_{\alpha_1}k_{\alpha_2}+\eta_{\alpha_1\alpha_3}k_{\alpha_2}k_{\alpha_4}+\eta_{\alpha_1\alpha_4}k_{\alpha_2}k_{\alpha_3}\\
&\left.\left.+\eta_{\alpha_2\alpha_3}k_{\alpha_1}k_{\alpha_4}+\eta_{\alpha_2\alpha_4}k_{\alpha_1}k_{\alpha_3}\right)\right]\rho+\frac{8}{5!}k_{\alpha_1}k_{\alpha_2}k_{\alpha_3}k_{\alpha_4}\left.\right\}\\
&-\frac{i\pi^2}{5!2}\left(\eta_{\alpha_1\alpha_2}\eta_{\alpha_3\alpha_4}+\eta_{\alpha_2\alpha_3}\eta_{\alpha_1\alpha_4}+\eta_{\alpha_2\alpha_4}\eta_{\alpha_1\alpha_3}\right)\left[\ln\left(\rho-i0\right)-\frac{137}{60}\right]\rho^2\\
&+i\frac{\pi^2}{4!}\left\{\left(\eta_{\alpha_1\alpha_2}k_{\alpha_3}k_{\alpha_4}+\eta_{\alpha_3\alpha_4}k_{\alpha_1}k_{\alpha_2}\right)\left[\ln\left(\rho-i0\right)-\frac{11}{6}\right]\right.\\
&-\frac{1}{24}\left(\eta_{\alpha_1\alpha_2}k_{\alpha_3}k_{\alpha_4}+\eta_{\alpha_3\alpha_4}k_{\alpha_1}k_{\alpha_2}+\eta_{\alpha_1\alpha_3}k_{\alpha_2}k_{\alpha_4}+\eta_{\alpha_1\alpha_4}k_{\alpha_2}k_{\alpha_3}\right.\\
&\left.\left.+\eta_{\alpha_2\alpha_3}k_{\alpha_1}k_{\alpha_4}+\eta_{\alpha_2\alpha_4}k_{\alpha_1}k_{\alpha_3}\right)\left[\ln\left(\rho-i0\right)+\ln\pi+2C-\frac{101}{30}\right]\right\}\rho\\
&\left.-i\frac{\pi^2}{30}k_{\alpha_1}k_{\alpha_2}k_{\alpha_3}k_{\alpha_4}\left[\ln\left(\rho-i0\right)-\frac{47}{60}\right]+\sum_{n=1}^{\infty}a_n\lambda^n\right\}.
\end{aligned}
\tag{6.5}
$$

The exact value of the convolution we are interested in, *i.e.*, the left hand side of (5.5), is given by the independent term above, as everyone knows. Should the reader be unfamiliar with this scenario, we direct him/her to [10]. We now get

$$
\begin{aligned}
&\Sigma_{G\alpha_1\alpha_2\alpha_3\alpha_4}\left(k\right)=k_{\alpha_1}k_{\alpha_2}\left(\rho-i0\right)^{-1}*k_{\alpha_3}k_{\alpha_4}\left(\rho-i0\right)^{-1}\\
&=-\frac{i\pi^2}{5!2}\left(\eta_{\alpha_1\alpha_2}\eta_{\alpha_3\alpha_4}+\eta_{\alpha_2\alpha_3}\eta_{\alpha_1\alpha_4}+\eta_{\alpha_2\alpha_4}\eta_{\alpha_1\alpha_3}\right)\left[\ln\left(\rho-i0\right)+\ln\pi+C-\frac{46}{15}\right]\rho^2\\
&+i\frac{\pi^2}{4!}\left\{\left(\eta_{\alpha_1\alpha_2}k_{\alpha_3}k_{\alpha_4}+\eta_{\alpha_3\alpha_4}k_{\alpha_1}k_{\alpha_2}\right)\left[\ln\left(\rho-i0\right)+\ln\pi+C-\frac{8}{3}\right]\right.\\
&-\frac{1}{24}\left(\eta_{\alpha_1\alpha_2}k_{\alpha_3}k_{\alpha_4}+\eta_{\alpha_3\alpha_4}k_{\alpha_1}k_{\alpha_2}+\eta_{\alpha_1\alpha_3}k_{\alpha_2}k_{\alpha_4}+\eta_{\alpha_1\alpha_4}k_{\alpha_2}k_{\alpha_3}\right.\\
&\left.\left.+\eta_{\alpha_2\alpha_3}k_{\alpha_1}k_{\alpha_4}+\eta_{\alpha_2\alpha_4}k_{\alpha_1}k_{\alpha_3}\right)\left[\ln\left(\rho-i0\right)+\ln\pi+2C-\frac{101}{15}\right]\right\}\rho\\
&\left.-i\frac{\pi^2}{30}k_{\alpha_1}k_{\alpha_2}k_{\alpha_3}k_{\alpha_4}\left[\ln\left(\rho-i0\right)+\ln\pi+C-\frac{47}{30}\right]\right\}.
\end{aligned}
\tag{6.6}
$$

We face here 1296 diagrams of this type.

7. Axions Enter the Picture

Axions are hypothetical elementary particles conjectured by the 1977 Peccei-Quinn theory so as to tackle the strong CP problem in quantum chromodynamics. Should they exist and have low enough mass (within a certain range), they may be of some interest as putative components of cold dark matter [18]. We thus consider now a massive scalar field (axions) interacting with the graviton and the pertinent Lagrangian becomes

$$\mathcal{L}_{GM} = \frac{1}{\kappa^2}\boldsymbol{R}\sqrt{|g|} - \frac{1}{2}\eta_{\mu\nu}\partial_\alpha h^{\mu\alpha}\partial_\beta h^{\nu\beta} - \frac{1}{2}\left[h^{\mu\nu}\partial_\mu\psi\partial_\nu\psi + m^2\psi^2\right]. \tag{7.1}$$

It is possible to recast the Lagrangian now as

$$\mathcal{L}_{GM} = \mathcal{L}_L + \mathcal{L}_I + \mathcal{L}_{LM} + \mathcal{L}_{IM}, \tag{7.2}$$

where

$$\mathcal{L}_{LM} = -\frac{1}{2}\left[\partial_\mu\psi\partial^\mu\psi + m^2\psi^2\right], \tag{7.3}$$

so that $\mathcal{L}_{LM}$ is the Lagrangian for the axion-graviton action

$$\mathcal{L}_{IM} = -\frac{1}{2}\kappa\gamma^{\mu\nu}\phi\partial_\mu\psi\partial_\nu\psi. \tag{7.4}$$

A new term in the interaction Hamiltonian appears

$$\mathcal{H}_{IM} = \frac{\partial\mathcal{L}_{IM}}{\partial\partial^0\psi}\partial^0\psi - \mathcal{L}_{IM}. \tag{7.5}$$

8. Graviton's Complete Self Energy

Axions necessarily generate a new contribution to a graviton's self energy

$$\Sigma_{GM\,\mu rvs}(k) = k_\mu k_r\left(\rho + m^2 - i0\right)^{-1} * k_v k_s\left(\rho + m^2 - i0\right)^{-1}. \tag{8.1}$$

To evaluate it face the customary four-dimensional integral together with the Feynman-parameters denoted by the letter *x*. After a Wick rotation, we find

$$\begin{aligned} &k_\mu k_r\left(\rho + m^2 - i0\right)^{\lambda-1} * k_v k_s\left(\rho + m^2 - i0\right)^{\lambda-1} \\ &= i\int_0^1 x^{-\lambda}(1-x)^{-\lambda}\int\frac{k_\mu k_r\left(p_v - k_v\right)\left(p_s - k_s\right)}{\left[\left(k - px\right)^2 + a\right]^{2-2\lambda}}\mathrm{d}^4k\mathrm{d}x, \end{aligned} \tag{8.2}$$

where

$$a = p^2x - p^2x^2 + m^2. \tag{8.3}$$

Effecting a variables-change $u = k - px$ we encounter

$$\begin{aligned} &k_\mu k_r\left(\rho + m^2 - i0\right)^{\lambda-1} * k_v k_s\left(\rho + m^2 - i0\right)^{\lambda-1} \\ &= i\int_0^1 x^{-\lambda}(1-x)^{-\lambda}\int\frac{f(u,x,\mu,r,v,s)}{\left(u^2 + a\right)^{2-2\lambda}}\mathrm{d}^4u\mathrm{d}x \end{aligned} \tag{8.4}$$

where

$$\begin{aligned} &f(u,x,\mu,r,v,s) \\ &= u_\mu u_r p_v p_s(1-x)^2 + u_\mu u_r u_v u_s - u_\mu u_s p_r p_v x(1-x) \\ &\quad - u_\mu u_v p_r p_s x(1-x) - u_r u_s p_\mu p_v x(1-x) \\ &\quad - u_r u_v p_\mu p_s x(1-x) + p_\mu p_r p_v p_s x^2(1-x)^2 + u_v u_s p_\mu p_r x^2. \end{aligned} \tag{8.5}$$

After computing the associated integrals we find

$$
\begin{aligned}
&k_\mu k_r\left(\rho+m^2-i0\right)^{\lambda-1} * k_\nu k_s\left(\rho+m^2-i0\right)^{\lambda-1}\\
&=\frac{i\pi^{\frac{5}{2}}2^{2\lambda}m^{2+4\lambda}}{16}\frac{\Gamma(-1-2\lambda)}{\Gamma(1-\lambda)}\left(\eta_{\mu r}k_\nu k_s+\eta_{\nu s}k_\mu k_r\right)\\
&\times\left[\frac{F\left(1-2\lambda,-1-2\lambda,\frac{3}{2}-\lambda;-\frac{\rho}{4m^2}\right)}{\Gamma\left(\frac{3}{2}-\lambda\right)}+\frac{F\left(1-\lambda,-1-2\lambda,\frac{5}{2}-\lambda;-\frac{\rho}{4m^2}\right)}{2\Gamma\left(\frac{5}{2}-\lambda\right)}\right]\\
&+i\frac{i\pi^{\frac{5}{2}}2^{2\lambda-1}m^{4+4\lambda}}{4}\left(\eta_{\mu r}\eta_{\nu s}+\eta_{\mu\nu}\eta_{rs}+\eta_{\mu s}\eta_{\nu r}\right)\\
&\frac{\Gamma(-2-2\lambda)}{\Gamma(1-\lambda)\Gamma\left(\frac{3}{2}-\lambda\right)}F\left(-2-2\lambda,1-\lambda,\frac{3}{2}-\lambda;-\frac{\rho}{4m^2}\right)\\
&-i\frac{i\pi^{\frac{5}{2}}2^{2\lambda}m^{2+4\lambda}}{64}\left(\eta_{\mu s}k_r k_\nu+\eta_{\mu\nu}k_r k_s+\eta_{rs}k_\mu k_\nu+\eta_{r\nu}k_\mu k_s\right)\\
&\times\frac{\Gamma(2-\lambda)\Gamma(-1-2\lambda)}{\Gamma(1-\lambda)^2\Gamma\left(\frac{5}{2}-\lambda\right)}F\left(-1-2\lambda,2-\lambda,\frac{5}{2}-\lambda;-\frac{\rho}{4m^2}\right)\\
&+i\frac{i\pi^{\frac{5}{2}}2^{2\lambda}m^{4\lambda}}{32}k_\mu k_r k_\nu k_s\frac{\Gamma(3-\lambda)\Gamma(-2\lambda)}{\Gamma(1-\lambda)^2\Gamma\left(\frac{5}{2}-\lambda\right)}F\left(-2\lambda,2-\lambda,\frac{5}{2}-\lambda;-\frac{\rho}{4m^2}\right).
\end{aligned}
\tag{8.6}
$$

Computing the Self-Energy ($\lambda=0$)

We appeal once again to a Laurent's expansion and have

$$
\begin{aligned}
&k_\mu k_r\left(\rho+m^2-i0\right)^{\lambda-1} * k_\nu k_s\left(\rho+m^2-i0\right)^{\lambda-1}\\
&=i\frac{\pi^2}{4\lambda}\left\{m^2\left(\eta_{\mu r}k_\nu k_s+\eta_{\nu s}k_\mu k_r\right)\left[\frac{1}{3}+\frac{1}{5}\frac{\rho}{4m^2}\right]\right.\\
&-m^4\left(\eta_{\mu r}\eta_{\nu s}+\eta_{\mu\nu}\eta_{rs}+\eta_{\mu s}\eta_{r\nu}\right)\times\left[\frac{1}{4}+\frac{1}{3}\frac{\rho}{4m^2}+\frac{4}{15}\left(\frac{\rho}{4m^2}\right)^2\right]\\
&-\frac{m^2}{4m^2+k^2-i0}\left(\eta_{\mu s}k_r k_\nu+\eta_{\mu\nu}k_r k_s+\eta_{rs}k_\mu k_\nu+\eta_{r\nu}k_\mu k_s\right)\\
&\left.\times\frac{k^2-m^2}{12}+\frac{m^2}{4}+\frac{k^2-m^2}{30}\frac{\rho}{4m^2}-\frac{1}{6}k_\mu k_r k_\nu k_s\right\}\\
&+i\frac{m^2\pi^2}{2}\left(\eta_{\mu r}k_\nu k_s+\eta_{\nu s}k_\mu k_r\right)\\
&\times\left[\frac{1}{3}\left(\ln m^2+\frac{1}{12}\right)+\frac{1}{5}\frac{\rho}{4m^2}\left(\ln m^2+\frac{13}{15}\right)\right]\\
&+i\frac{m^2\pi^2}{30}\left(\eta_{\mu r}k_\nu k_s+\eta_{\nu s}k_\mu k_r\right)\frac{\rho}{4m^2}\\
&\times\left[F\left(1,1,\frac{7}{2};-\frac{\rho}{4m^2}\right)+\frac{1}{7}F\left(1,1,\frac{9}{2};-\frac{\rho}{4m^2}\right)\right]\\
&-i\frac{\pi^2m^4}{4}\left(\eta_{\mu r}\eta_{\nu s}+\eta_{\mu\nu}\eta_{rs}+\eta_{\mu s}\eta_{\nu r}\right)
\end{aligned}
$$

$$
\begin{aligned}
&\times\left\{\left[\frac{1}{2}-\frac{2}{3}\frac{\rho}{4m^2}-\frac{8}{15}\left(\frac{\rho}{4m^2}\right)^2\right]\right.\\
&\left.\times\left(\ln m^2+1\right)-\frac{1}{2}\left[\frac{3}{2}-\frac{1}{9}\left(\frac{\rho}{4m^2}\right)+\frac{52}{225}\left(\frac{\rho}{4m^2}\right)^2\right]\right\}\\
&-i\frac{2\pi^2m^4}{105}\left(\eta_{\mu r}\eta_{vs}+\eta_{\mu v}\eta_{rs}+\eta_{\mu s}\eta_{vr}\right)\left(\frac{\rho}{4m^2}\right)^3F\left(1,1,\frac{9}{2};-\frac{\rho}{4m^2}\right)\\
&-i\frac{\pi^2m^2\left(k^2-m^2\right)}{12\left(4m^2+k^2-i0\right)}\left(\eta_{\mu s}k_rk_v+\eta_{\mu v}k_rk_s+\eta_{rs}k_\mu k_v+\eta_{rv}k_\mu k_s\right)\\
&\times\left[\frac{1}{2}\left(\ln m^2+\frac{1}{3}\right)+\frac{1}{5}\left(\ln m^2+\frac{5}{6}\right)\frac{k^2}{4m^2}\right]\\
&-i\frac{\pi^2m^2}{8\left(4m^2+k^2-i0\right)}\left(\eta_{\mu s}k_rk_v+\eta_{\mu v}k_rk_s+\eta_{rs}k_\mu k_v+\eta_{rv}k_\mu k_s\right)\\
&\times m^2\left[\left(\ln m^2+\frac{2}{3}\right)+\frac{k^2}{12}+\frac{k^2}{30}\frac{k^2}{4m^2}\right]-\frac{i\pi^2m^4}{40\left(4m^2+k^2-i0\right)}\frac{k^2}{4m^2}\\
&-i\frac{\pi^2m^2}{10}\left(\eta_{\mu s}k_rk_v+\eta_{\mu v}k_rk_s+\eta_{rs}k_\mu k_v+\eta_{rv}k_\mu k_s\right)\\
&\times\frac{k^2-m^2}{21\left(4m^2+k^2-i0\right)}F\left(1,1,\frac{9}{2};-\frac{\rho}{4m^2}\right)\left(\frac{k^2}{4m^2}\right)^2\\
&-i\frac{\pi^2}{12}k_\mu k_rk_vk_s\left[\left(\ln m^2+\frac{3}{4}\right)+\frac{k^2-4m^2}{2\left(4m^2+k^2-i0\right)}\right]\\
&-i\frac{\pi^2m^2}{30}k_\mu k_rk_vk_s\frac{k^2-m^2}{4m^2+k^2-i0}\frac{k^2}{4m^2}F\left(1,1,\frac{7}{2};-\frac{k^2}{4m^2}\right)+\sum_{n=0}^{\infty}a_n\lambda^n.
\end{aligned}
\tag{8.7}
$$

Once again, the exact result for our four-dimensional convolution is

$$
\begin{aligned}
&\Sigma_{GM\,\mu\nu rs}\left(k\right)=k_\mu k_r\left(\rho+m^2-i0\right)^{-1}*k_vk_s\left(\rho+m^2-i0\right)^{-1}\\
&=i\frac{m^2\pi^2}{2}\left(\eta_{\mu r}k_vk_s+\eta_{vs}k_\mu k_r\right)\times\left[\frac{1}{3}\left(\ln m^2+\frac{1}{12}\right)+\frac{1}{5}\frac{\rho}{4m^2}\left(\ln m^2+\frac{13}{15}\right)\right]\\
&+i\frac{m^2\pi^2}{30}\left(\eta_{\mu r}k_vk_s+\eta_{vs}k_\mu k_r\right)\frac{\rho}{4m^2}\\
&\times\left[F\left(1,1,\frac{7}{2};-\frac{\rho}{4m^2}\right)+\frac{1}{7}F\left(1,1,\frac{9}{2};-\frac{\rho}{4m^2}\right)\right]\\
&-i\frac{\pi^2m^4}{4}\left(\eta_{\mu r}\eta_{vs}+\eta_{\mu v}\eta_{rs}+\eta_{\mu s}\eta_{vr}\right)\times\left\{\left[\frac{1}{2}-\frac{2}{3}\frac{\rho}{4m^2}-\frac{8}{15}\left(\frac{\rho}{4m^2}\right)^2\right]\right.\\
&\left.\times\left(\ln m^2+1\right)-\frac{1}{2}\left[\frac{3}{2}-\frac{1}{9}\left(\frac{\rho}{4m^2}\right)+\frac{52}{225}\left(\frac{\rho}{4m^2}\right)^2\right]\right\}\\
&-i\frac{2\pi^2m^4}{105}\left(\eta_{\mu r}\eta_{vs}+\eta_{\mu v}\eta_{rs}+\eta_{\mu s}\eta_{vr}\right)\left(\frac{\rho}{4m^2}\right)^3F\left(1,1,\frac{9}{2};-\frac{\rho}{4m^2}\right)\\
&-i\frac{\pi^2m^2\left(k^2-m^2\right)}{12\left(4m^2+k^2-i0\right)}\left(\eta_{\mu s}k_rk_v+\eta_{\mu v}k_rk_s+\eta_{rs}k_\mu k_v+\eta_{rv}k_\mu k_s\right)
\end{aligned}
$$

$$\times\left[\frac{1}{2}\left(\ln m^2+\frac{1}{3}\right)+\frac{1}{5}\left(\ln m^2+\frac{5}{6}\right)\frac{k^2}{4m^2}\right]$$
$$-i\frac{\pi^2m^2}{8\left(4m^2+k^2-i0\right)}\left(\eta_{\mu s}k_rk_v+\eta_{\mu v}k_rk_s+\eta_{rs}k_\mu k_v+\eta_{rv}k_\mu k_s\right)$$
$$\times m^2\left[\left(\ln m^2+\frac{2}{3}\right)+\frac{k^2}{12}+\frac{k^2}{30}\frac{k^2}{4m^2}\right]-\frac{i\pi^2m^4}{40\left(4m^2+k^2-i0\right)}\frac{k^2}{4m^2}$$
$$-i\frac{\pi^2m^2}{10}\left(\eta_{\mu s}k_rk_v+\eta_{\mu v}k_rk_s+\eta_{rs}k_\mu k_v+\eta_{rv}k_\mu k_s\right)$$
$$\times\frac{k^2-m^2}{21\left(4m^2+k^2-i0\right)}F\left(1,1,\frac{9}{2};-\frac{\rho}{4m^2}\right)\left(\frac{k^2}{4m^2}\right)^2 \tag{8.8}$$
$$-i\frac{\pi^2}{12}k_\mu k_rk_vk_s\left[\left(\ln m^2+\frac{3}{4}\right)+\frac{k^2-4m^2}{2\left(4m^2+k^2-i0\right)}\right]$$
$$-i\frac{\pi^2m^2}{30}k_\mu k_rk_vk_s\frac{k^2-m^2}{4m^2+k^2-i0}\frac{k^2}{4m^2}F\left(1,1,\frac{7}{2};-\frac{k^2}{4m^2}\right)$$

Accordingly, our desired self-energy total is a combination of $\Sigma_{G\alpha_1\alpha_2\alpha_3\alpha_4}(k)$ and $\Sigma_{GM\alpha_1\alpha_2\alpha_3\alpha_4}(k)$.

9. Axion's Self Energy

The self-energy reads

$$\Sigma^{\mu s}(k)=\frac{2\gamma^{\mu v}\gamma^{rs}}{\gamma_{\rho\lambda}\gamma^{\rho\lambda}}k_vk_r\left(\rho+m^2-i0\right)^{-1}*\left(\rho-i0\right)^{-1}. \tag{9.1}$$

In four dimensions, we have

$$k_vk_r\left(\rho+m^2-i0\right)^{-1}*\left(\rho-i0\right)^{-1}=\int\frac{k_vk_r}{\left(k^2+m^2-i0\right)\left[\left(p-k\right)^2-i0\right]}\mathrm{d}^4k. \tag{9.2}$$

Using the same Feynman parameters as above, we have

$$k_vk_r\left(\rho+m^2-i0\right)^{\lambda-1}*\left(\rho-i0\right)^{\lambda-1}$$
$$=i\int_0^1x^{-\lambda}\left(1-x\right)^{-\lambda}\int\frac{k_vk_r}{\left[\left(k-px\right)^2+a\right]^{2-\lambda}}\mathrm{d}^4k\mathrm{d}x, \tag{9.3}$$

where

$$a=\left(p^2+m^2\right)x-p^2x^2. \tag{9.4}$$

We compute the integral (3) and encounter

$$k_vk_r\left(\rho+m^2-i0\right)^{\lambda-1}*\left(\rho-i0\right)^{\lambda-1}$$
$$=i\frac{\eta_{vr}m^{2+4\lambda}\pi^2}{4}\frac{\Gamma\left(2+\lambda\right)}{\Gamma\left(1-\lambda\right)}\Gamma\left(-1-2\lambda\right)F\left(-1-2\lambda,1-\lambda,3;-\frac{\rho}{m^2}\right) \tag{9.5}$$
$$+\frac{ik_vk_rm^{4\lambda}\pi^2}{6}\frac{\Gamma\left(3+\lambda\right)}{\Gamma\left(1-\lambda\right)}\Gamma\left(-2\lambda\right)F\left(-2\lambda,1-\lambda,4;-\frac{\rho}{m^2}\right).$$

Self-Energy Computation ($\lambda = 0$)

We Laurent-expand again, this time (5) around $\lambda = 0$.

$$
\begin{aligned}
& k_v k_r \left(\rho + m^2 - i0\right)^{\lambda-1} * \left(\rho - i0\right)^{\lambda-1} \\
& = i\pi^2 \left\{ \frac{1}{2\lambda} \left(\frac{\eta_{vr} m^2}{4} - \frac{1}{3} k_v k_r \right) + \frac{\eta_{vr} m^2}{4} \left[\left(1 + \frac{1}{3} \frac{\rho}{m^2} \right) \left(\ln m^2 + \frac{1}{2} \right) \right. \right. \\
& \left. - \left(1 + \frac{1}{6} \frac{\rho}{m^2} \right) \right] - \frac{k_v k_r}{3} \left(\ln m^2 + \frac{3}{4} \right) \\
& \left. + \frac{1}{4} \left(\frac{\rho}{m^2} \right) \left[\frac{\eta_{vr} m^2}{12} \frac{\rho}{m^2} - \frac{k_v k_r}{3} \right] F\left(1,1,5;-\frac{\rho}{m^2}\right) + \sum_{n=1}^{\infty} a_n \lambda^n \right\}
\end{aligned}
\tag{9.6}
$$

The λ -independent term yields the exact convolution result we need

$$
\begin{aligned}
\Sigma_{vr}(k) &= k_v k_r \left(\rho + m^2 - i0\right)^{-1} * \left(\rho - i0\right)^{-1} \\
&= i\pi^2 \left\{ \frac{\eta_{vr} m^2}{4} \left[\left(1 + \frac{1}{3} \frac{\rho}{m^2} \right) \left(\ln m^2 + \frac{1}{2} \right) \right] \right. \\
&\quad - \left(1 + \frac{1}{6} \frac{\rho}{m^2} \right) \Bigg] - \frac{k_v k_r}{3} \left(\ln m^2 + \frac{3}{4} \right) \\
&\quad \left. + \frac{1}{4} \left(\frac{\rho}{m^2} \right) \left[\frac{\eta_{vr} m^2}{12} \frac{\rho}{m^2} - \frac{k_v k_r}{3} \right] F\left(1,1,5;-\frac{\rho}{m^2}\right) \right\}
\end{aligned}
\tag{9.7}
$$

10. Conclusions

We have developed above an approximate quantum field theory (QFT) of Einstein's gravity (EG) that is both unitary and finite. This treatment considerably simplifies the mathematical handling so that it may constitute a valuable tool in the theorist's arsenal.

This paper addressed the same problem tackled in [19], with different mathematical techniques. Both papers dealt with gravity's quantization (GQ) via an approximate graviton's approach. The difference between that reference and the present paper resides in the fact that here we base our discourse on a general GQ formulation using Ultrahyperfunctions. In [19], instead, we constitute a special instance, based on Explicitly Lorentz Invariant Schwartz' Distributions (ELISD). The predictions of the two papers are similar, a remarkable fact given that the two types of mathematics involved are very different.

Our approximation consists of defining the graviton field as $\phi^{\mu\nu} = \gamma^{\mu\nu}\phi$ with $\gamma^{\mu\nu}$ a constant tensor and ϕ an scalar field.

Summing up, we have evaluated in finite fashion.

- A graviton's self-energy in the EG-field.
- The self-energy in the presence of a massive scalar field (axions, for example). Two sorts of diagram emerge: the original ones of the pure EG field plus the ones generated by the addition of a scalar field.
- An axion's self-energy.

Conflicts of Interest

The authors declare no conflicts of interest regarding the publication of this paper.

References

[1] Plastino, A. and Rocca, M.C. (2020) *Journal of Physics Communications*, **4**, Article ID: 035014. https://doi.org/10.1088/2399-6528/ab8178

[2] Plastino, A. and Rocca, M.C. (2020) *Journal of Modern Physics*, **11**, 378-394. https://doi.org/10.4236/jmp.2020.113024

[3] Gupta, S.N. (1956) *Proceedings of the Physical Society. Section A*, **65**, 161. https://doi.org/10.1088/0370-1298/65/3/301

[4] Gupta, S.N. (1956) *Proceedings of the Physical Society. Section A*, **65**, 608-619. https://doi.org/10.1088/0370-1298/65/8/304

[5] Gupta, S.N. (1968) *Physical Review*, **172**, 1303. https://doi.org/10.1103/PhysRev.172.1303

[6] Bollini, C.G., Escobar, T. and Rocca, M.C. (1999) *International Journal of Theoretical Physics*, **38**, 2315-2332. https://doi.org/10.1023/A:1026623718239

[7] Bollini, C.G. and Rocca, M.C. (2004) *International Journal of Theoretical Physics*, **43**, 1019-1051. https://doi.org/10.1023/B:IJTP.0000048599.21501.93

[8] Bollini, C.G. and Rocca, M.C. (2004) *International Journal of Theoretical Physics*, **43**, 59-76. https://doi.org/10.1023/B:IJTP.0000028850.35090.24

[9] Bollini, C.G., Marchiano, P. and Rocca, M.C. (2007) *International Journal of Theoretical Physics*, **46**, 3030-3059. https://doi.org/10.1007/s10773-007-9418-y

[10] Plastino, A. and Rocca, M.C. (2018) *Journal of Physics Communications*, **2**, Article ID: 115029. https://doi.org/10.1088/2399-6528/aaf186

[11] Grothendieck, A. (1955) Produits Tensoriels Topologiques et Espaces Nucleaires (Memoirs of the American Mathematical Society, Number 16). American Mathematical Society, Providence. https://doi.org/10.1090/memo/0016

[12] Sebastiao e Silva, J. (1958) *Mathematische Annalen*, **136**, 58-96. https://doi.org/10.1007/BF01350287

[13] Feynman, R.P. (1963) *Acta Physica Polonica*, **24**, 697.

[14] Visconti, A. (1969) Quantum Field Theory. Pergamon Press, Oxford.

[15] Delbourgo, R. and Prasad, V.B. (1975) *Journal of Physics G: Nuclear Physics*, **1**, 377. https://doi.org/10.1088/0305-4616/1/4/001

[16] Barci, D.G., Bollini, C.G. and Rocca, M.C. (1995) *Il Nuovo Cimento*, **108**, 797-808. https://doi.org/10.1007/BF02731021

[17] Kleinert, H. (2016) Particles and Quantum Fields Free Web Version. https://doi.org/10.1142/9915

[18] Peccei, R.D. (2008) The Strong CP Problem and Axions. In: Kuster, M., Raffelt, G. and Beltrán, B., Eds., *Axions: Theory, Cosmology, and Experimental Searches*, Lecture Notes in Physics, Vol. 741, Springer, Heidelberg, 3-17. https://doi.org/10.1007/978-3-540-73518-2_1

[19] Plastino, A. and Rocca, M.C. (2020) *Journal of High Energy Physics, Gravitation and Cosmology*. (In Press)

Journal of Modern Physics, 2020, 11, 581-592
https://www.scirp.org/journal/jmp
ISSN Online: 2153-120X
ISSN Print: 2153-1196

Complete Solution for Quasicrystals

Antony J. Bourdillon

UHRL, San Jose, CA, USA
Email: bourdillona@sbcglobal.net

How to cite this paper: Bourdillon, A.J. (2020) Complete Solution for Quasicrystals. *Journal of Modern Physics*, **11**, 581-592.
https://doi.org/10.4236/jmp.2020.114038

Received: March 25, 2020
Accepted: April 21, 2020
Published: April 24, 2020

Abstract

A set of discoveries are described that complete the structural model and diffraction theory for quasicrystals. The irrational diffraction indices critically oppose Bragg diffraction. We analyze them as partly rational; while the irrational part determines the metric that is necessary for measurement. The measurement is verified by consistency with the measured lattice parameter, now corrected with the metric and index. There is translational symmetry and it is hierarchic, as is demonstrated by phase-contrast, optimum-defocus imaging. In Bragg's law, orders are integral, periodic and harmonic; we demonstrate harmonic quasi-Bloch waves despite the diffraction in irrational, geometric series. The harmonicity is both local and long range. A breakthrough in understanding came from a modified structure factor that features independence from scattering angle. Diffraction is found to occur at a given "quasi-Bragg condition" that depends on the special metric. This is now analyzed and measured and verified: the *metric function* is derived from the irrational part of the index in three dimensions. The inverse of the function is exactly equal to the metric that was first discovered independently by means of "quasi-structure factors". These are consistent with all structural measurements, including diffraction by the quasicrystal, and with the measured lattice parameter.

Keywords

Quasicrystal, Icosahedra, Hierarchic, Integral, Periodic, Harmonic, Irrational, Geometric Series, Metric

1. Introducing Harmonics in Hierarchy

"A metallic phase with long range order but with no translational symmetry" [1], how come? The greater the prize, the worse the gaff: the translational symmetry is strictly hierarchic [2]-[15]. How, in particular, can the diffraction represent long range order when it occurs as irrational numbers, aperiodically ordered, and in geometric series? Since Bohr's atom, all of modern wave physics

have required harmonic solutions; how does that strange series harmonize? This study shows precisely how the exceptional harmony occurs.

The original solid-state phase was discovered in 1982 and published in 1984 [1], shortly before my hierarchic proposal in 1986. After twenty years in the doldrums, Senechal wrote for the American Mathematical Society, "What is a quasicrystal?" The paper began, "The short answer is no one [knows]" [16]. She was mistaken: I had by then discovered the quasi-structure factor and metric [2] [3] [6]. These were based on phase-contrast, optimum-defocus images [17] which identify the locations of the heavier atom in the Al_6Mn icosahedral alloy, owing to high atomic scattering factor. Knowing all of the microscope magnification, the image pattern, and the diffraction pattern, it was obvious that the unit cell is $Al_{12}Mn$, with stoichiometry Al_6Mn because of edge sharing. These cells are hierarchically arranged, each order having 6 five-fold rotation axes. In particular, four tiers of hierarchic structure are evident in the data and this structure was shown to be infinitely extensible: it is logarithmically periodic with period τ^2, the square of the golden section $\tau = \left(1+5^{1/2}\right)/2$ [18].

To calculate the diffraction pattern from the known structure, it was necessary to correctly index [9] the original diffraction pattern [1] [2]. From stereographic projections of the icosahedral axes and diffraction planes, the indexation was shown to be three dimensional, in geometric series, simple and complete. The planes are normal to the three-dimensional axes. Mathematicians choose six dimensions; physicists falsify them.

A breakthrough in understanding of the diffraction pattern followed our realization that the structure factor is independent of scattering angle and can be simply calculated from our knowledge of the structure [2] [14]. *Prima facie*, the structure factor was inconsistent with data. This inconsistency was half expected because of known "quasi-periodicity", so we included two adjustments to the formulae. Firstly, a coherence term c_s which has the effect similar to making the structure breath so that the quasi-Bragg condition became evident by sudden diffractive coherence, that is similar to Bragg coherence observed by rotation of a crystal through the Bragg condition: suddenly on and suddenly off. Bragg diffraction is bi-planar where quasi-Bragg diffraction is multi-planar [14], but the breathing coherence provides sharp diffraction at the quasi-Bragg condition [12], in spite of the "quasiperiodic lattice". Actually of course, there is no mechanical breathing strain; the coherence is due to axial contraction owing to the peculiar hierarchic optics as will be described below by a new law in physics. Secondly, it became obvious that because our unit cells do not repeat periodically in linear order, we had to sum our quasi-structure not just over the unit cell as in crystals; but over the whole quasicrystal (QC) in hierarchic order. The quasi-structure factor formula (QSF) allowed an important iterative procedure that was necessary for the summation of high orders: the iteration overcame computing truncation errors. The final result is consistent with experimental diffraction data [2] [5]. An example will be given in **Figure 1**. This shows four peaks in

geometric series, offset from the Bragg condition by the metric 0.894. This will be elaborated in the next section.

The outstanding question remained, what is the metric and how does the geometric series diffraction occur? It is not consistent with Bragg diffraction; but rather diametrically opposed by geometric, aperiodic, and anharmonic orders n, and multiple spacings d at any given Bragg condition. The new quasi-Bragg law was evident: $\tau^m \lambda = 2d' \sin(\theta')$, where through multiple simulations, the role of the metric defined all of the lattice parameter a; the order $n' \to m$; the quasi-interplanar spacing d'; and quasi-Bragg angle θ' (the compliment to the angle of incidence). *After completely understanding the metric in this unique diffraction, the varieties of data verify both the structure and the diffraction.*

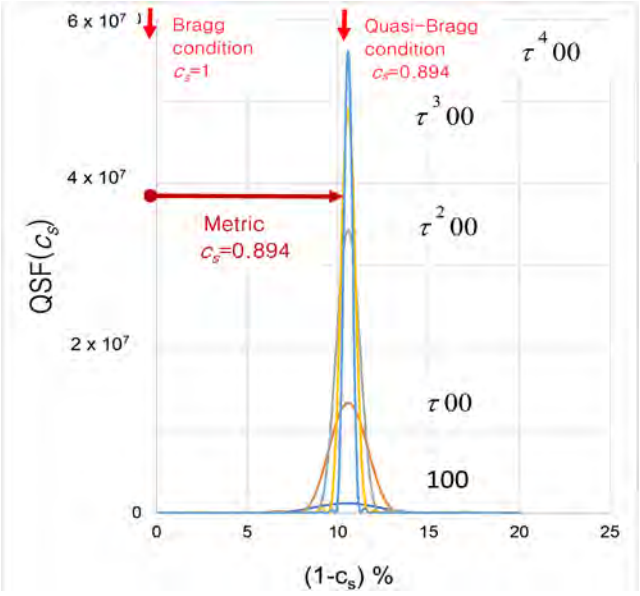

Figure 1. Quasi structure factors calculated by scanning for five peaks in geometric series against the coherence factor c_s [14]. At the Bragg condition, $c_s = 1$ (ordinate axis), and there is no diffraction; the diffraction peaks occur at the quasi-Bragg condition when the metric $c_s = 0.894$. All peaks in the diffraction pattern of ref. [1] are calculated to occur at this condition. Geometric series indices are shown level with the tops of corresponding QSF peaks.

2. Quasi Structure Factor (QSF) Suppresses Diffraction

The sites of atoms and cell centers in icosahedral clusters are known [2] [13] [14], and also sites of higher order p of supercluster centers, where radii multiply by τ^{2p}:

$$\text{Unit cell } (r_u): \quad \text{Mn} \quad (0,0,0)$$

$$\text{Al} \quad \frac{1}{2}(\pm\tau, 0, \pm 1), \frac{1}{2}(0, \pm 1, \pm\tau), \frac{1}{2}(\pm 1, \pm\tau, 0) \tag{1}$$

and

$$\text{Cell or cluster centers } (r_{cc}) \quad \frac{1}{2}(\pm\tau^2, 0, \pm\tau), \frac{1}{2}(0, \pm\tau, \pm\tau^2), \frac{1}{2}(\pm\tau, \pm\tau^2, 0) \tag{2}$$

The QSF formula is adapted from classical crystallography with two differences:

$$F_{hkl} = \sum_{i=1}^{\text{all atoms}} f_i \cos\left(2\pi \cdot c_s \left(\overline{h_{hkl}} \cdot \overline{r_i}\right)\right) \tag{3}$$

firstly, because the diffraction is sharp in spite of multiple interplanar spacings d, a coherence factor c_s is inserted. Its value will be derived analytically below. The factor is used as a scanned variable (Figure 1) to illustrate the variance of quasi-Bragg diffraction from Bragg diffraction in crystals.

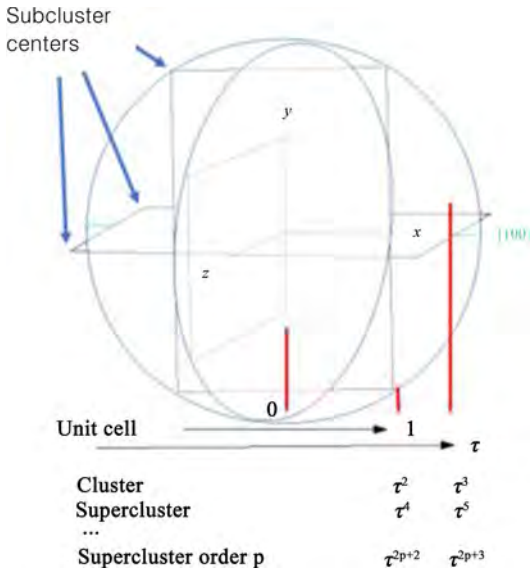

Figure 2. Each golden triad has three principal planes on each dimension that intersect (red pointers) at normals on the [100] axis in the diagram. Each corner of each golden rectangle locates the center of a cell or subcluster. Intercluster spacings are arranged at intervals 0, 1, τ, for the unit cell. By scaling the triad for clusters and superclusters, the spacings continue $\tau^2, \tau^3, \tau^4, \cdots$ in geometric series, as observed in diffraction indices.

Secondly, because the unit cells are not periodic as in crystals, the summation is made over all atoms in the QC; not just the unit cell. The summation is taken in two steps: over the unit cell and cluster, and iteratively over the superclusters in hierarchic order p. Write the vector from the origin to each atom in a cluster $\overline{r_{cl}}$ as the sum of a unit cell vector $\overline{r_u}$, with a vector to the cell centers in the cluster $\overline{r_{cc}}$: $\overline{r_{cl}} = \overline{r_{cc}} + \overline{r_u}$. Then since:

$$\sum_{i}^{N_{\text{cluster}}} \exp\left(\overline{h_{hkl}} \cdot \overline{r_{cl}}\right) = \sum_{i}^{12} \exp\left(\overline{h_{hkl}} \cdot \overline{r_{cc}}\right) \times \sum_{i}^{13} \exp\left(\overline{h_{hkl}} \cdot \overline{r_u}\right) \tag{4}$$

with corresponding summations over unit cell sites and cell centers, and knowing that $N_{\text{cluster}} = N_{cc} \cdot N_u$, the QSF for the cluster is calculated:

$$F_{hkl}^{\text{cluster}} = \sum_{i=1}^{12} \cos\left(2\pi \cdot c_s \left(\overline{h_{hkl}} \cdot \overline{r_{cc}}\right)\right) \cdot F_{hkl}^{\text{cell}} \tag{5}$$

and repeating iteratively over superclusters by using the known stretching factor τ^{2p}:

$$F_{hkl}^{p} = \sum_{i=1}^{\text{all atoms}} \cos\left(2\pi \cdot c_s \left(\overline{h_{hkl}} \cdot \tau^{2p} \overline{r_{cc}}\right)\right) \cdot F_{hkl}^{p-1} \quad (6)$$

The example in **Figure 1** is for a simple axial series, but all beams in the original data [1] display the same metric deviance from the Bragg condition on the ordinate axis where $c_s = 1$. In the QCs all beams peak at the quasi-Bragg condition $c_s = 0.894$. *There is no Bragg diffraction*. From larger samples, the value of c_s is extremely precise [5]. As we shall see, this value is the result of harmonization of the incident, sine wave probe with the aperiodic, hierarchic structure. Notice that the QSF depends on the angle between a specific atomic plane-normal and the crystal structure; it is independent of the experimental Bragg angle. Elimination of the Bragg angle θ from the equation, allowed access to parameters n', d', and hierarchic lattice parameter a. (The value of the QSF depends greatly on the number of atoms in the simulated quasicrystal as also partly on atomic scattering factors: the number is much larger and more varied than the number of atoms in a crystal unit cell).

3. Stretching the Axis for Bloch

Bragg diffraction is bi-planar: the path difference between two rays reflected from neighboring Bragg planes is equal to the wavelength of light. QC diffractions multiplanar, as is observed in high resolution electron micrographs: within the "quasi-periodic solids" every atom scatters. To know how the phases of the various scattered rays add, it is necessary to calculate the QSF. The addition is iterative (Equation (6)). Subclusters locate on the corners of the golden rectangles shown in **Figure 2**, *i.e.* on principal planes. These planes, in hierarchic diffraction, replace Bragg planes in diffraction from crystals. Keeping the golden triad as basis in the hierarchy, the spacings between principal planes scale geometrically owing to the stretching factor τ^{2p} that determines axial dimensions with increasing order.

Interplanar spacings are ordered like the diffraction pattern: $0, 1, \tau, \tau^2, \tau^3, \tau^4, \tau^5, \cdots$ It is evident that whereas Bragg diffraction occurs by coherent scattering from Bragg planes, hierarchic diffraction occurs by coherent scattering from subcluster centers. How, more precisely, this happens will be illustrated with quasi-Bloch waves. These waves differ from both the Bloch wave in crystals and from the Bragg diffracted wave beam. Bloch waves are evident as lattice images in the two-beam condition [19]. The waves are due to interference between an incident X-ray or electron beam with its specularly reflected diffraction beam. However, because the interplanar spacings are not in linear order in the QC, an imagined pseudo-Bragg Bloch wave (blue waves in **Figure 3**) may be coherent in the unit cell but must then be incoherent with the geometric, principal-plane, hierarchic lattice that describes the higher order icosahedra. The pseudo interference is destructive. To construct interference, the interfering sine wave must be stretched by the inverse of the metric. This makes the quasi-Bloch wave commensurate and approximately harmonic with the principal planes. The interfe-

rence is accompanied by a small (10.6%) change in scattering angle, away from the Bragg condition *i.e.* smaller than would occur in crystals having equivalent interplanar spacing. The result is the quasi-Bragg angle θ' to be used below in the quasi-Bragg law. Before we reach for this conclusion, we must explain the origin for the metric that was calculated in the QSFs, and that is critically needed to find the function $f(n', d', \theta', c_s) = 0$ for the quasi-Bragg diffraction. The strong explanation is principally numerical, and will be described in the next section.

Meanwhile, it is obvious in Figure 3, that whereas long range order is evident from the diffraction of quasicrystals, it is not true that there is no translational symmetry: the quasi-Bloch wave is invariant in all translations $a\tau^m$. There is additional symmetry because the hierarchic model is also centrosymmetric. Notice the extraordinary feature: the quasi-Bloch wave symmetry is both long range and local at each intercept in Figure 3(b).

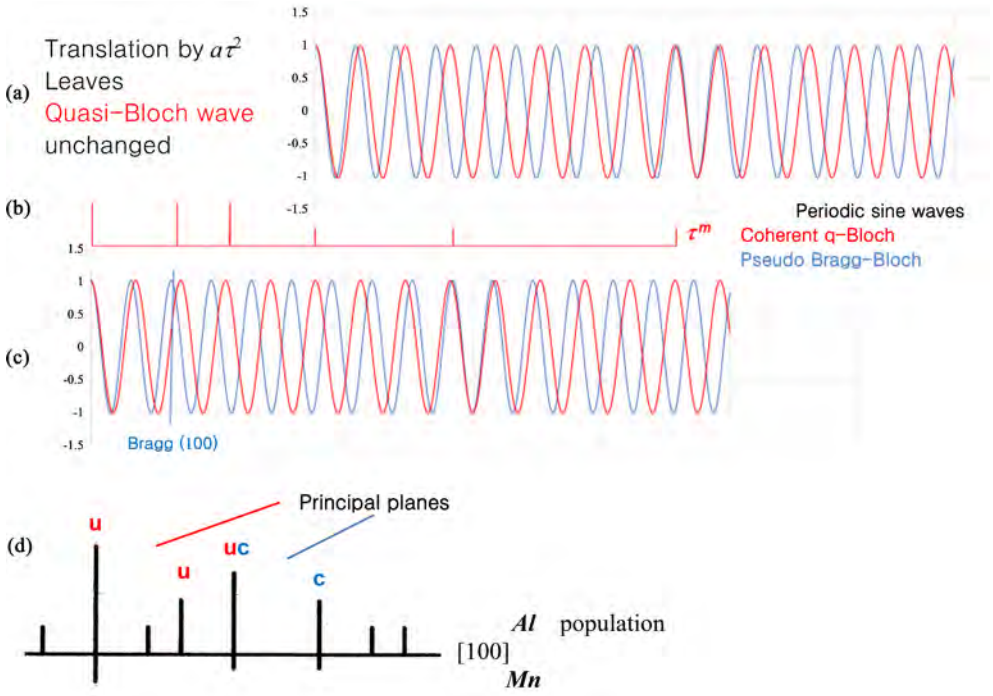

Figure 3. (a) Red Quasi-Bloch wave invariant under translation $a\tau^m$ compared with blue pseudo-Bragg Bloch wave that is incommensurate with the structure below in d. (b) Geometric series that mark locations of principal plane intercepts in the unit cell and cluster as below. (c) Same traces as (a), but translated to demonstrate local and long range invariance of the quasi-Bloch wave, and approximate coherence with structure. (d), Atomic planes in the semi-cluster that cross the [100] axis, including principal planes: u for the unit cell; c for the cluster. Where the pseudo-Bragg Bloch wave is incoherent.

4. Irrational Metric Function

Column 7 in Table 1 lists the *geometric series*, *base* τ. Corresponding values are shown in col.9. They are irrational excepting the first. The exact Fibonacci equivalents are shown in cols 2 - 5. They can be rationalized by replacing the irrational number t by the fraction 3/2. For harmony, the fraction should be

Table 1. The bold type in column 7 shows the *geometric series* that correctly indexes the observed diffraction pattern. Corresponding irrational values are shown in col. 9 and the common Fibonacci sequence (cols 2 - 5), which sums a rational part and an irrational part. By substituting the rational fraction 3/2 for irrational τ in col.5, the rational series in col.10 is derived. QSFs calculated for this imaginary structure are Bragg-like with $c_s = 1$. This fact confirms the supposition that the metric, calculated in the quasi-Bragg QSFs, is due to the irrational part of col.9 (*i.e.* completely absent in Bragg diffraction). Subtract it from col.9 and harmonize the residue by dividing col. 11/col. 12 (corresponding to harmonics in **Figure 3**). Derive the metric in the final col. 14. This value is identical to the metric simulated universally in QSFs. N.B. $\tau^m = F_m(1,\tau) = F_m(0,1) + F_{m+1}(0,1)\tau$; where $m > 0$; ratios $F_{m+1}(0,1)/F_m(0,1)$ oscillate about τ; contrasting $F_{m+1}(1,\tau)/F_m(1,\tau) = \tau$, as in the diffraction data.

	Fibonacci series				Geometric series		Irrational values	Rational Approx.	Irr.-Rat. residue	Commensurate divisor	Residue/ divisor	Metric
					τ^{m-1}							c_s
m	F_m		F_{m+1}	τ				$a+3b/2$		$/F_{m+1}$	$\Delta = \tau - 3/2$	$1/(1+\Delta)$
			0	τ	τ^0	=	1	1	0	0		
1	0		1	τ	τ	=	1.618034...	1.5	0.11803	1	0.118034	0.894427
2	1	+	1	τ	τ^2	=	2.618034…	2.5	0.11803	1	0.118034	0.894427
3	1	+	2	τ	τ^3	=	4.236068…	4	0.23607	2	0.118034	0.894427
4	2	+	3	τ	τ^4	=	6.854102	6.5	0.3541	3	0.118034	0.894427
5	3	+	5	τ	τ^5	=	11.09017	10.5	0.59017	5	0.118034	0.894427
6	5	+	8	τ	τ^6	=	17.944272	17	0.94427	8	0.118034	0.894427
7	8	+	13	τ	τ^7	=	29.034443	27.5	1.53444	13	0.118034	0.894427
8	13	+	21	τ	τ^8	=	46.978715	44.5	2.47872	21	0.1180341	0.894427
9	21	+	34	τ	τ^9	=	76.013159	72	4.01316	34	0.1180341	0.894427
10	34	+	55	τ	τ^{10}	=	122.99188	116.5	6.49188	55	0.1180341	0.894427
11	55	+	89	τ	τ^{11}	=	199.00504	188.5	10.505	89	0.1180341	0.894427
12	89	+	144	τ	τ^{12}	=	321.99691	305	16.9969	144	0.1180341	0.894427

integral or half integral. QSF calculations show it is half integral. The rational approximation to the geometric series indices is listed in col. 10. Calculation of the QSFs for this imaginary series is Bragg-like with $c_s = 1$. This demonstrates the fact that t*he metric is an expression of the irrational part of the geometric sequence* in col. 7. To derive the metric, subtract the rational part from the irrational sequence (col. 7 - col. 10) to give the residue in column 11. Notice that this is a growing number down the sequence, and that it can be harmonized by the integers $F_{m+1}(0,1)$ in col. 12, *i.e.* the Fibonacci sequence $F_{m+1} = 0,1,1,2,3,5,\cdots$, with the argument representing the first two terms. The re-normalization corresponds to the increasing number of periods between intercepts illustrated in **Figure 3**. Division of the irrational residue by this sequential harmonization leaves the constant, irrational number. When this is represented as an increment on the $c_s = 1$ at the Bragg condition, and then inverted, we derive, from the irrational

indices, the analytic metric which is exactly the same as was discovered, by the perfectly independent numerical method of QSF simulations on the QC. The exact and identical values make the probability for error infinitesimally small and practically impossible.

The result is summarized in Figure 4. The "metric function" is the inverse of the metric and is equal to:

$$
\begin{aligned}
{}^{1}/_{c_s} &= 1+(\tau-{}^{3}/_{2}) = 1+0.118034 = {}^{1}/_{c_s}\\
&= 1+(\tau^{2}-{}^{5}/_{2})\\
&= 1+\frac{(\tau^{3}-4)}{2}\\
&= 1+\frac{(\tau^{4}-{}^{13}/_{2})}{3}\\
&= 1+\frac{(\tau^{5}-{}^{21}/_{2})}{5}\\
&= 1+\frac{(\tau^{6}-{}^{34}/_{2})}{8}\\
&\ \ \vdots\\
&= 1+\frac{(\tau^{m}-{}^{F_{m+4}}/_{2})}{F_{m+1}} = \frac{1}{0.894}
\end{aligned}
$$

irrational index; rational semi-integer subtraction; Fibonacci divisor; : Metric function

Figure 4. The metric function is derived by subtraction of the rational part from the irrational index $F_m(1,\tau)=1,\tau,\tau^2,\tau^3,\cdots$ (see Table 1). After division by a commensurating harmonic number, $F_{m+1}(0,1)=0,1,1,2,3,5,8,11,\cdots$, (also Fibonacci, see Figure 3), the metric expresses computational "breathing" of the QC axes that are necessary for coherence. This condition was obtained by scanning c_s to find the maximum QSF. The metric function is the inverse of the metric that is simulated universally in QSFs. The first six terms are evaluated as examples. The wave expands when the metric contracts the axes.

$$\frac{1}{c_s}=1+\frac{\tau^m-F_{m+4}/2}{F_{m+1}}=\frac{1}{0.894} \tag{7}$$

To illustrate, the first six terms are shown in the figure: the metric is exactly derived from the irrational part of the index, the part that is completely absent in the Bragg formula.

The metric may be derived in several ways, one is as follows: An index τ^m is separated into rational and irrational parts while τ is separated into the rational semi-integral 3/2 and an irrational residue $\Delta=\tau-3/2$ (Table 1):

$$
\begin{aligned}
\tau^m &= F_m+F_{m+1}\cdot\tau\\
&= F_m+F_{m+1}+F_{m+1}/2+F_{m+1}\cdot\Delta\\
&= F_{m+2}+F_{m+1}/2+F_{m+1}\cdot\Delta\\
&= F_{m+4}/2+F_{m+1}\cdot\Delta
\end{aligned} \tag{8}
$$

Since, by general properties of the Fibonacci sequence:

$$
\begin{aligned}
F_{m+4}/2 &= F_{m+3}/2+F_{m+2}/2\\
&= F_{m+2}/2+F_{m+1}/2+F_{m+2}/2\\
&= F_{m+2}+F_{m+1}/2
\end{aligned} \tag{9}
$$

Equation (8) is thereby systematically confirmed from Table 1 and Figure 4, and rearranged:

$$\Delta = \frac{\tau^m - F_{m+4}/2}{F_{m+1}} \tag{10}$$

So that the metric function:

$$\frac{1}{c_s} = 1 + \Delta = \frac{1}{0.894} \tag{11}$$

in complete agreement with the QSF simulations where $c_s = 1/1.1180$, and $\Delta = \tau - 3/2 = 0.1180$. This irrational part (Table 1, col. 11), can be written $F_{m+1}(1, \tau - 3/2)\Delta$, consistent with Equation (8).

The metric can be derived in further ways: notice, for example, that if τ is supposed to vary, then $c_s \to 1$ as $\tau \to 0$, *i.e.* at the Bragg condition. Generally however, the metric commensurates and harmonizes the diffracted sine wave onto a geometric grid [2] [14], as is simulated in the QSFs.

A summary of the structural result is shown in Figure 5. Notice, in particular, that the lattice parameter for the QC that was measured a long time ago on an assumption of Bragg diffraction [20] [21], is now corrected for the metric and index under the quasi-Bragg law: $a = 0.205 \cdot \tau \cdot c_s$ nm. Within errors, a is equal to both the known diameter of *Al* and to the edge width of the unit cell (Figure 6). To understand this, consider the edge of the unit cell. Twelve *Al* atoms are closely packed around the central *Mn* atom. The edge width of the unit cell is the sum of the radii of two *Al* atoms [5] [14] [15]. The experimental value of *a* is a necessary consistency test for any model that has been proposed, and the test is only possible with a systematic and complete theory of the unique diffraction. There is a further fact beyond the strong evidence from imaging and

Bragg	Hierarchic	Comment
$n = 2d\sin(\theta)/\lambda$	$\tau^m = 2d'\sin(\theta')/\lambda$	Harmonic laws Give us $\theta' = \theta/c_s$
$F_{hkl} = \Sigma f_i \cos(2\pi \mathbf{h}_{hkl} \cdot \mathbf{r}_i)$	$F'_{hkl} = \Sigma f_i \cos(2\pi c_s (\mathbf{h}_{hkl} \cdot \mathbf{r}_i))$ *including iteration*	Structure factors Give c_s, a and d'
$d = a/h$	$d' = a\, c_s/h$	$\theta' = \theta/c_s$
	$a = 0.206\ \tau c_s$ nm [1] $a^* = 2\pi/a$	Measured lattice parameter $a \approx$ Diameter of Al

Measured & Verified

n:	Bragg order	F_i:	Structure factors
d:	Bragg interplanar spacing	f_i:	atomic scattering factor for atom i
θ:	Bragg angle	c_s:	metric
λ:	wavelength	r_i:	atom position
τ:	golden section	h_{hkl}:	plane normal for indices h,k,l
prime	Hierarchic equivalent	a:	lattice parameter (cubic lattice) ~ *Al* dia reciprocal lattice vector $a^*=1/a'$

Figure 5. Comparison of Bragg parameters in crystals with quasi-Bragg parameters in quasicrystals. Notice especially the corrections (col. 2, row 5) to the lattice parameter a, derived from the earlier, false assumption of Bragg diffraction.

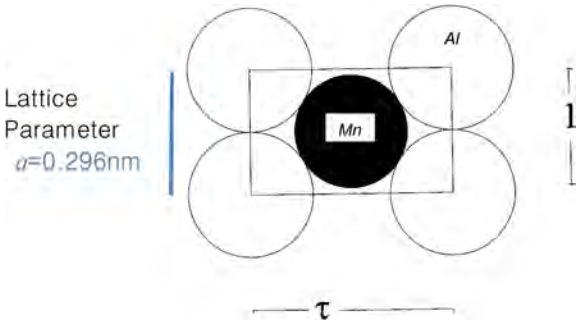

Figure 6. Cross-section of icosahedral unit cell showing central *Mn* atom touching outer *Al* atoms centered on corners of the golden rectangle. The measured lattice parameter, $a = 0.296$ nm , equals the width of the golden rectangle and the diameter of *Al*. The dense unit cell has 15 identical cross-sections between the 30 edges on the Platonic solid. Alongside the imaging of hierarchies and theory of diffraction, the measurement verifies the structure.

diffraction, namely that all diatomic, icosahedral QCs have atomic diameter ratios: $D_{\text{solute}}/D_{\text{solvent}} = \left(1+\tau^2\right)^{1/2} - 1$, as indeed do $D_{\text{Mn}}/D_{\text{Al}}$ in the figure. The fact is consistent with high local density as the structural driving force.

The true measurement of the lattice parameter, with the correction given by the metric and index under the quasi-Bragg law (**Figure 5**), verifies the structure and diffraction of the QC.

5. Welcome Hierarchic Physics

The quasicrystal has inter-related icosahedral symmetry with diffraction in geometric series: an incident X-ray or electron beam scatters off the hierarchic lattice into geometric space. *The metric, that is measured and experimentally verified, is now completely understood*. This is unique and novel in QCs. Quasicrystallographers have, for 38 years refused to accept this fact, though some, like Senechal have acknowledged shortcomings. For example, a sub-editor of *Acta Crystallographica* wrote that you don't measure the lattice parameter, "You just have to choose 'd_h'", the interplanar spacing [[5] p. 82]. This is a category error: mathematicians choose their axioms; physicists falsify them [22] [23]. He went on to write, "Bragg's equation cannot be applied if we do not know how to handle the term d_h". He doesn't "know" since he "chooses" a in $d_{hkl} = a/m \cdot \left(h,k,l^2\right)$ falsely and inaccurately (without metric); while Bragg's law *never* applies. His is first rank, mainstream, quasi-physics. As we have shown, the dimensions that mathematicians invent are multiplied without necessity; it is ironic that the metric function supplies the new dimensionality that they sought. Whatever, they do not review papers objectively when their own writings and readings are made irrelevant. The formal and informal logic that has guided science for two millenia are observed by neglect, and this is evident in published reviews. Other mathematical theories are equally quasi [23] [24], as Feynman famously observed, "No one understands quantum mechanics". But obviously, whatever is not understood is not physics.

6. Conclusion

The quasi-Bragg law is a new law in physics. Now that the structure and diffraction are clear for anybody to see and understand, we should *turn our attention to outlying problems*. These include quasicrystalloids in which planar five-fold, six-fold and eight-fold quasicrystal symmetries link to regular linear symmetries on planar normals. The icosahedral unit cell may share edges in various ways, and metrics are likely dependent on them individually. Another class of problems is defects, especially in rapidly quenched material. Some anomalous microstructures have been recorded, by convergent beam diffraction for example [21], so these, along with grain boundaries [14], might give important information about hierarchic crystal growth. Supposing that the dense unit cell nucleates in the melt before solidification, it is not obvious how clusters, superclusters and higher orders grow and agglomerate during solidification. It may become necessary to discover methods that can be used on samples that are more bulky than thin foils observed in typical transmission electron microscopy. Hierarchic crystals present ever more interesting phenomena, where mature and complete understanding now graduates them as a new field in physics.

Conflicts of Interest

The author declares no conflicts of interest regarding the publication of this paper.

References

[1] Shechtman, D., Blech, I., Gratias, D. and Cahn, J.W. (1984) *Physical Review Letters*, **53**, 1951-1953. https://doi.org/10.1103/PhysRevLett.53.1951

[2] Bourdillon, A.J. (2009) Quasicrystals and Quasi Drivers. UHRL, San Jose.

[3] Bourdillon, A.J. (2011) Logarithmically Periodic Solids. Nova Science, New York.

[4] Bourdillon, A.J. (2010) Quasicrystals' 2D Tiles in 3D Superclusters. UHRL, San Jose.

[5] Bourdillon, A.J. (2012) Metric, Myth and Quasicrystals. UHRL, San Jose, 82.

[6] Bourdillon, A.J. (2009) *Solid State Communications*, **149**, 1221-1225. https://doi.org/10.1016/j.ssc.2009.04.032

[7] Bourdillon, A.J. (2014) *Journal of Modern Physics*, **5**, 488-496. https://doi.org/10.4236/jmp.2014.56060

[8] Bourdillon, A.J. (2014) *Journal of Modern Physics*, **5**, 1079-1084. https://doi.org/10.4236/jmp.2014.512109

[9] Bourdillon, A.J. (2013) *Micron*, **51**, 21-25. https://doi.org/10.1016/j.micron.2013.06.004

[10] Bourdillon, A.J. (2016) *Journal of Modern Physics*, **7**, 43-50. https://doi.org/10.4236/jmp.2016.71005

[11] Bourdillon, A.J. (2015) *Physical Chemistry & Biophysics*, **5**, 3.

[12] Bourdillon, A.J. (2016) *Journal of Modern Physics*, **7**, 1558-1567. https://doi.org/10.4236/jmp.2016.712142

[13] Bourdillon, A.J. (2019) *Journal of Modern Physics*, **10**, 624-634.

https://doi.org/10.4236/jmp.2019.106044

[14] Bourdillon, A.J. (2019) *Journal of Modern Physics*, **10**, 1364-1373.

[15] Bourdillon, A.J. (2020) Complete Solution for Quasicrystals. https://www.youtube.com/watch?v=OFcSDKCecDA

[16] Senechal, M. (2006) *Notices to the American Mathematical Society*, **3**, 886-887.

[17] Bursill, L.L. and Peng, J.L. (1985) *Nature*, **316**, 50-51. https://doi.org/10.1038/316050a0

[18] Huntley, H.E. (1970) The Divine Proportion. Dover, Mineola.

[19] Hirsch, P., Howie, A., Nicholson, R.B., Pashley, D.W. and Whelan, M.J. (1977) Electron Microscopy of Thin Crystals. Krieger, New York.

[20] Tsai, A.P. (2008) *Science and Technology of Advanced Materials*, **9**, 1-20. https://doi.org/10.1088/1468-6996/9/1/013008

[21] Bourdillon, A.J. (1987) *Philosophical Magazine Letters*, **55**, 21-26. https://doi.org/10.1080/09500838708210435

[22] Popper, K.R. (1959) The Logic of Scientific Discovery. Hutchinson, London. https://doi.org/10.1063/1.3060577

[23] Popper, K.R. (1982) Quantum Theory and the Schism in Physics. Hutchison, London.

[24] Bourdillon, A.J. (2019) *Journal of Modern Physics*, **11**, 365-377. https://doi.org/10.4236/jmp.2019.106044

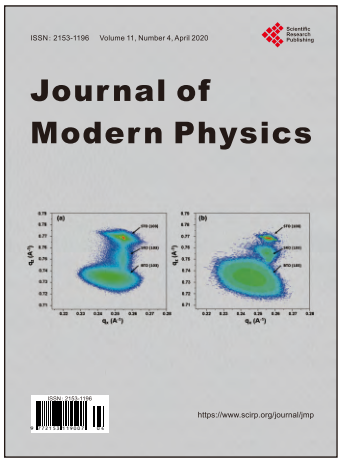

Call for Papers

Journal of Modern Physics

ISSN: 2153-1196 (Print) ISSN: 2153-120X (Online)
https://www.scirp.org/journal/jmp

Journal of Modern Physics **(JMP)** is an international journal dedicated to the latest advancement of modern physics. The goal of this journal is to provide a platform for scientists and academicians all over the world to promote, share, and discuss various new issues and developments in different areas of modern physics.

Editor-in-Chief

Prof. Yang-Hui He City University, UK

Subject Coverage

Journal of Modern Physics publishes original papers including but not limited to the following fields:

Biophysics and Medical Physics
Complex Systems Physics
Computational Physics
Condensed Matter Physics
Cosmology and Early Universe
Earth and Planetary Sciences
General Relativity
High Energy Astrophysics
High Energy/Accelerator Physics
Instrumentation and Measurement
Interdisciplinary Physics
Materials Sciences and Technology
Mathematical Physics
Mechanical Response of Solids and Structures
New Materials: Micro and Nano-Mechanics and Homogeneization
Non-Equilibrium Thermodynamics and Statistical Mechanics
Nuclear Science and Engineering
Optics
Physics of Nanostructures
Plasma Physics
Quantum Mechanical Developments
Quantum Theory
Relativistic Astrophysics
String Theory
Superconducting Physics
Theoretical High Energy Physics
Thermology

We are also interested in: 1) Short Reports—2-5 page papers where an author can either present an idea with theoretical background but has not yet completed the research needed for a complete paper or preliminary data; 2) Book Reviews—Comments and critiques.

Notes for Intending Authors

Submitted papers should not have been previously published nor be currently under consideration for publication elsewhere. Paper submission will be handled electronically through the website. All papers are refereed through a peer review process. For more details about the submissions, please access the website.

Website and E-Mail

https://www.scirp.org/journal/jmp **E-mail: jmp@scirp.org**

What is SCIRP?

Scientific Research Publishing (SCIRP) is one of the largest Open Access journal publishers. It is currently publishing more than 200 open access, online, peer-reviewed journals covering a wide range of academic disciplines. SCIRP serves the worldwide academic communities and contributes to the progress and application of science with its publication.

What is Open Access?

All original research papers published by SCIRP are made freely and permanently accessible online immediately upon publication. To be able to provide open access journals, SCIRP defrays operation costs from authors and subscription charges only for its printed version. Open access publishing allows an immediate, worldwide, barrier-free, open access to the full text of research papers, which is in the best interests of the scientific community.

- High visibility for maximum global exposure with open access publishing model
- Rigorous peer review of research papers
- Prompt faster publication with less cost
- Guaranteed targeted, multidisciplinary audience

Scientific Research Publishing

Website: https://www.scirp.org

Subscription: sub@scirp.org

Advertisement: service@scirp.org